Western Graduate&PostdoctoralStudies

Western University
Scholarship@Western

Electronic Thesis and Dissertation Repository

9-30-2022 10:30 AM

Characterization of the Role of miR156-SPL12 Regulatory Module in Root Architecture and Stress Response in Medicago sativa (alfalfa)

Vida Nasrollahi, *The University of Western Ontario*

Supervisor: Hannoufa, Abdelali, *The University of Western Ontario*
Co-Supervisor: Kohalmi, Susanne, *The University of Western Ontario*
A thesis submitted in partial fulfillment of the requirements for the Doctor of Philosophy degree in Biology
© Vida Nasrollahi 2022

Follow this and additional works at: https://ir.lib.uwo.ca/etd

Recommended Citation

Nasrollahi, Vida, "Characterization of the Role of miR156-SPL12 Regulatory Module in Root Architecture and Stress Response in Medicago sativa (alfalfa)" (2022). *Electronic Thesis and Dissertation Repository*. 8898.
https://ir.lib.uwo.ca/etd/8898

This Dissertation/Thesis is brought to you for free and open access by Scholarship@Western. It has been accepted for inclusion in Electronic Thesis and Dissertation Repository by an authorized administrator of Scholarship@Western. For more information, please contact wlswadmin@uwo.ca.

Abstract

The highly conserved plant microRNA156 (miR156) regulates various aspects of plant development and stress response by silencing a group of SQUAMOSA-PROMOTER BINDING PROTEIN-LIKE (SPL) transcription factors. The Hannoufa lab previously showed that transgenic alfalfa (*Medicago sativa* L.) plants overexpressing *miR156* display increased nodulation, nitrogen fixation, and root regenerative capacity during vegetative propagation. In alfalfa, transcripts of 11 *SPL*s, including *SPL12*, are targeted by miR156. Our understanding of the functions of SPLs and their mode of action in alfalfa's nodulation and nitrogen fixation is still elusive, and thus this study was aimed at filling this gap in knowledge.

Here, I carried out a functional characterization of SPL12 by investigating the transcriptomic and phenotypic changes associated with altered transcript levels of *SPL12*, and by determining SPL12 regulatory targets using *SPL12*-silencing and -overexpressing alfalfa plants. Phenotypic analyses showed that silencing of *SPL12* in alfalfa caused an increase in root regeneration, nodulation, and nitrogen fixation. In addition, *AGL6* and *AGL21* that encode respective AGAMOUS-like MADS box transcription factors were identified as being directly targeted for silencing by SPL12, based on Next Generation Sequencing-mediated transcriptome analysis and chromatin immunoprecipitation assays. Phenotypic and molecular analysis showed that silencing *AGL6* also increased nodulation in alfalfa.

The role of SPL12 and AGL6 in nodulation was also investigated under osmotic stress using *SPL12*-RNAi and *AGL6*-RNAi plants, where the SPL12/AGL6 module appears to have a negative role in maintaining nodulation. Additionally, examination of the role of SPL12 in nodulation under nitrate treatment, suggested that SPL12 may regulate nodulation under nitrate treatment in alfalfa by targeting *AGL21*. Moreover, I also investigated the role of the alfalfa SPL12 homolog, *Lj*SPL12, in the model legume *Lotus japonicus* for nodulation and found that *Lj*SPL12 negatively affects the nodulation in *spl12* mutant plants. Taken together, these results suggest that SPL12, AGL6 and AGL21 form a genetic module that regulates root development and nodulation in alfalfa.

Considering the important role already shown for another SPL, SPL13, in vegetative state transition and abiotic stress tolerance in alfalfa, I also successfully applied the CRISPR/Cas9 technique to edit the *SPL13* gene in alfalfa, however, the overall efficiency was low.

Keywords

Medicago sativa L., nodule organogenesis, nitrogen fixation, alfalfa, miR156, SPL, AGL, CRISPR/Cas9

Summary for lay audience

With an increasing global population that is projected to reach nine billion people by 2050, demand for more resource-intensive foods is predicted to rise even faster than it currently is. In addition, agricultural production is predicted to be severely affected by climate change, resulting in major challenges for crop production and food security. The availability of major nutrients in the plant rhizosphere is critical for sustainable crop production, including nitrogen a major limiting factor in crop growth and productivity. Leguminous plants, including alfalfa (*Medicago sativa* L.), can withstand nitrogen scarcity to a certain extent due to their ability to host nitrogen-fixing bacteria in root nodules. At the molecular level, the highly conserved plant microRNA156 (miR156) affects plant growth and development, and is involved in regulating response to various stress conditions, including nutritional scarcity, drought and diseases, by silencing a group of SQUAMOSA-PROMOTER BINDING PROTEIN-LIKE (SPL) transcription factors. It is thus critical to determine if the miR156-SPL regulatory network plays a role in modulating alfalfa's root-related traits.

In the current study, the role of the transcription factor protein, SPL12, as well as downstream genes that are regulated by SPL12 was investigated to understand their potential roles in root-related traits, including root development, nodule formation and nitrogen assimilation. This study involved the phenotypic and molecular genetic characterization of alfalfa plants with increased and decreased levels of *SPL12* and other downstream genes. The analyses showed that SPL12 plays a negative role in root regeneration, nodulation and nitrogen fixation by regulating downstream target genes, such

as *AGL6* and *AGL21*. Phenotypic and molecular analyses further showed that silencing *AGL6* also increased nodulation in alfalfa. Analysis of plant-wide changes in gene expression revealed that at least 169 genes were affected by *SPL12* silencing in alfalfa. Alfalfa plants with reduced *SPL12* levels maintained nodulation under osmotic stress by partially regulating sulfate transportation.

Understanding the molecular function of miR156-targeted SPL12 and its targets in alfalfa root architecture and nodulation will provide an important molecular tool that can be used in marker-assisted improvements not only for alfalfa, but also potentially for other legume crops.

Co-Authorship Statements

The following thesis includes material from manuscripts under revision, and in preparation. For these manuscripts and my thesis, my supervisor, Dr. Abdelali Hannoufa, provided insight and strategic direction of the projects as well as editing. My co-supervisor, Dr. Susanne Kohalmi, provided insightful comments along with editing.

I performed all of the experiments described in the following thesis with the following exceptions:

A construct for *SPL12*-RNAi was made previously in the Hannoufa lab by Banyar Aung. The RNAi construct was used in *Agrobacterium*-mediated alfalfa transformation which I performed myself.

SPL12 overexpression (*35S::SPL12*) and *AGL6*-RNAi transgenic plants were generated by Banyar Aung in the Hannoufa lab and Qing Shi Mimmie Lu in the Lining Tian lab at AAFC-London, respectively.

Sections 3.1, 3.2, 4.1 and 4.2 contain material from an accepted article for publication with the following authors' contributions:

Nasrollahi, V., Z.-C. Yuan, Q. Lu, T. McDowell, S. E. Kohalmi and A. Hannoufa 2022. Deciphering the role of SPL12 and AGL6 from a genetic module that functions in nodulation and root regeneration in *Medicago sativa*. Manuscript accepted for publication in Plant Molecular Biology (2022-07-17; PLAN-D-22-00039R1).

AH conceived the research and secured the funding. VN and AH designed the experiments. VN performed the experiments, analyzed the data and drafted the manuscript. TM, QSML and ZCY assisted in generating the transgenic plants and in conducting nitrogen fixation experiments. SEK and AH supervised the project. ZCY, TM, QSML, SEK and AH edited the manuscript.

Sections 3.3, 4.5 and 4.6 contain material under preparation for possible publication with the following authors' contributions:

Nasrollahi, V., Z.-C. Yuan, S. E. Kohalmi and A. Hannoufa,. SPL12 regulates *AGL6* and *AGL21* to modulate nodulation and root regeneration under osmotic stress and nitrate sufficiency conditions in *Medicago sativa* (under preparation).

AH conceived the study and participated in its design as well as securing the funding. VN performed the experiments, analyzed the data and drafted the manuscript. SEK and AH supervised the project. VN drafted the manuscript. ZCY, SEK and AH edited the manuscript.

Dedication

To my brother Hamid, without whose help I would not be here!

Acknowledgments

I would like to thank my supervisor Dr. Abdelali Hannoufa for his continuous support, encouragement, and guidance during my study period.

I am grateful to my co-supervisor, Dr. Susanne Kohalmi for her guidance and manuscript editing skills, along with the final reading of my thesis. I would also like to thank the members of my advisory committee, Dr. Sangeeta Dhaubhadel and Dr. Hugh Henry for providing helpful feedback and advice during my PhD studies.

I would also like to thank past and current members of Dr. Hannoufa's lab (Ling, Gigi, Matei, Jonathan, Lisa, Biruk, and Lexi) for their helpful advice, and for contributing towards a wonderful working environment. I appreciate the work Qing Shi Mimmie Lu did in developing the *AGL6*-RNAi alfalfa, and I thank Tim McDowell for his help with conducting nitrogen fixation experiments. I am also grateful for the support and friendship I have received from past and present students at AAFC research center, in London, ON. Thank you Nishat, Shabnam, Mandana, Jie, Alpa, Arina, Raj, Gebb, and too many others to name.

Lastly, I would like to thank my parents and my siblings (Hamid, Leily, and Majid) for supporting me throughout this research. I would particularly like to thank Hamid for his help, support, and encouragement during the most challenging parts of this degree.

I am very much grateful to my husband Georges Kovari. Thank you for believing in me and for your endless support.

Table of Contents

Abstract i

Summary for lay audience iii

Co-Authorship Statements v

Dedication vii

Acknowledgments viii

Table of Contents ix

List of Tables xiv

List of Figures xv

List of Appendices xviii

List of Abbreviations xx

Chapter 1 1

1 Introduction 1

1.1 The importance and benefits of alfalfa and leguminous crops 1

1.2 Nodulation and nitrogen fixation in legume plants 4

1.2.1 Flavonoids as signals in plant-rhizobia interactions 8

1.2.2 Autoregulation of nodulation 15

1.3 Root architecture 18

1.4 Regulation of root architecture and nodulation 20

1.5 The regulatory role of microRNAs in root development and nodulation 21

1.6 The role of miR156 in regulating root architecture, nodulation and nitrogen fixation 24

1.7 SPL transcription factors and their role in the regulation of root architecture, nodulation and nitrogen fixation 25
1.8 Role of MADS box proteins in the regulation of root architecture 27
1.9 Hypothesis and objectives of the study 28
Chapter 2 30
2 Materials and Methods 30
2.1 Plant material 30
2.1.1 Alfalfa plants 30
2.1.2 *Lotus japonicus* plants 30
2.2 Generation of vector constructs and plant transformation 31
2.2.1 *SPL12*-RNAi and *AGL6*-RNAi 31
2.2.2 *35S::SPL12* and *35S::SPL12m-GFP* 32
2.2.3 sgRNA design and construction of sgRNA-Cas9 expression vector 35
2.3 Alfalfa transformation and screening for alfalfa transformants 36
2.4 Identification of *spl12* mutant lines in *L. japonicus* 38
2.5 Nodulation test 39
2.5.1 Nodulation test in Alfalfa 39
2.5.2 Nodulation test in *Lotus japonicus* 39
2.6 Evaluation of nitrogen fixation by nitrogenase activity assay 40
2.7 Nitrate treatment 41
2.8 Mannitol treatment 42
2.9 RNA extraction, reverse transcription-real time quantitative PCR 42
2.10 Next Generation RNA sequencing transcriptome analysis 43

2.11 Analysis of differentially expressed genes and GO enrichment 44

2.12 Phylogenetic tree construction 45

2.13 Southern blot analysis 45

2.14 Extraction of SPL12-GFP fusion protein and Western blot analysis 46

2.15 ChIP-qPCR analysis 46

2.16 T7 Exonuclease 1 Assay 48

2.17 Microscopy 49

2.18 Statistical analysis 49

Chapter 3 50

3 Results 50

3.1 Generating alfalfa *spl13* mutants by CRISPR-Cas9 editing 50

3.1.1 Designing sgRNA for editing *SPL13* in alfalfa 50

3.1.2 Screening of CRISPR-modified alfalfa plants by T7 endonuclease 1 digestion 53

3.1.3 Validation of edited *SPL13* locus by Sanger Sequencing 56

3.2 SPL12 plays a role in root architecture, nodulation and nitrogen fixation 56

3.2.1 *SPL12* transcript levels in *SPL12*-RNAi and *35S::SPL12* plants 59

3.2.2 Effect of *SPL12* silencing on root regenerative capacity 59

3.2.3 Effect of inoculation with *Sinorhizobium meliloti* on *SPL12* transcript levels 64

3.2.4 Role of SPL12 in nodulation 67

3.2.5 Silencing of *SPL12* enhances nitrogen fixation 72

3.2.6 *SPL12* silencing affects nodulation-related genes 75

3.3 Effect of *SPL12* silencing on root transcriptome 78

3.3.1 Differentially expressed genes between *SPL12*-RNAi and WT alfalfa plants 78

3.3.2 Gene ontology enrichment analysis of DEGs 80

3.3.3 RNA-Seq data validation by quantitative real time PCR 80

3.3.4 Comparison of differentially expressed genes between the two *SPL12*-RNAi genotypes 84

3.3.5 SPL12 regulation of *AGL6* and *AGL21* 84

3.3.6 Expression profiles of *SPL12*, *AGL6* and *AGL21* genes in alfalfa 87

3.3.7 SPL12 is a direct regulator of *AGL6* 92

3.3.8 *AGL6* silencing enhances nodulation 95

3.4 SPL12 and AGL6 affect nodulation in alfalfa under osmotic stress and nitrate application 95

3.4.1 Effect of *SPL12* silencing on response to osmotic stress 95

3.4.2 *SPL12* silencing mitigates nodulation inhibition under osmotic stress 98

3.4.3 Changes in the transcript levels of *AGL21* and *AGL6* in *SPL12*-RNAi alfalfa under osmotic stress 101

3.4.4 Sulfate transporters are enhanced in *SPL12*-silenced plants 106

3.4.5 Effect of *SPL12* silencing on expression of stress-related genes under mannitol treatment 109

3.4.6 *AGL6* silencing maintains nodulation under osmotic stress 112

3.4.7 *SPL12* silencing reduces effect of nitrate on nodulation 115

3.4.8 Effect of nitrate on expression of *SPL12* and *AGL21* 115

3.4.9 SPL12 is a direct regulator of *AGL21* 122

3.5 Characterization of *Lotus japonicus spl12* mutants 125

3.5.1 Nodulation is enhanced in *spl12* mutant of *L. japonicus* 128

Chapter 4 131

4 Discussion 131

4.1 Role of SPL12 in root regeneration capacity 131

4.2 Role of SPL12 in nodulation and nitrogen fixation 132

4.3 Genes and pathways affected by *SPL12* silencing 136

4.4 Direct regulatory interaction between SPL12 and *AGL6* to control nodulation 138

4.5 The role of SPL12 and AGL6 in regulating nodulation under osmotic stress in alfalfa 139

4.6 How nitrate availability affects nodulation through SPL12-*AGL21* regulatory pathway 142

4.7 Efficiency of *SPL13* mutagenesis by CRISPR-Cas9 in alfalfa 144

Conclusion and future research directions 149

References 154

Appendices 177

Curriculum Vitae 210

List of Tables

Table 3. 1 Validation of RNA-Seq data using RT-qPCR. 83

List of Figures

Figure 1.1 The process of rhizobia infection and nodule development in legume roots 5

Figure 1.2 Sulfate transporters are involved in the regulation of plant response to drought stress 9

Figure 1.3 Symbiotic signaling pathway 12

Figure 1.4 Autoregulation of Nodulation..... 16

Figure 1.5 Mechanism of miR156 post-transcriptional gene regulation 22

Figure 2.1 Mutagenesis of *SPL12* to prevent miR156 complementarity..... 33

Figure 3.1 CRISPR/Cas9 mutagenesis of *SPL13* in alfalfa 51

Figure 3.2 Detection and molecular analysis of CRISPR/Cas9-modified alfalfa plants by T7E1 assay 54

Figure 3.3 Confirmation of *SPL13* editing in 13-CR-6 genotype with gRNA1. 57

Figure 3.4 Relative transcript levels of *SPL12* in different genotypes of alfalfa plants ... 60

Figure 3.5 Effect of *SPL12* silencing on root regeneration in alfalfa 62

Figure 3.6 Relative transcript levels of *SPL12* and early nodulation genes upon rhizobium infection 65

Figure 3.7 The effect of *SPL12* silencing on nodulation 68

Figure 3.8 Effect of *SPL12* overexpressing on root regeneration and nodule numbers in alfalfa 70

Figure 3.9 Analysis of nitrogen fixation activity in alfalfa..... 73

Figure 3.10 Effect of *SPL12* silencing on the nodulation-related gene transcription level 76

Figure 3.11 Gene Ontology enrichment analysis of DEGs between *SPL12*-RNAi and WT 81

Figure 3.12 Numbers of DEGs based on RNA-Seq of WT and *SPL12*-RNAi plants..... 85

Figure 3.13 SPL12 regulation of *AGL21* in alfalfa..... 88

Figure 3.14 Tissue-specific transcript profiles of *SPL12*, *AGL6*, and *AGL21*..... 90

Figure 3.15 Detection of SPL12 binding to *AGL6* promoter..... 93

Figure 3.16 Effect of the *AGL6* silencing on nodulation..... 96

Figure 3.17 Effect of *SPL12* silencing on response to osmotic stress 99

Figure 3.18 Effect of *SPL12* silencing on nodulation under osmotic stress 102

Figure 3.19 Transcript levels of *AGL21*, *AGL6* and *CLE13* in *SPL12*-RNAi and WT alfalfa under osmotic stress..... 104

Figure 3.20 Relative transcript levels of sulfate transporter genes based on NGS and RT-qPCR in WT and *SPL12*-RNAi alfalfa plants..... 107

Figure 3.21 Relative transcript levels of stress-related genes in response to osmotic stress..... 110

Figure 3.22 The effect of *AGL6* silencing on nodulation under osmotic stress..... 113

Figure 3.23 Effect of 8 mM nitrate on nodulation phenotype in *SPL12*-RNAi roots..... 116

Figure 3.24 Effect of 20 mM nitrate on nodulation phenotype in *SPL12*-RNAi roots... 118

Figure 3.25 Phylogenetic tree of *M. truncatula* and Arabidopsis MADS-box proteins. 120

Figure 3.26 Detection of *SPL12* binding to *AGL21* promoter 123

Figure 3.27 PCR genotyping of LORE1 insertions in *Lotus japonicus*..... 126

Figure 3.28 Analysis of nodulation in spl12 *L. japonicus* mutant 129

List of Appendices

Apendix 1:

Supplementary Figures

Figure S1 The original coding sequence of *SPL13* in alfalfa and positions of different gRNAs selected for CRISPR experiments 177

Figure S2 Promoter sequence of the alfalfa *AGL6* gene with putative SBD binding elements 178

Figure S3 Effect of nitrate on nodulation in *SPL12*-RNAi plants 179

Figure S4 Promoter sequence of the alfalfa *AGL21* gene with putative SBD binding elements 180

Apendix 2:

Supplementary Tables

Table S1 Primers utilized and their nucleotide sequences 181

Table S2 Composition of alfalfa transformation media 186

Table S3 Buffers and extraction reagent used in Southern blot analysis and their components 190

Table S4 Buffers used in ChIP assay and their components 191

Table S5 Top 50 out of 1710 differentially expressed genes and their functions in RNAi12-29 197

Table S6 Top 50 out of 840 differentially expressed genes and their functions in RNAi12-24 199

Table S7 Differentially increased genes and their functions common in both *SPL12*-RNAi plants 201

Table S8 Differentially decreased genes and their functions common in both *SPL12*-RNAi plants 204

Table S9 GO-term analysis represented molecular function, biological process and cellular components in leaf tissues 207

List of Abbreviations

ABA	abscisic acid
ANOVA	analysis of variance
AON	autoregulation of nodulation
ARA	acetylene reduction activity
ATP	adenosine triphosphate
bp	base pairs
BME	β-mercaptoethanol
ChIP	chromatin immunoprecipitation
CLE	CLAVATA3/EMBRYO SURROUNDING REGION
CRISPR	clustered regularly interspaced short palindromic repeats
Cys	Cysteine
dai	days after inoculation
DCL1	DICER-LIKE 1
DEGs	differentially expressed genes
DIG	Digoxigenin
EDTA	ethylenediaminetetraacetic acid
gDNA	genomic DNA
GFP	GREEN FLUORESCENT PROTEIN

GMO	genetically modified organism
GO	gene ontology
HEN1	HUA ENHANCER1
IT	infection thread
LORE1	*L. japonicus* retrotransposon 1
MADS	MCM1/AGAMOUS/DEFICIENS/SRF
Met	Methionine
miRNAs	microRNAs
miR156	microRNA156
MSTFA	*N*-methyl-*N*-trimethylsilyl trifluoroacetamide
NF	nodulation or nod factors
NR	NITRATE REDUCTASE
NiR	NITRITE REDUCTASE
OE	Overexpression
PAM	protospacer-adjacent motifs
REVIGO	reduced visualization gene ontology
RISC	RNA-INDUCED SILENCING COMPLEXES
RNAi	RNA interference
RNS	root nodule symbiosis

RT-qPCR	reverse transcription-real time quantitative PCR
SBD	SPL binding domain
SBP	SQUAMOSA PROMOTOR BINDING PROTEIN
SDS	sodium dodecyl sulfate
sgRNA	single guide RNA
SPL	SQUAMOSA-PROMOTER BINDING PROTEIN-LIKE
SULTRs	SULFATE TRANSPORTERS
SYM	symbiotic signaling
T7E1	T7 EXONUCLEASE I
v/v	volume per volume
w/v	weight per volume
WT	wild-type
W/m2	watts over a square meter surface

Chapter 1

1 Introduction

1.1 The importance and benefits of alfalfa and leguminous crops

Legume crops, including soybean, pea, clover, chickpea, and alfalfa represent the second most important crop in terms of global economy, just after cereals (Ferguson et al. 2010). They are nutritionally important and economically significant, as they are cultivated globally on an area of 201,728 thousand ha, and are responsible for more than 25% of the world's primary crop production (Mahmood et al. 2018). These plants are rich in oils, fiber, micronutrients, minerals, and proteins suitable for livestock feed and human consumption (Kamboj and Nanda 2018). Furthermore, legumes are more agronomically sustainable than other crops, as they require less chemical fertilizer (Stagnari et al. 2017). Legume crops can enrich soil nitrogen by supplying nitrogen to agro-ecosystems via beneficial symbioses with soil rhizobia that can fix atmospheric nitrogen to convert it into ammonia (Oldroyd et al. 2011). As such, legumes are considered keystone species for agricultural and natural ecosystems due to their natural ability to release fixed nitrogen into soils (Canfield et al. 2010). It is estimated that leguminous plants convert 40 to 60 million metric tons of nitrogen from the atmosphere annually (Graham and Vance 2003).

Nitrogen-fixing symbioses between plants and bacteria can be divided into two main classes: plant-cyanobacteria symbiosis and root nodule symbiosis (RNS) (Delaux et al. 2015). Plants that possess the nitrogen-fixing nodulation trait are distributed across species

belonging to four orders of flowering plants, namely Fabales, Cucurbitales, Fagales, and Rosales (Sprent 2007). Although these orders are known as the nitrogen-fixing clade, there are many non-nodulating species in this clade, with the majority of nodulating species belonging to the Leguminosae (Fabaceae) within the order Fabales (Soltis et al. 1995; van Velzen et al. 2019). The symbiotic relationship between legumes and their rhizobial partners is mutually beneficial, since the host legume provides the rhizobia carbon and energy in exchange for an essential nutrient, nitrogen (Prell and Poole 2006).

Of the nitrogen fixing forage crops, alfalfa (*Medicago sativa* L.) is the most widely cultivated around the world (Annicchiarico et al. 2015), grown on about 30 million ha (Annicchiarico et al. 2015; Rozema and Flowers 2008). Due to its being the highest-yielding perennial forage crop with relatively high protein content compared to other forage legumes, alfalfa can be grown alone or in combination with different grass species. Well-managed alfalfa can be grown for three or more successive years (Bélanger et al. 2006; Sheaffer and Seguin 2003).

Alfalfa has a long taproot system ranging on average from 1.5 to 2.1 m in length (Abdul-Jabbar et al. 1983), which penetrates more deeply into the soil than the roots of various common temperate crops including wheat, corn, various beans, cereals, and oilseeds (Fan et al. 2016). A deep rooting system helps plants to access water and nutrients stored deep in the soil, and hence helps ensure plant production and survival under drought and nutrient stress (Comas et al. 2013). While alfalfa is used mainly as a feed for livestock, it is also used for crop rotations and soil improvement, because of its ability to form a symbiotic relationship with rhizobium bacteria, which improve soil nitrogen balance and quality

through nitrogen fixation (Ferguson et al. 2010; Sheaffer and Seguin 2003). Although alfalfa's relationship with these bacteria is one of the most efficient relationships between rhizobia and legume plants, the amount of fixed nitrogen is variable in different planting areas and crop management systems. It is estimated that alfalfa can fix about 200-400 kg/ha/year of nitrogen, depending on the area and environment (Angus and Peoples 2012; Issah et al. 2020). While breeding efforts have focused on improving other agronomically important traits such as abiotic stress tolerance and forage productivity (Jia et al. 2018; Kumar et al. 2018; Lei et al. 2017; Singer et al. 2018), nitrogen traits have received little attention in alfalfa.

Classical breeding is generally challenging and time consuming, especially in alfalfa where it is made even more difficult by the plant's outcross-pollinating reproductive nature (Choi et al. 2004), and its large (800-1000 Mb) autotetraploid (2n = 4x = 32) genome (Blondon et al. 1994), further adding to its genomic diversity and complicating the use of conventional breeding approaches (Volenec et al. 2002). Given the difficulties associated with classical breeding in alfalfa, alternative approaches, such as the development and use of modern biotechnology tools need to be explored for genetic improvement of this crop. It should be noted that the full sequence of the cultivated alfalfa genome was only recently made public (https://figshare.com/articles/dataset/genome_fasta_sequence_and_annotation_files/12327602) (Chen et al. 2020). Prior to this, researchers had to rely on the genome sequence of the closely related species *Medicago truncatula* (http://www.medicagogenome.org/) to develop and expand alfalfa's genomic toolbox (Arshad et al. 2018; Gao et al. 2016).

1.2 Nodulation and nitrogen fixation in legume plants

Unlike animals, the vast majority of plants have to acquire nitrogen, usually in the form of nitrates and ammonium, from the soil. Although nitrogen gas (N_2) is plentiful in the atmosphere, the biologically active forms of nitrogen are often so limited that they can constrain plant growth. For nodule-forming plants, however, the limitation of nitrogen fixation can be overcome to some extent by acquiring nitrogen from the rhizosphere (Oldroyd et al. 2011). While some species-specific factors may be involved, in general, development of nitrogen-fixing root nodules is controlled by two parallel processes that are initiated by the host plant. First, nodule organogenesis, which is formed from the re-initiation of cell division in the root cortex (Madsen et al. 2010; Oldroyd et al. 2011); and second, rhizobia infect the inside of the root hair cells that curl around rhizobia to entrap bacteria, which eventually grow and form infection threads (ITs) (Oldroyd et al. 2011) **(Figure 1.1)**. ITs are plant-derived conduits that are capable of crossing cell boundaries to direct rhizobia into the root cortex targets, the site of developing primordia (Held et al. 2010; Madsen et al. 2010). Finally, the rhizobia are released from the ITs into the inner cells in the nodule while remaining encapsulated within a plant membrane. In these organelle-like structures, called symbiosomes, rhizobia are responsible for the reduction of atmospheric di-nitrogen to ammonia by expressing the nitrogenase enzyme (Oldroyd and Downie 2008).

As nitrogenase is exceptionally rich in sulfur (Becana et al. 2018; Heim et al. 2016; Scherer 2008), this element becomes limiting in symbiosis. There is a high demand for sulfur in nodulated legumes, and hence nitrogen fixation is more sensitive to sulfur deficiency than

Figure 1.1 The process of rhizobia infection and nodule development in legume roots

The release of flavonoids by the legume roots triggers the synthesis of rhizobial Nodulation Factors (Nod Factors) that are recognized by the plant and lead to the invasion of plant root cells by rhizobia through root hair cells. Infection threads are initiated at the site of root hair curls and extend through root hairs towards the cortical cells of the root. Pre-infection threads are formed in advance, and define the path of infection thread growth through the outer cortex. The infection thread grows towards the nodule primordia (which are formed by dividing cortical cells), ramifies and releases rhizobia into the cells.

Figure modified from Wang et al. (2018).

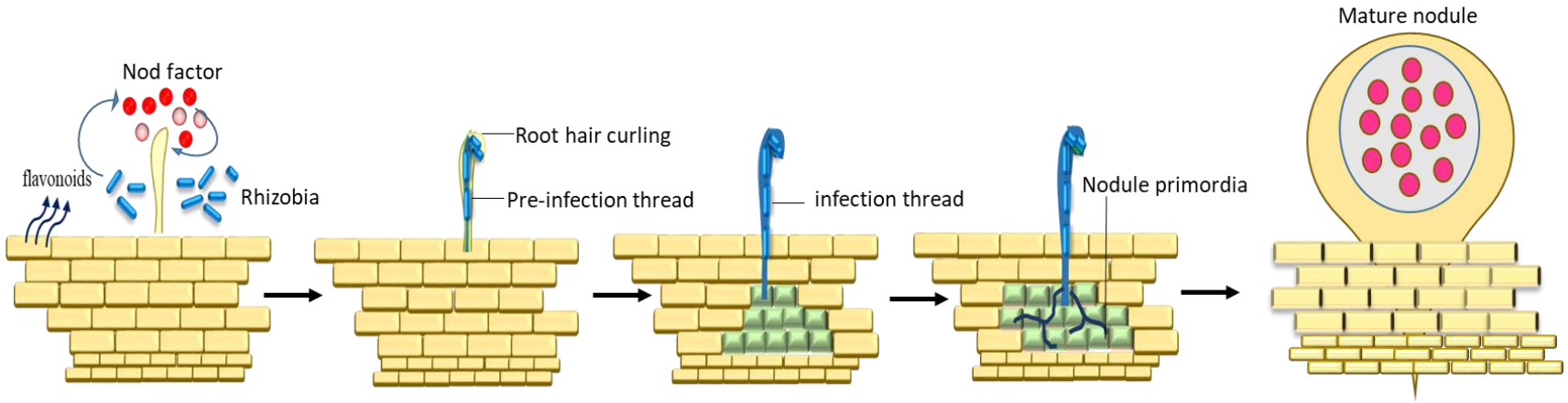
Nod factor
flavonoids
Rhizobia
Root hair curling
Pre-infection thread
infection thread
Nodule primordia
Mature nodule

to nitrate uptake (Varin et al. 2010). Sulfur is an indispensable and limiting nutrient for plants because it is used for the formation of the sulfur-containing amino acids, cysteine (Cys) and methionine (Met), which are incorporated into protein synthesis, and also function as metal cofactors and coenzymes (Davidian and Kopriva 2010). An abundant supply of sulfur in plants markedly increases nodulation and nitrogen fixation (Anderson and Spencer 1950; Scherer and Lange 1996; Varin et al. 2010). Sulfur-deficiency in plants, on the other hand, leads to decreases in nodulation, nodule metabolism, and nitrogenase biosynthesis and activity, presumably due to the low-availability of Cys and Met (Becana et al. 2018). In addition, it has been reported that low nitrogen fixation observed in sulfur-deficient legumes is due to low leghemoglobin, glucose, ATP, and ferredoxin, which suggests a limitation in energy production for nitrogen fixation (Pacyna et al. 2006; Scherer 2008; Varin et al. 2010). Sulfur from the soil is taken up as sulfate by plant cells through several classes of sulfate transporters (SULTRs) (Takahashi et al. 2012). In *Lotus japonicus*, the *SYMBIOTIC SULFATE TRANSPORTER1* (*SST1*) gene encodes a sulfate transporter that is specifically and highly expressed in the nodules, suggesting a major role in the transport of sulfate from the plant to the bacteroids (Krusell et al. 2005). In *M. truncatula*, a Group 3 SULTR (*SULTR3.5*), homolog *LjSST1*, is strongly expressed in nodules (Roux et al. 2014). In addition, it has been shown that *MtSULTR3.5* expression is strongly up-regulated in roots subjected to salt stress (Gallardo et al. 2014). Members of the SULTR3 class of transporters have been less well studied, although the five *At*SULTR3 transporters in *Arabidopsis thaliana* were well characterized by Chen et al. (2019), who found that all of them are localized to the chloroplast membrane, and facilitate the import of sulfate to this organelle. Interestingly, the *SULTR3.1* and *SULTR3.4* genes are

up-regulated in roots of both Arabidopsis and *M. truncatula* plants subjected to drought stress (Gallardo et al. 2014). Cys, whose precursor is sulfate, induces abscisic acid (ABA) biosynthesis (Batool et al. 2018), which is a drought-induced messenger that coordinates rapid adaptive responses such as stomatal closure (Ernst et al. 2010). Sulfur and ABA metabolisms are co-regulated to control the environmental stresses in Arabidopsis (Cao et al. 2014). During drought, sulfate concentration increases quickly in the xylem sap. Subsequently, sulfate is transported to the green tissues and sequestered into the chloroplasts, where it undergoes reduction and is used for Cys biosynthesis (Malcheska et al. 2017), and stimulates the synthesis of the drought hormone ABA (Batool et al. 2018), which is a key regulator of response to abiotic stress (Cao et al. 2014) **(Figure 1.2)**. The rapid drought response in Arabidopsis was shown to depend on all five *At*SULTR3 transporters, since Cys and ABA contents were reduced to 67% and 20%, respectively, in the *AtSULTR3* quintuple mutant (lacking activities of all SULTR3 members), as compared to wild type plants (Chen et al. 2019).

1.2.1 Flavonoids as signals in plant-rhizobia interactions

Nodulation is initiated by plant root exudates containing phenolic flavonoid compounds, which act as chemotactic signals under low nitrogen conditions (Liu and Murray 2016) to attract symbiotic bacteria in the rhizosphere (Ferguson et al. 2010; Oldroyd et al. 2011). While leguminous plants produce an array of flavonoids, only specific subsets of these play a role in nodulation. For example, the chalcone-4, 40-dihydroxy-20-methoxychalcone (methoxychalcone) identified in root exudates of alfalfa and other *Medicago* spp. is the

Figure 1.2 Sulfate transporters are involved in the regulation of plant response to drought stress

Sulfate transporters facilitate sulfate (SO_4^{2-}) uptake throughout the plant. Drought stress results in sulfate accumulation in the xylem and movement toward the green tissues. The Group3 SULTRs (SULTR3), localized in the plastid membrane, transfer the sulfate into the chloroplasts where sulfur is incorporated into Cys, which triggers ABA production, a hormone that regulates stomatal opening and closure.

Figure modified from Gommers (2019).

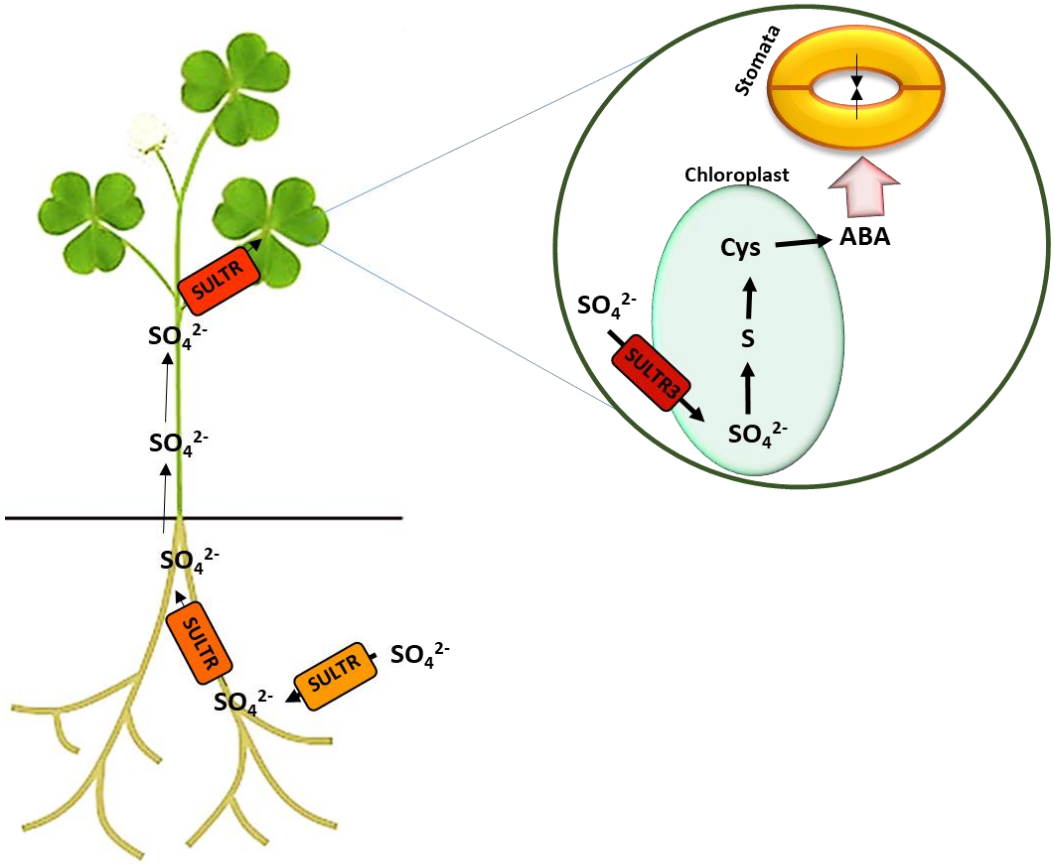
Stomata
Chloroplast
Cys
ABA
S
SULTR3
SULTR
SULTR
SULTR
SO_4^{2-}
SO_4^{2-}
SO_4^{2-}
SO_4^{2-}
SO_4^{2-}
SO_4^{2-}
SO_4^{2-}
SO_4^{2-}

strongest inducer of *NOD* genes in compatible rhizobial symbionts, including *Sinorhizobium meliloti* (Dakora et al. 1993; Maxwell et al. 1989). The enzyme CHALCONE O-METHYLTRANSFERASE (ChOMT) is required for the biosynthesis of methoxychalcone from isoliquiritigenin (Maxwell et al. 1992). In *M. truncatula*, *MtChOMT1* and three other closely homologous genes (*MtChOMT2*, *MtChOMT3*, and *MtChOMT4*) were induced in root hairs inoculated with rhizobia (Breakspear et al. 2014), and two of these (*MtChOMT2*, *MtChOMT3*) were also detected in the infection zone of mature nodules of this plant (Chen et al. 2015; Roux et al. 2014).

The specific interaction between legumes and nitrogen-fixing rhizobia starts when host-specific flavonoids released by the plant into the rhizosphere are recognized by NodD. NodD induces the expression of *NOD* genes by binding to the nod box, the conserved sequences located upstream of *NOD* genes (Chen et al. 2005). The NOD proteins control the production of the rhizobial lipo-chito-oligosaccharide, also known as Nodulation Factors (NF) (Lerouge et al. 1990; Peters et al. 1986). The bacterial secreted NF are the key signal molecules that initiate nodule organogenesis (Lerouge et al. 1990). The perception of rhizobial NF is necessary and sufficient to induce nodule organogenesis (Truchet et al. 1991) through activation of the plant common symbiotic signaling (SYM) pathway (Oldroyd and Downie 2004). By analyzing a range of mutants, these processes have been intensively studied in the past two decades to help gain an understanding of the genetic elements of the pathway **(Figure 1.3)** in a number of leguminous species (Oldroyd 2013; Suzaki et al. 2015). Briefly, NFs are perceived by receptor-like kinases with extracellular Lysine Motif (LysM) domains (Limpens et al. 2003). In *M. truncatula*, NFs produced by *S. meliloti*, are recognized by LysM RECEPTOR KINASE3 (LYK3) and

Figure 1.3 Symbiotic signaling pathway

Bacterial Nod factors are perceived by the receptors LYK3 and NFP at the plasma membrane of epidermal cells. Activation of these receptor complexes leads to depolarization of cell membranes and changes in ion fluxes which initiate calcium spiking, driven by proteins in the nuclear envelope. Calcium spiking is dependent on various nuclear envelope proteins including the calcium channels DMI1, CNGC15, and three nuclear pore proteins, NENA, NUP85, and NUP133. Calcium spiking is perceived by nuclear calcium-calmodulin kinase (DMI3). The activation of DMI3 results in the phosphorylation of IPD3 with the help of DELLA to regulate expression of NIN and its downstream genes NF-YA1, ERN1, and NPL, leading to nodulation. LYK3: LysM RECEPTOR KINASE 3; NFP: NOD FACTOR PERCEPTION; DMI1,2,3: DOES NOT MAKE INFECTIONS 1,2,3; CNGC15: CYCLIC NUCLEOTIDE-GATED CALCIUM; IPD3: INTERACTING PROTEIN OF DMI3; NIN: NODULE INCEPTION; NPL: NODULATION PECTATE LYASE; NFYA1: NUCLEAR FACTOR YA1; ERN: ERF REQUIRED FOR NODULATION.

Figure modified from Roy et al., (2020).

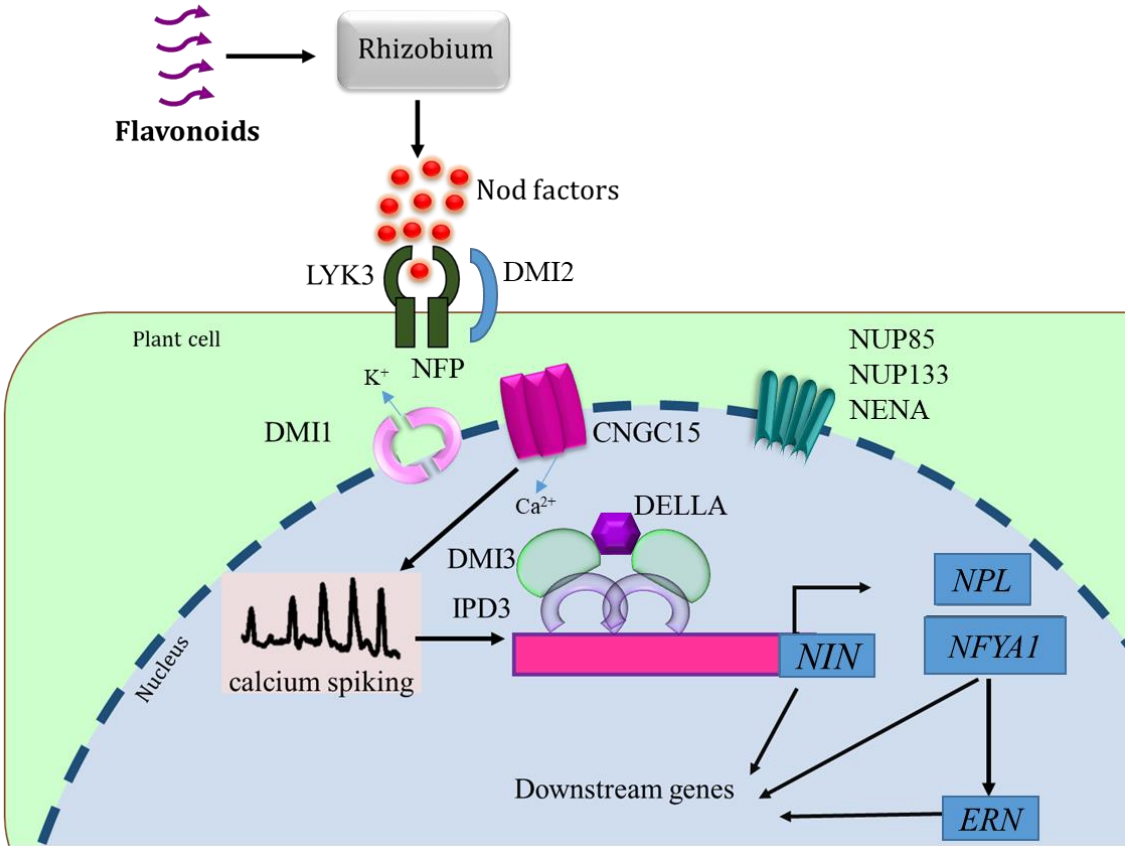
Flavonoids
Rhizobium
Nod factors
LYK3
DMI2
Plant cell
K+
NFP
NUP85
NUP133
NENA
DMI1
CNGC15
Ca2+
DELLA
DMI3
IPD3
NPL
NIN
NFYA1
Nucleus
calcium spiking
Downstream genes
ERN

NOD FACTOR PERCEPTION (NFP) (Arrighi et al. 2006; Limpens et al. 2003). Recognition of NFs leads to the induction of a signaling pathway that activates a leucine-rich repeat-RLK, known as DOES NOT MAKE INFECTIONS2 (DMI2) in *M. truncatula* (also known as SYMbiosis RK, SYMRK, in *L. japonicas*) (Bersoult et al. 2005). Secondary signals initiate calcium oscillation in the nuclear region, a process known as calcium spiking (Charpentier et al. 2016). Activation of this signaling pathway requires three components of the nuclear pore, NUP85, NUP133, and NENA (Groth et al. 2010; Kanamori et al. 2006; Saito et al. 2007), and the cation channels located on the nuclear envelope, encoded by a single inner-membrane-localized channel, DMI1, in *M. truncatula* (CASTOR-POLLUX in *L. japonicus*) (Ané et al. 2004; Capoen et al. 2011). The CYCLIC NUCLEOTIDE-GATED CALCIUM (*Mt*CNGC15) that interacts with *Mt*DMI1 was also shown to be required for nuclear calcium oscillations (Charpentier et al. 2016). Perception of the calcium spiking signature is decoded by a nuclear calcium/calmodulin-dependent protein kinase (*Lj*CCaMK, known as DMI3 in *M. truncatula*). *Mt*DMI3 interacts with and subsequently phosphorylates INTERACTING PROTEIN OF DMI3 (*Mt*IPD3) (known as CYCLOPS in *L. japonicus*) (Messinese et al. 2007; Yano et al. 2008). *Mt*DMI3 interacts with the nuclear protein *Mt*IPD3 and other downstream components, such as two GRAS family proteins, NODULATION SIGNALING PATHWAY1 (NSP1), and NSP2 to activate expression of NODULE INCEPTION (NIN) and its downstream genes that encode NUCLEAR FACTOR YA1 (NF-YA1)/YA2, and ERF REQUIRED FOR NODULATION2 (ERN2), which are essential for rhizobium infection and nodule organogenesis (Andriankaja et al. 2007; Hirsch et al. 2009; Marsh et al. 2007; Middleton et al. 2007; Schauser et al. 1999; Smit et al. 2005).

In *M. truncatula*, DELLA proteins were shown to promote the phosphorylation of *Mt*IPD3 in response to rhizobia, and consequently enhance its interaction with other transcriptional regulators such as *Mt*NSP1 and *Mt*NSP2 (Jin et al. 2016), which form a heterocomplex that associates with the promoter of Nod factor-inducible genes, such as *EARLY NODULIN11* (*MtENOD11)* and *MtERN1* (Hirsch et al. 2009).

1.2.2 Autoregulation of nodulation

Forming and maintaining nodules is an energy-demanding process, and consequently excessive nodulation (super-nodulation) can negatively affect plant growth and development (Matsunami et al. 2004). The host plant, therefore, tightly regulates the total root nodule number depending on the metabolic status of the shoot (carbon source) and root (nitrogen source) (Suzaki et al. 2015). To that end, legumes have evolved a negative regulatory pathway called autoregulation of nodulation (AON) **(Figure 1.4)** that functions systemically through the shoot to maintain an optimal number of nodules (Caetano-Anollés and Gresshoff 1991; Kosslak and Bohlool 1984; Reid et al. 2011b). The nitrogen regulation pathway is activated in root cortical cells during rhizobial infection and nodule development to inhibit nodulation under nitrogen-rich conditions, helping the plant to conserve energy resources (Lim et al. 2014; Reid et al. 2011b). Following the initial rhizobial infection events, root-derived nodulation-specific CLAVATA3/EMBRYO SURROUNDING REGION (CLE) peptides, including CLE12 and CLE13 in *M. truncatula* (Mortier et al. 2010), CLE ROOT SIGNAL1 (CLE-RS1) and CLE-RS2 in *L. japonicus*, or RHIZOBIA-INDUCED CLE1 (RIC1) and RIC2 in soybean (*Glycine max*) (Magori and Kawaguch 2010; Reid et al. 2011a), are triggered to activate AON. Following

Figure 1.4 Autoregulation of Nodulation

Upon activation of the nod factor signaling pathway and perception of rhizobia, the expression of *CLE12* and *CLE13* is increased, and CLE12 and CLE13 are then transported through the xylem to the shoot. Perception of the peptides in the shoot requires the receptor kinase *Mt*SUNN in *M. truncatula* (*Lj*HAR1 in *L. japonicus* or *Gm*NARK in soybean). A second pathway is involved the transport of miR2111 to the root to affect *TML* expression. TML1 and TML2 inhibit the expression of NIN leading to suppression of the downstream genes that regulate nodulation. In soybean, *Gm*NIN activates the expression of miR172c, which in turn silences *GmNNC1*. *Gm*NIN and *Gm*NNC1 activate or repress the expression of *GmRIC1* and *GmRIC2,* respectively. CLE12/13: CLAVATA3/EMBRYO SURROUNDING REGION12/13; SUNN: SUPER NUMERIC NODULES; HAR1: HYPERNODULATION ABERRANT ROOT FORMATION1; NARK: NODULE AUTOREGULATION RECEPTOR KINASE; TML1/2: TOO MUCH LOVE1/2; NIN: NODULE INCEPTION; NNC1: NODULE NUMBER CONTROL1; CLE-RS1/2: CLE ROOT SIGNAL1/2; RIC1/2: RHIZOBIA-INDUCED CLE1/2.

Figure modified from Wang et al., (2020).

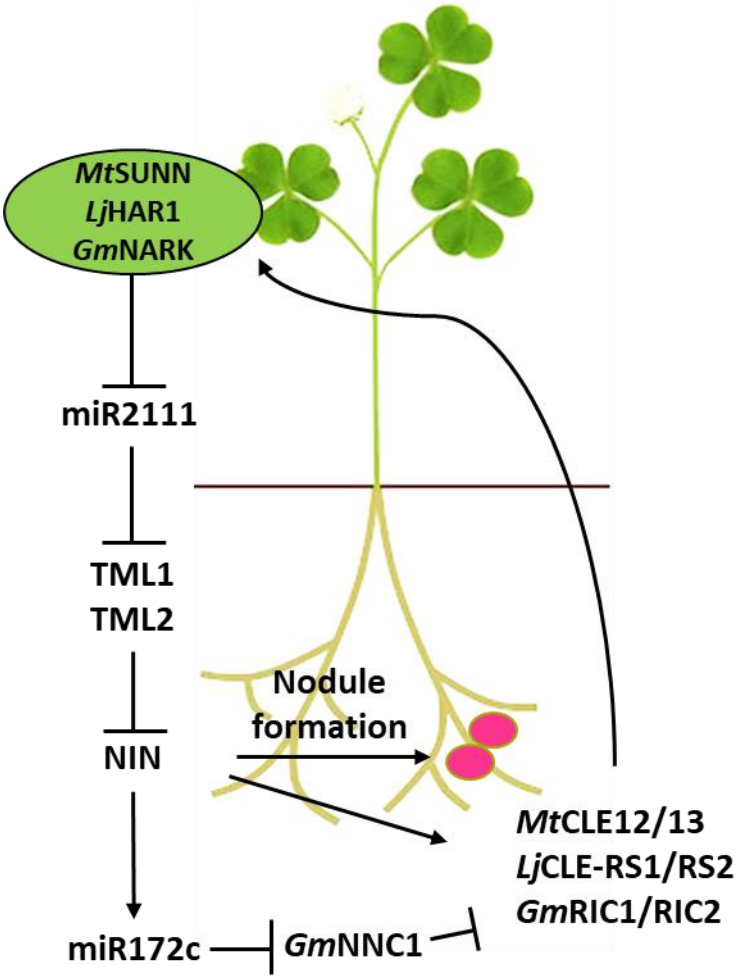
*Mt*SUNN
*Lj*HAR1
*Gm*NARK
miR2111
TML1
TML2
NIN
miR172c
*Gm*NNC1
Nodule
formation
*Mt*CLE12/13
*Lj*CLE-RS1/RS2
*Gm*RIC1/RIC2

processing, these small functional CLE peptides translocate from the root to the shoot through the xylem (Okamoto et al. 2013), where they bind to a specific homodimeric or heterodimeric receptor complex that includes HYPERNODULATION ABERRANT ROOT FORMATION1 (HAR1) in *L. japonicus* (Krusell et al. 2002; Nishimura et al. 2002; Okamoto et al. 2013), SUPER NUMERIC NODULES (SUNN) in *M. truncatula* (Schnabel et al. 2005), or NODULE AUTOREGULATION RECEPTOR KINASE (NARK) in soybean (Searle et al. 2003). In *L. japonicus*, *Lj*CLE-RS2 binds to *Lj*HAR1, and the application of *Lj*CLE-RS2 peptide through the xylem was found to inhibit nodulation in wild-type but not in *har1* mutants, showing that the *Lj*HAR1 receptor kinase is required for regulating the AON pathway through *Lj*CLE peptide (Okamoto et al. 2013).

Recently, Gautrat et al. (2020) reported that the shoot-produced *Mt*miR2111 is involved in AON and negatively regulates its target genes, *TOO MUCH LOVE1* (*MtTML1*) and *MtTML2* to keep the plant susceptible to nodulation in *M. truncatula*. Moreover, *Gm*NIN was shown to directly target *GmRIC1* and *GmRIC2* to activate their expression, and NODULE NUMBER CONTROL1 (*Gm*NNC1) inhibits the expression of these two genes by interacting with *Gm*NIN. In addition, *Gm*NINa can also activate *GmRIC1* and *GmRIC2* by activating miR172c, which silences *GmNNC1* via transcript cleavage and reduces the suppressive effect of *Gm*NNC1 on *GmRIC1* and *GmRIC2* (Wang et al. 2019).

1.3 Root architecture

As the underground organ of terrestrial plants, roots are important living components that, in most cases act as an anchor that holds the plant upright, absorb water and minerals, and transport them to stems for plant growth and development. In addition, roots are a source

of phytohormones, such as cytokinins, and specialized metabolites, such as flavonoids, terpenoids, and isoflavonoids, that are involved in various aspects of plant adaptation to the surrounding environment (Jogawat et al. 2021; Takahashi and Shinozaki 2019). Vigorous and deep rooting systems are in most cases important for plant productivity and survival, and therefore optimization of root system architecture can be important for plant survival, because of its potential to reduce soil erosion (Reubens et al. 2007), improve nutrient cycling, enhance water use efficiency (Lynch 2007), and improve resistance to stress (Castonguay et al. 2006; Khan et al. 2016). Root system architecture is controlled at the genetic level, differs across species, and is highly variable even within a species (Osmont et al. 2007).

While crop breeding programs have focused on increasing yield by improving aboveground plant traits, the roots ('the hidden half' of the plant) have fallen by the wayside (Den Herder et al. 2010). Given the fact that roots play an important role in the establishment and performance of plants, the second 'green revolution' has been focused on crop yield improvement through exploiting and modifying root architecture systems (Lynch 2007). Root system optimization in crops may enable plants to overcome the challenges posed by their sessile status, and to increase stress tolerance (Koevoets et al. 2016). A deep rooting system helps plants to access water and nutrients stored deep in the soil, and hence allowing for plant production and survival under unfavorable growth condition (Comas et al. 2013).

1.4 Regulation of root architecture and nodulation

In legumes, depending on the environmental conditions, two types of lateral organs determine root system architecture, lateral roots and nitrogen fixing root nodules. Both root nodule and lateral root organogenesis involve divisions of cells located close to the root apical meristem (Bensmihen 2015; Crespi and Frugier 2008; Herrbach et al. 2014). Nodules are induced by common environmental cues such as low nitrogen-availability conditions in the presence of the specific *Rhizobium* spp. in the rhizosphere (Reid et al. 2011b). In legumes, nitrogen is utilized through assimilation regardless of whether it enters the plant as nitrate and ammonium from soil, or by fixation of atmospheric nitrogen (Murray et al. 2017). Nitrate is absorbed by the root from the external environment using two nitrate transporters, NITRATE TRANSPORTER1 (NRT1) and NRT2, which function as low affinity and high affinity nitrate transporters, respectively (Tsay et al. 2007). The nitrate imported into the cells is sequentially reduced into nitrite by NITRATE REDUCTASE (NR) and into ammonium by NITRITE REDUCTASE (NiR) (Glass et al. 2002). Ammonium is assimilated into amino acids through the glutamine synthase (GS) and glutamine oxoglutarate aminotransferase (GOGAT) cycle (Potel et al. 2009).

Serving as an important signal to regulate gene expression, nitrate also impacts on root architecture, as the initiation, formation and development of lateral roots depend on nitrate availability (Sun et al. 2017). In addition, root architecture is the basis of plant growth as it controls the uptake and utilization of nutrients and affects the plant's growth and biomass (Zhao et al. 2018). In general, lateral root growth is dually regulated by nitrate availability, including stimulatory and inhibitory effects of nitrate on lateral root development. While

nitrate stimulates lateral root growth (Linkohr et al. 2002; Zhang and Forde 1998), too high nitrate concentration has an inhibitory effect on lateral root growth (Tian et al. 2009; Zhang and Forde 1998). Factors that contribute to the regulation of lateral organ formation include mobile phytohormones (Fukaki and Tasaka 2009), microRNAs (miRNAs) (Chen 2012), and proteins (Murphy et al. 2012) .

1.5 The regulatory role of microRNAs in root development and nodulation

MicroRNAs (miRNAs) are small (~22 nt in length), endogenous, non-coding RNAs that have a central role in regulating gene expression at the post-transcriptional level in a sequence-specific manner by either transcript cleavage or inhibition of mRNA translation (Sun 2012). miRNAs are processed primarily from larger precursor RNAs by endonuclease DICER-LIKE 1 (DCL1) (Bernstein et al. 2001; Rogers and Chen 2013). The mature miRNA/miRNA duplexes are processed with a 3' two-nucleotide overhang that are methylated by HUA ENHANCER 1 (HEN1) to prevent degradation (Yu et al. 2005). The processed miRNA/miRNA duplexes are then exported into the cytoplasm by EXPORTIN 5 (XPO5) (Muqbil et al. 2013) and recruited by a RNA-INDUCED SILENCING COMPLEX (RISC) in the cytoplasm. The miRNA duplex is then unwound and only the leading strand is kept to target genes in a sequence specific manner by transcript cleavage or by translation inhibition while the second strand is degraded in the cytoplasm (Felekkis et al. 2010; Yu et al. 2017) **(Figure 1.5)**. By targeting major transcription factors, miRNAs control essential processes, including stress responses, phytohormone regulation, organ morphogenesis, and developmental process (Liu et al. 2018; Ma et al. 2022). Regulatory

Figure 1.5 Mechanism of miR156 post-transcriptional gene regulation

The endonuclease DCL1 creates a short miRNA-duplex with two-nucleotide 3' overhangs that are exported to the cytoplasm via EXPORTIN 5. The miRNA/miRNA duplex binds to RISC endonucleases in the cytoplasm and the leading strand is used as a guide to target transcripts (including *SPLs*) in a sequence-specific manner, resulting in the silencing of downstream complementary mRNA targets through cleavage or translational repression. DCL1: DICER-LIKE1; RISC: RNA-INDUCED SILENCING COMPLEXES; SPL: SQUAMOSA-PROMOTER BINDING PROTEIN-LIKE; XPO5: EXPORTIN 5. *SPL* and SPL downstream target genes are indicated with green and purple boxes respectively. Diagram is created with BioRender.com.

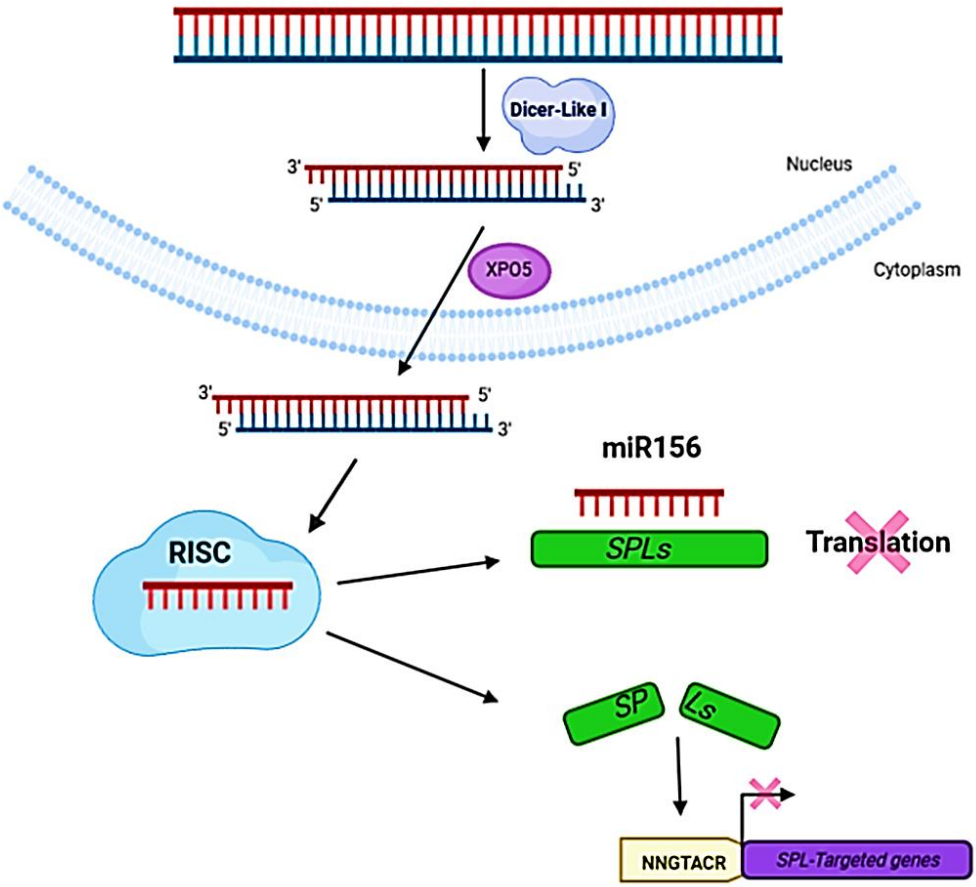
Dicer-Like I
3'
5'
5'
3'
Nucleus
XPO5
Cytoplasm
3'
5'
5'
3'
miR156
RISC
SPLs
Translation
SP
Ls
NNGTACR
SPL-Targeted genes

miRNAs can influence nitrate-regulated root architecture. For example miR167 and its target AUXIN RESPONSE FACTOR 8 (ARF8) play an important role in controlling lateral root growth in response to nitrate in Arabidopsis (Gifford et al. 2008; Wu et al. 2006). In addition, miR172 positively regulates nodulation in legumes, as shown in soybean, whereas overexpression of miR172 resulted in plants with increased nodule number and nitrogen fixation (Yan et al. 2013). Nova-Franco et al. (2015) also showed similar results in common bean (*Phaseolus vulgaris*). The miR2111/TML module is also involved in regulating nodulation in legumes, as overexpression of miR2111 or mutations in *TML* caused hyper-nodulation in *L. japonicus* (Tsikou et al. 2018).

1.6 The role of miR156 in regulating root architecture, nodulation and nitrogen fixation

The miR156/SPL regulatory module plays a fundamental role in the regulation of a range of plant growth and development processes, such as transition from vegetative to reproductive stages, fertility, and response to stresses (Cardon et al. 1999; Wang and Wang 2015; Xu et al. 2016). Previously, it was shown that overexpression of *miR156* in alfalfa (miR156-OE) resulted in plants displaying delayed flowering, improved vegetative and root growth, enhanced branching, and caused an increase in number of nodes, collectively culminating in an overall improvement in biomass yield and quality (Aung et al. 2015). miR156-OE plants were also shown to have increased ability to survive heat (Matthews et al. 2019), salinity (Arshad et al. 2017b) and drought stress (Arshad et al. 2017a; Feyissa et al. 2019). Moreover, overexpression of *miR156* was shown to play a role in nodulation in legume plants. A previous study found that overexpression of miR156 enhanced nodule

numbers and nitrogenase activity in alfalfa (Aung et al. 2017), but miR156s appear to play species-specific roles in different leguminous plants, as a reduction in nodulation was reported in other studies for miR156 overexpression plants. For example, when *GmmiR156* was overexpressed in soybean , it repressed nodulation through its negative regulation of *Gm*miR172 (Yan et al. 2013). Similarly in *L. japonicus*, *LjmiR156* was found to reduce nodule numbers (Wang et al. 2015). More recently, Yun et al. (2022) reported that the miR156-SPL9 regulatory system in soybean acts as an upstream master regulator of nodulation by targeting and regulating the transcript levels of nodulation genes in soybean. It has been shown that overexpressed and reduced *GmmiR156* resulted in increased expression of *GmNINa* and *GmENOD40-1* (nodulation markers) (Yun et al. 2022).

1.7 SPL transcription factors and their role in the regulation of root architecture, nodulation and nitrogen fixation

miR156 targets a number of *SPL* genes for post-transcriptional silencing in various plant species (Feyissa et al. 2021; Gao et al. 2016; Preston and Hileman 2013). The SPLs constitute a diverse family of transcription factors characterized by a highly conserved SQUAMOSA PROMOTER BINDING PROTEIN (SBP) domain, which is typically 76 amino acids long (Klein et al. 1996; Yamasaki et al. 2004). SPLs are involved in binding to a consensus DNA binding site, known as the SPL Binding Domain (SBD), with a 'NNGTACR' core consensus sequence, where N is any nucleotide but identical sequentially, and R is either A or G. (Birkenbihl et al. 2005; Yamasaki et al. 2006). While 76 amino acid SBP domain is required for binding to the target sequences in downstream genes, this binding is also determined by other factors. In alfalfa, 11 out of 16 *SPLs* (*SPL2*,

SPL3, *SPL4*, *SPL6*, *SPL7a*, *SPL8*, *SPL9*, *SPL11*, *SPL12*, *SPL13* and *SPL13a*) are repressed by miR156 via transcript cleavage (Aung et al. 2015; Feyissa et al. 2021; Gao et al. 2016; Ma et al. 2021). Of the known SPLs in alfalfa, SPL13 has been well characterized, and has been shown to regulate flowering time and vegetative development, with increased lateral shoot branching in *SPL13*-silenced alfalfa plants (Gao et al. 2018b). SPL13 also negatively regulates alfalfa's tolerance to drought, heat and flooding (Arshad et al. 2017a; Feyissa et al. 2021; Matthews et al. 2019). Hanly et al. (2020) showed that SPL9 also is a negative regulator of drought stress in alfalfa. Downregulation of *SPL9* led to enhanced drought tolerance in transgenic alfalfa, as *SPL9*-RNAi alfalfa showed less leaf senescence and more relative water content under drought conditions compared to WT plants (Hanly et al. 2020). Furthermore, Gou et al. (2018) reported that SPL8 has a negative role in regulating salt and drought stress in alfalfa, as plants with downregulated *SPL8* showed enhanced salt and drought tolerance and increased biomass yield (Gou et al. 2018). Alfalfa plants with CRISPR knockdown *SPL8* also exhibited phenotypic changes and enhanced tolerance to drought (Singer et al. 2021). In Arabidopsis, SPL9 is a potential nitrate regulatory hub and may target the primary nitrate-responsive genes (Krouk et al. 2010). Transcript levels of nitrate-responsive genes, *AtNiR*, *AtNR2* and *AtNRT1.1* significantly increased in response to nitrate in *AtSPL9* overexpressing transgenic Arabidopsis plants (Krouk et al. 2010). In soybean, *GmSPL9* positively regulates nodulation by targeting the *GmNINa*, *GmENOD40-1* and *GmmiR172* during nodulation (Yun et al. 2022). In Arabidopsis, *AtSPL3*, *AtSPL9*, and *AtSPL10* are involved in the regulation of Arabidopsis lateral root development, with *At*SPL10 playing the most dominant role (Yu et al. 2015b). Gao et al.

(2018c) reported that *At*SPL10 directly regulates *AGAMOUS-like MADS box protein 79* (*AtAGL79*) expression by binding to its promoter.

1.8 Role of MADS box proteins in the regulation of root architecture

The MADS (MINICHROMOSOME MAINTENANCE1/AGAMOUS/DEFICIENS/ SERUM RESPONSE FACTOR) box proteins are a family of transcription factors that participate in many aspects of plant development and morphogenesis (Gramzow and Theissen 2010). Although MADS-box proteins were initially found to be involved in floral organ speciation (De Folter et al. 2006; Dong et al. 2013; Huang et al. 2017; Michaels et al. 2003), they recently became a focus of research into the genetic regulation of root development (reviewed by Alvarez-Buylla et al. 2019). For example, ANR1 (ARABIDOPSIS NITRATE REGULATED1) was the first MADS-box transcription factor shown to stimulate lateral root development in the presence of high nitrate concentrations (Gan et al. 2012). *AGL21*, a MADS-box gene, which is highly expressed in lateral root primordia, was found to control lateral root development by regulating auxin biosynthesis genes in Arabidopsis (Yu et al. 2014). In rice, *OsMADS25*, an *ANR1*-like gene, positively regulates lateral and primary root development by promoting nitrate accumulation and increasing the expressions of nitrate transporter genes at high nitrate concentrations (Yu et al. 2015a). In common bean, *PvAGL21* is expressed in nodules, and its expression is higher in roots compared to pods, seeds and stems (Íñiguez et al. 2015). These observations link AGLs to nodulation- and root architecture-related traits in plants.

Collectively, while previous research has shown that miR156 regulates nodulation and nitrogen fixation in alfalfa (Aung et al. 2017); research has yet to be conducted to determine

the biochemical and molecular mechanisms underpinning these effects, or which of the SPL proteins regulate nitrogen traits in this plant.

1.9 Hypothesis and objectives of the study

I hypothesize that miR156 effects on root architecture, nodulation, nitrogen fixation and abiotic stress are mediated by specific SQUAMOSA-PROMOTER BINDING PROTEIN-LIKE (SPL) transcription factors, specifically SPL12, and other SPL-regulated downstream genes.

Objectives: The main purpose of this research was to investigate the role of SPL12 and its downstream target genes in root architecture, nodulation and nitrogen fixation. The specific objectives were:

Short-term objectives

1. Determining the role of *SPL12* in root architecture, nodulation, and nitrogen fixation.
2. Investigating whether *AGL6* and *AGL21* are downstream target genes of SPL12.
3. Investigating the role of SPL12 and AGL6 in nodulation under osmotic stress.
4. Investigating the role of SPL12 in nitrate inhibition of nodule formation.
5. Mutating *SPL13* by CRISPR-Cas9 editing to improve stress tolerance and increase forage yield in alfalfa.

Long-term objective

The long-term objective of this project is to make a significant contribution to our knowledge of the mechanisms of actions of miR156 and SPLs in root architecture, nodulation, nitrogen fixation activity, and stress tolerance in alfalfa, and to generate molecular tools for use in promoting resilience and productivity in this crop and potentially others.

Chapter 2

2 Materials and Methods

2.1 Plant material

2.1.1 Alfalfa plants

Alfalfa clone N4.4.2 (Badhan et al. 2014) was obtained from Daniel Brown (Agriculture and Agri-Food Canada, London, ON, Canada) and was used as the wild-type (WT) genotype. Plants overexpressing miR156 (miR156-OE) at different levels (A11, A11a and A17) were generated by Dr. Hannoufa's group in a previous study (Aung et al. 2015). WT and transgenic alfalfa plants were grown under greenhouse conditions at 21-23°C, 16 hrs light/8 hrs dark, light intensity of 380–450 W/m2 (approximately 500 W/m2 at high noon time), and a relative humidity of 56% for the duration of all experiments. Because of the obligate outcrossing nature of alfalfa, WT and transgenic alfalfa plants were propagated by rooted stem cuttings to maintain the genotype throughout the study. The stem cuttings, containing the same number of nodes, were grown in vermiculite for three weeks. Rooted cuttings were then inoculated and used in phenotypic characterization, osmotic stress and nitrate treatment experiments.

2.1.2 *Lotus japonicus* plants

Seeds of wild-type Gifu (Handberg and Stougaard 1992) and mutant *L. japonicus* plants were scarified using sand paper and surface-sterilized following the previously established

methods (Szczyglowski et al. 1998). Briefly, seeds were subjected to two consecutive one-minute washes with 0.1% (w/v) sodium dodecyl sulfate (SDS) in 70% (v/v) ethanol and 0.1% (w/v) SDS in 20% (v/v) bleach. Sterilized seeds were then rinsed with sterile Milli-Q water 10 times and allowed to imbibe overnight. Imbibed seeds were transferred to Petri dishes containing six layers of sterilized Whatman filter paper moistened with sterilized Milli-Q water and allowed to germinate for seven days at 23°C, under 16 hrs /8 hrs light/dark regime.

2.2 Generation of vector constructs and plant transformation

2.2.1 *SPL12*-RNAi and *AGL6*-RNAi

SPL12-RNAi (RNAi12-7, RNAi12-24 and RNAi12-29), and *AGL6*-RNAi (L9, L13A and L13B) genotypes were generated to investigate the role of SPL12 and AGL6 in root architecture and nodulation. For *SPL12*-RNAi and *AGL6*-RNAi, 250 bp and 256 bp fragments, respectively, were amplified from alfalfa cDNA using primers RNAiMsSPL12-F2 and RNAiMsSPL12-R2 (*SPL12*-RNAi), and MsAGL6-RNAi-F2 and MsAGL6-RNAi-R2 (*AGL6*-RNAi) (**Table S1**) and cloned into pENTR entry vector (Invitrogen, Carlsbad, CA, USA). After PCR screening and analysis by Sanger sequencing, LR reactions were performed for RNAi constructs to recombine the fragments into the pHELLSGATE12 (RNAi) destination vector (Helliwell and Waterhouse 2003) using the Gateway cloning system (Thermo Fisher Scientific, Mississauga ON). The pHELLSGATE12 (RNAi) vectors were transferred into *E. coli* by the heat shock method (Froger and Hall 2007) and the presence of the insert was confirmed by Sanger sequencing

of the plasmid DNA. Subsequently, RNAi constructs were transferred into *Agrobacterium tumefaciens* (LBA4404) by heat shock (Höfgen and Willmitzer 1988). *A. tumefaciens* strains were then used in the transformation of alfalfa N.4.4.2 germplasm as described below (see Section 2.3).

2.2.2 *35S::SPL12* and *35S::SPL12m-GFP*

To generate *SPL12* overexpression constructs, the full-length coding region of *SPL12* (1314 bp) was amplified from alfalfa cDNA using primers OEMsSPL12 F and OEMsSPL12 R (**Table S1**), and then cloned into the pMDC32 (Curtis and Grossniklaus 2003) vector using Gateway cloning (Thermo Fisher Scientific, Mississauga ON). For *35S::SPL12m-GFP* construct, the *Mlu*I-SPL12-*Spe*I fragment was synthesized with a mutated miR156 recognition site based on Wei et al. (2012) (**Figure 2.1**). Each mutation changes a single nucleotide and causes no change in the SPL12 amino acid sequence, but introduces changes into the predicted miR156 binding site to prevent complementary binding and subsequent cleavage. The fragments were then cloned into the pGreen-GFP (Yu et al. 2004) vector using a T4 ligation method according to manufacturer's description (Thermo Fisher Scientific, Mississauga ON). The vectors were transferred into *E. coli* using the heat shock method (Froger and Hall 2007) and the presence of the insert was confirmed by Sanger sequencing of plasmid DNA. Subsequently, these overexpression constructs were transformed into *A. tumefaciens* (LBA4404 or EHA105) by heat shock (Höfgen and Willmitzer 1988), and the resulting strains were then used in the transformation of alfalfa N.4.4.2 germplasm as described below (see Section 2.3).

Figure 2.1 Mutagenesis of *SPL12* to prevent miR156 complementarity

The seven point mutations (red) were introduced into the *SPL12* coding sequence within the region complementary to miR156 to produce *SPL12m*. Asterisks indicate mismatches between miR156 and the mRNA sequence (red: between miR156 and *SPL12m* mRNA sequence; black: between miR156 and *SPL12m* and *SPL12* mRNA sequence).

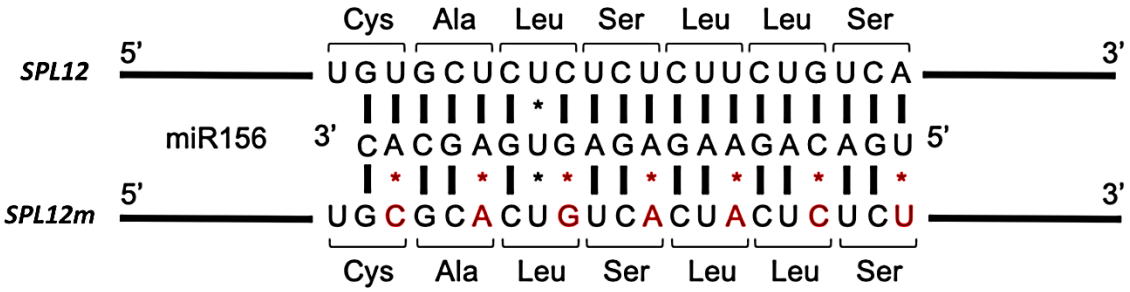
Cys Ala Leu Ser Leu Leu Ser
SPL12
5'
3'
UGUGCUCUCUCUCUUCUGUCA
miR156
3'
CACGAGUGAGAGAAGACAGU
5'
SPL12m
5'
3'
UGCGCACUGUCACUACUCUCU
Cys Ala Leu Ser Leu Leu Ser

2.2.3 sgRNA design and construction of sgRNA-Cas9 expression vector

The sgRNAs, 20 nt sequences that flank a protospacer-adjacent motif (PAM) sequence, were designed using the web-based tool CRISPR-P 2.0 (Liu et al. 2017) to target three specific sites in the exons of the *SPL13* gene in alfalfa (**Figure S1**). Based on the scoring system in the web application tool CRISPR-P (Liu et al. 2017), three sgRNAs were selected that possessed the highest ON-target scores (Doench et al. 2014), the lowest OFF-target scores and OFF-target numbers (Doench et al. 2016), and a GC content between 30 and 80% (Doench et al. 2014; Liang et al. 2016).

The chosen sgRNAs, considering the secondary structure, also had to have more criteria including no more than 12 total complementary base pairs with the scaffold sequence, no more than six internal base pairs, and an intact secondary structure (a repeat and anti-repeat region, a stem loop 2, and a stem loop 3) except for stem loop 1 (Liang et al. 2016). The three guide RNAs met these criteria. The *MtU6*:sgRNA fragments containing a *M. truncatula U6* promoter (*MtU6*) and each guide RNA, flanked by In-Fusion reaction adaptors were synthesized by Bio Basic Inc. and cloned into the linearized destination vector pFGC5941 (Meng et al. 2017) digested with *Xba*I, using the In-Fusion cloning system (Takara Bio Inc.) protocol. The pFGC5941 binary vector, which expresses Cas9 and guide RNA, was transferred to *E. coli* using the heat shock method (Froger and Hall 2007) and plasmid DNA was extracted from positive clones and sequenced to confirm the presence of the insert. Plasmid DNA was then introduced into *A. tumefaciens* (EHA 105) by heat shock (Höfgen and Willmitzer 1988), and the resulting *A. tumefaciens* strain was

then used in the transformation of alfalfa N.4.4.2 germplasm as described below (see Section 2.3).

2.3 Alfalfa transformation and screening for alfalfa transformants

Alfalfa transformation by *A. tumefaciens* was carried out according to Tian et al. (2002) with slight modifications. Tissue culture material was kept in a growth chamber at 26°C with a photoperiod of 16 hrs /8 hrs light/dark for all stages. Leaves and petioles (~0.8 cm) from *M. sativa* N4.2.2 plants were used in this study by first pre-culturing them for two days on basal SH2K medium in a growth chamber (the ingredients for all of media are listed in **Table S2**). For the co-cultivation stage the explant fragments were infected with *A. tumefaciens* cells suspended in liquid co-cultivation medium supplemented with 20 μM acetosyringone, by soaking the explant fragments in *A. tumefaciens* culture for 10 min. The explant fragments were then blot-dried on sterile filter paper, placed on Basal SH2K media supplemented with 20 μM acetosyringone, and incubated for five days in the dark to facilitate *A. tumefaciens* infection. After rinsing in Basal SH2K media, the infected tissues were transferred to callus induction medium (basal SH2K medium, 300 mg/L timentin) to induce callus formation for two weeks. The transformed calli were then selected by transferring calli to callus induction medium containing the appropriate antibiotics; 50 mg/L hygromycin B was used to select for *35S::SPL12*, 10 mg/L glufosinate ammonium for *SPL13*-CRISPR, and 50 mg/L kanamycin for *SPL12*-RNAi, *AGL6*-RNAi and *35S::SPL12m-GFP*, respectively. After 10 days, the antibiotic concentrations were increased to 75 mg/L for hygromycin B and kanamycin and to 15 mg/L for glufosinate ammonium. Embryo induction was then initiated by transferring calli to embryo induction

medium supplemented with the same antibiotic concentration that was used in the second callus selection phase, and incubated for 6-8 weeks. During these periods, the calli were transferred to fresh media every two weeks to ensure the media were fresh to facilitate embryo development. Green embryos were subsequently transferred to embryo germination and plant development media containing the same antibiotic concentration used in the second callus selection phase, and kept on embryo germination until the well-formed cotyledons were observed. Following development of plantlets, and when roots formed, excess media were rinsed and rooted plants were transferred to 10.2 cm square plastic pots filled with BX Mycorrhizae (PRO-MIX®, Smithers-Oasis North America) soil mix and covered with a magenta box for a week. These tissue culture plantlets were placed in the greenhouse (16 hrs light/8 hrs dark, 56 relative humidity, 23°C). Finally, acclimatized plants were transferred to 22.2 cm pots, and subsequently used to propagate alfalfa for different experiments.

Prior to characterization, regenerated alfalfa plants derived from transformation with overexpression and RNAi constructs were analyzed by PCR to determine the presence of respective transgenes in the genome. For that, genomic DNA (gDNA) from leaves of putative *SPL12*-RNAi, *AGL6*-RNAi, *35S::SPL12*, *35S::SPL12m-GFP* and *SPL13*-CRISPR alfalfa was extracted according to the ChargeSwitch gDNA Plant Kit (Thermo Fisher Scientific) protocol and used directly for PCR.

The presence of the transgene in *SPL12*-RNAi and *AGL6*-RNAi alfalfa genotypes was confirmed by PCR of gDNA using a *35S* promoter- and pHellgate12 intron-specific primers (pHELLGATE12intron) (**Table S1**). Similarly, *SPL12* overexpression alfalfa

genotypes (*35S::SPL12* and *35S::SPL12m-GFP*) were screened by PCR using a *35S* promoter- and gene-specific primers (OEMsSPL12-R) (**Table S1**). Positive transgenic plants were then analyzed for *SPL12* and *AGL6* transcript abundance by RT-qPCR using primers LA-MsSPL12-F1 and LA-MsSPL12-R1 (*SPL12*), and qMsAGL6-1F and qMsAGL6-1R (*AGL6*) (**Table S1**).

The presence of the transgene in the transgenic *SPL13*-CRISPR alfalfa genotypes was confirmed by PCR amplification of genomic DNA using *SpCas9* gene primers LH_Cas9_F1 and LH_Cas9_R1 (**Table S1**).

2.4 Identification of *spl12* mutant lines in *L. japonicus*

The LORE1 insertional mutation alleles *spl12-1* (line no. 30088823) and *spl12-2* (line no. 30080688) were identified from the *L. japonicus* LORE1 retrotransposon mutant resource (https://lotus.au.dk/). For all the selected LORE1 insertion lines, the R3 generation seeds (3rd generation of plants derived from tissue culture) were acquired from the Lotus Base. Seeds of the LORE1 insertion lines for each allele were germinated and the resulting plants were genotyped by PCR. PCR-based genotyping was used to identify homozygous and heterozygous plants for all LORE1 insertion lines. gDNA from leaves was isolated according to the ChargeSwitch gDNA Plant Kit (Thermo Fisher Scientific) protocol and used directly for PCR. PCR was performed using both the gene- and LORE1-specific primers (**Table S1**), following an established procedure (Urbański et al. 2012).

2.5 Nodulation test

2.5.1 Nodulation test in Alfalfa

Root development from the stems was determined for transgenic and WT alfalfa plants grown in vermiculite at 13 days after initiation of vegetative propagules by determining the number of main roots generated from stem cuttings.

For the nodulation test, the number of nodules was determined at 14 and 21 days after inoculation (dai) with *S. meliloti* Sm1021. To eliminate potential microbial contamination, equipment, vermiculite and water used in the experiment were all sterilized. *S. meliloti* Sm1021 strain was cultured on Yeast Extract Broth agar (Beringer 1974) for 2 days at 28°C. A single colony was then inoculated in liquid TY medium and incubated at 28°C to an optical density OD_{600} nm of 1.5. The 3-week-old rooted stems were inoculated by applying 5 mL of the bacterial suspension or sterilized water (non-inoculated control) into each pot containing rooted alfalfa stem. The plants were then kept on a bench in the greenhouse and watered with distilled water once a week. The total number of nodules from each stem was counted two and three weeks after inoculation with *S. meliloti*. At least 10 biological replicates per genotype were used, and the experiment was repeated three times.

2.5.2 Nodulation test in *Lotus japonicus*

Under sterile conditions, seven-day-old seedlings of WT and mutant *L. japonicus* were transplanted into 10.2 cm square plastic pots containing vermiculite that was supplemented

with Murashige & Skoog Modified Basal Salt Mixture without Nitrogen (PhytoTech) and allowed to grow under greenhouse conditions of 16 hrs light/8 hrs dark at 23°C with 56% humidity. Seven days after transplanting, the seedlings were inoculated using *Mesorhizobium loti* strain NZP2235. The seedlings were inoculated by applying 5 mL of the bacterial suspension or sterilized water (non-inoculated control) and allowing growth to proceed for two and three additional weeks. The total number of nodules from each seedling was counted two and three weeks after inoculation with the *M. loti*. Twenty biological replicates per genotype were used, and the experiment was repeated twice.

2.6 Evaluation of nitrogen fixation by nitrogenase activity assay

To determine the rate of nitrogen fixation activity in *SPL12*-RNAi and WT alfalfa plants, the nitrogenase activity was tested by measuring the conversion of acetylene to ethylene (Dilworth 1966; Aung et al. 2017). Nitrogenase activity was determined in nodulated roots at 14 dai. For this, three-week-old rooted stems were transplanted into 10.2 cm square plastic pots containing soil (three rooted plants per pot), followed by inoculation with *S. meliloti* as described in section 2.5.1. For the un-inoculated control, sterilized MilliQ water was used instead of rhizobia. Two weeks after inoculation, roots from *SPL12*-RNAi and WT alfalfa plants were harvested and the acetylene reduction assay (ARA) was conducted using a Hewlett Packard 5890 Series II gas chromatograph (GC) (Agilent Technologies) with flame ionization detection (FID). To measure the amount of ethylene, nodulated roots were sealed in 20 mL glass vials with rubber lids. Air (10 µL) was then removed from the vial and replaced with 10 µL of acetylene gas to create an acetylene atmosphere in the vial. The vial was incubated for 1 hr at room temperature, and ethylene was quantified by GC

as described in Aung et al. (2017). At least 10 biological replicates per genotype were used, and the experiment was repeated twice. The amount of ethylene released from acetylene reduction was then calculated and expressed as nmol/plant per hr.

2.7 Nitrate treatment

To explore if SPL12-related regulation of nodulation is affected by nitrate, the nodulation test was performed upon treatment with this nutrient. WT and *SPL12*-RNAi alfalfa stem cuttings were grown on vermiculite for 21 days, inoculated with *S. meliloti* Sm1021 as described above (Section 2.5.1), and treated with KCl or KNO_3. For this, the 21-day-old inoculated transgenic and WT plants were watered with 3, 8, or 20 mM KNO_3 or KCl twice a week for two and three weeks. The entire experiment was repeated twice under the same growth and nitrate treatment conditions to test the reproducibility of the results. Effects on nodulation were studied by counting the number of active (pink) nodules as described in Section 2.5.1.

To investigate whether treatment with KNO_3 affects expression of *SPL12* and *AGL21* genes, WT and *SPL12*-RNAi alfalfa plants were grown on vermiculite for 21 days, then the plants were transferred to Murashige & Skoog Modified Basal Salt Mixture without Nitrogen (PhytoTech) liquid media and left overnight under room temperature. For the nitrate signaling test, the samples were treated with 20 mM KNO_3 for 0, 5, and 24 hrs, then roots were collected and flash frozen in liquid nitrogen and stored at -80°C for later transcript analysis of *SPL12* and *AGL21*.

2.8 Mannitol treatment

To investigate whether SPL12 affects nodulation when plants are grown under osmotic stress, WT, *SPL12*-RNAi and *AGL6*-RNAi alfalfa plants were grown on vermiculite for 21 days, and then inoculated with *S. meliloti* Sm1021 for two days, followed by treatment with mannitol (to mimic osmotic stress) (Vera-Estrella et al. 2004). For the mannitol treatment, 23-day-old inoculated WT and transgenic plants were watered with 400 mM mannitol or distilled water once a week for two and three weeks. The below ground phenotypic parameters were measured according to Aung et al. (2017). The phenotypes included in the characterization were the number of main roots, lateral roots, and root length. The roots directly emerging from the stem were considered as main roots while those that emerged from the main roots were counted as lateral roots. Root length was determined as the length of the longest root. The entire experiment was repeated twice under the same growth and osmotic stress conditions to test the reproducibility of the results. Root samples were harvested from *SPL12*-RNAi and WT plants under osmotic and control conditions and were flash frozen in liquid nitrogen and kept at -80°C for later transcript analysis of *SPL12*, *AGL21*, *AGL6*, *CLE13*, *SULTR3.4*, *SULTR3.5*, *GSH* and *WD40-1* (**Table S1**).

2.9 RNA extraction, reverse transcription-real time quantitative PCR

Transcript levels of different genes of interest in alfalfa tissues were determined by reverse transcription-real time quantitative PCR (RT-qPCR). For that, different alfalfa tissues, such as stems, leaves and roots were collected and flash frozen in liquid nitrogen and stored in a -80°C freezer until used for RNA extraction. Approximately 100 mg fresh weight was

used for total RNA extraction using the RNeasy Plant Mini-prep Kit (Qiagen, Hilden, Germany, Cat # 1708891) for leaf and stem tissues, and the Total RNA Purification Kit (Norgen Biotek, Canada, Thorold, Cat # 25800) for root tissues. Tissue was homogenized using a PowerLyzer®24 bench top bead-based homogenizer (Cat # 13155) according to the manufacturer's manual. Approximately 500 ng of Turbo DNase (Invitrogen, Cat # AM1907)-treated RNA was used to generate cDNA using the iScript cDNA synthesis kit (Bio-Rad, Cat # 1708891). Transcript levels of the target genes were analyzed by RT-qPCR using a CFX96 TouchTM Real-Time PCR Detection System (Bio-Rad) and SsoFast™ EvaGreen® Supermixes (Bio-Rad Cat # 1725204). Each reaction consisted of 2 µL of cDNA template, 0.5 µL forward and reverse gene-specific primers (10 µM each) (**Table S1**), 5 µL SsoFast Eva green Supermix and topped with to 10 µL ddH_2O. Each sample was analyzed in three or four biological replicates, and each biological replicate was tested using three technical replicates. Transcript levels were analyzed relative to three reference genes: *CYCLOPHILIN* (Cyclo) (Guerriero et al. 2014), *β-actin* (*ACTB*) (Castonguay et al. 2015) and *ACTIN DEPOLYMERIZING FACTOR* (*ADF*) (Castonguay et al. 2015; Guerriero et al. 2014) (**Table S1)**.

2.10 Next Generation RNA sequencing transcriptome analysis

To determine global changes in gene transcript levels due to *SPL12* silencing, about 5 cm of root tips from WT and two *SPL12*-RNAi genotypes (RNAi12-24 and RNAi12-29) were used for Next Generation RNA sequencing. Total RNA was extracted using the RNeasy PowerPlant Kit (Qiagen, Cat # 13500-50) and quantified using a NanoDrop 2000C (Thermo Scientific). RNA quality was assessed with the Agilent Bioanalyzer 2100 RNA

Nano chip (Agilent Technologies). Three biological replicates were used, and RNA libraries were constructed and sequenced on an Illumina NovaSeq6000 with 100 bp fragment pair end reads at Genome Quebec (Montreal, Canada) through a fee-for-service contract. RNA-seq raw data can be accessed from the National Center for Biotechnology Information, NCBI, BioProject PRJNA818300.

2.11 Analysis of differentially expressed genes and GO enrichment

RNAseq data were analyzed using published protocols (Trapnell et al. 2012) on Biocluster with Linux shell scripts. The published *M. truncatula* Mt4.0 V2 sequence (http://www.medicagogenome.org/downloads) was used as a reference genome as the full genome sequence of alfalfa had not been published by the time this research was carried out. Firstly, the Quality Control (QC) analyses were performed for all Raw Illumina pair-end reads using FastQC program (Andrews 2010). Raw sequence reads were then trimmed to obtain high quality reads (Q > 30), adapter sequences were removed and short reads dropped using custom Perl scripts. These high-quality reads were then mapped to the *M. truncatula* genome using TopHat (v2.0.10). TopHat output was then used as input files for Cufflink (v2.2.1) to detect differentially expressed genes (DEGs) between WT and *SPL12*-RNAi (Aung et al. 2017). Subsequently, DEGs were annotated and assigned to three major functional categories (biological process, molecular function, and cell component) using Reduced Visualization Gene Ontology (REVIGO) software (http://revigo.irb.hr/) as described in Supek et al. (2011). Venn diagrams were generated using the Venny tool (Oliveros 2007).

2.12 Phylogenetic tree construction

The phylogenetic tree was constructed based on an alignment of the MADS-box domain and using publicly available sequences of *M. sativa*, *M. truncatula* and Arabidopsis. Amino acids were aligned by visualization and nucleotides were subjected to ClustalW alignment analysis. The Phylogenetic tree was constructed using the neighbor-joining method of phylogenetic tree construction using MEGA7 (Kumar et al. 2016).

2.13 Southern blot analysis

To investigate the T-DNA insertion profiles in the *SPL12*-RNAi plants, Southern blot analysis was carried out using total genomic DNA. For that, genomic DNA was isolated using the CTAB method according to Murray and Thompson (1980). For Southern blot analysis, the method of Wang et al. (2015) was followed, in which about 20 µg of genomic DNA was digested overnight with *EcoR* I (Fermentas), size-separated on a 0.8% agarose gel, and transferred to a nylon membrane (ROCHE). A 250 bp fragment encompassing the *35S* promoter amplified from the *SPL12*-RANi construct using SPL12i-35S-F and SPL12i-35S-R primers (**Table S1**) was used as probe. The probe was labelled with digoxigenin (DIG) using a PCR DIG Probe Synthesis Kit (Roche, Mannheim, Germany)**.** Following cross-linking the DNA to the membrane, pre-hybridization was performed with incubation of the membrane in pre-hybridization buffer for 3-4 hrs at 65°C (all buffers are listed in **Table S3**). The membrane was then incubated with the probe in hybridization buffer overnight at 65°C with gentle shaking. After hybridization, the membrane was washed four times with wash buffer (**Table S3**), each time for 20-30 min to remove the un-

hybridized probe. After incubation in blocking buffer overnight, the membrane was incubated with 5 μL Anti-DIG antibody (Roche) in blocking buffer for 45 min to 1 hr with gentle agitation at room temperature. After washing with antibody wash buffer at room temperature, detection was performed according to manufacturer's instructions (CDPStar; Roche).

2.14 Extraction of SPL12-GFP fusion protein and Western blot analysis

To investigate the expression of SPL12-GFP at the protein level, Western blot analysis was carried out on crude protein extracted from fresh leaves of 30-day-old of *35S::SPL12m-GFP* alfalfa plants. The plant material was homogenized in 0.2 mL of protein extraction buffer (0.125 mM Tris, pH 6.8, 4% w/v SDS, 18% glycerol, 0.024% w/v bromophenol-blue, 1.43 M β-mercaptoethanol, 0.2% protease inhibitor). After centrifugation at 16,000 *g* for 15 min, the insoluble fraction was removed, and the supernatant (denatured protein) was separated on a 12% SDS PAGE gel. Separated proteins were then transferred onto a nitrocellulose membrane, which was then incubated with primary anti-GFP antibody (Abcam, ab290, Cambridge, MA) and secondary horseradish peroxidase (HRP)-conjugated goat antirabbit IgG (Abcam) antibody. The signals were developed using the Pierce ECL Western Blotting Substrate (Thermo Fisher Scientific, Waltham, MA).

2.15 ChIP-qPCR analysis

ChIP-qPCR analysis was used to determine the occupancy of SPL12 on promoters of candidate downstream genes that may be regulated by SPL12 to control nodulation. Shoot

tips of alfalfa plants overexpressing *SPL12* tagged with *GFP* driven by the *35S* promoter (*35S::SPL12m-GFP*) were used as materials for ChIP-qPCR analysis, which was performed based on a previously described protocol (Gendrel et al. 2005), with minor modifications, using the Chromatin Immunoprecipitation Assay kit (Lot:2382621, Millipore, Billerica, MS). Briefly, 1 g of shoot tips from WT and *35S::SPL12m-GFP* plants were collected and fixed with 1% formaldehyde under vacuum for 20 min. The reaction was stopped by adding 0.125 M glycine, and the fixed tissues were ground in liquid nitrogen. Powdered tissues were homogenized with 30 mL of pre-chilled Extraction Buffer 1 (Extraction reagents and buffers are listed in **Table S4**) and incubated for 10 min on ice, then the crude extract was filtered through two layers of Miracloth (Millipore, Canada). The filtrate was centrifuged at 3000*g* for 20 min and the supernatant was discarded while the pellets were re-suspended in 1 mL of pre-chilled Extraction Buffer 2. After centrifugation at 12000*g* for 10 min, the pellets were re-suspended in 300 μL pre-chilled Extraction Buffer 3 and centrifuged at 16000*g* for 1 hr. The supernatant was removed, and chromatin pellets were re-suspended in 300 μL of Nuclei Lysis Buffer by gentle pipetting. The chromatin solution was then sonicated twice at power 3 for 15 sec on ice into 500-1,000 bp fragments using a Sonic Dismembrator (Fisher Scientific). A 15 μL aliquot of the supernatant was removed to use as the Input DNA control. A total of 30 μL of protein A-agarose beads (Millipore, Canada) was added to the Chromatin Solution that was brought to 1.5 mL using ChIP Dilution Buffer, and this mixture was incubated with rotation for 1 hr at 4°C. Subsequently, the mixture was gently agitated, centrifuged (3500*g*) for 1 min, and the supernatant was transferred for immunoprecipitation while discarding the beads. A total of 5 μL of Ab290 GFP antibody was added to the Chromatin Solution and

the mixture was incubated with overnight gentle agitation at 4°C. After 12 hrs, 50 µL of protein A-agarose beads was added to each tube and immune complexes were collected by incubation at 4°C for at least 1 hr with gentle agitation and then centrifugation. After washing with a cycle of low normality salt, high salt, LiCl and TE (Tris-EDTA) buffer, the immunoprecipitate was eluted with 250 µL of Elution Buffer. The DNA reverse cross-linking procedure was performed with 20 µL of 5 M NaCl incubated at 65°C for 5 hrs. To each sample 10 µL 0.5 M EDTA, 20 µL 1 M Tris-HCl (pH 6.5) and 2 µL of 10 mg/mL proteinase K (Sigma- Aldrich, Canada) was added. DNA was extracted using phenol: chloroform (1:1, v:v), recovered by ethanol precipitation in the presence of 0.3 M sodium acetate (pH = 5.2) and 2 µL glycogen carrier 10 mg/mL (Sigma-Aldrich, Canada) after overnight incubation at -20°C. The DNA pellets were washed with 70% ethanol and each pellet was re-suspended in 16 µL of distilled water to be used for ChIP-qPCR analysis using qnMsAGL6 and qnMsAGL21 primers (**Table S1**). SPL12 occupancy on *AGL6* and *AGL21* was tested by comparing the fold enrichment in *35S::SPL12m-GFP* and WT plants. A DNA fragment containing a SBP binding consensus-like sequence was amplified from *LATERAL ORGAN BOUNDARES-1* (*LOB1*) (Shuai et al. 2002) and was used as a negative control.

2.16 T7 Exonuclease 1 Assay

To detect mismatch mutations by T7 exonuclease 1 (T7E1) assay at the *SPL13* locus of putative CRISPR-Ca9 transgenic plants, the genomic region encompassing the targeted *SPL13* gRNA sites was amplified using Phusion High Fidelity DNA Polymerase (Thermo Fisher Scientific). The primers CRISPR-SPL13g1-F and CRISPR-SPL13g1-R were used

for the gRNA1 site; CRISPR-SPL13g2-F and CRISPR-SPL13g2-R for the gRNA2 site; and CRISPR-SPL13g3-F and CRISPR-SPL13g3-R for the gRNA3 (**Table S1**). The PCR amplicons were purified using GeneJET PCR Purification Kit (Thermo Fisher Scientific). The purified PCR products were denatured and annealed in NEBuffer 2 (New England Biolabs) using a thermocycler under the following condition: 95°C for 10 min, ramp down to 85°C at 2°C/s and finally to 25°C at 0.3°C/s. The annealed DNA was then treated with 1 μL T7E1 (New England Biolabs) at 37°C for 15 min and then analyzed by 2% agarose gel electrophoresis.

2.17 Microscopy

All microscopic observations were performed under a stereo microscope (Nikon SMZ1500, Japan) using 1 mm magnification. The microscope was integrated with a DsRi2 digital camera (Nikon, Japan) and the magnification scope varied between 3.15x and 78.75x. All images captured were taken in a JPG format.

2.18 Statistical analysis

Statistical analyses were performed using Microsoft Excel software. Pairwise comparisons were made using a Student's t-test, which was the proper statistical test in this case, as I was comparing each of the transgenic plants with WT. The significant differences between sample means for three or more data sets were calculated using the one-way analysis of variance (ANOVA) where appropriate. A P value of 0.05 or less was used as a statistically significant difference.

Chapter 3

3 Results

3.1 Generating alfalfa *spl13* mutants by CRISPR-Cas9 editing

SPL13 is one of the *SPL* genes that are targeted for transcript cleavage by miR156 in alfalfa (Aung et al. 2015). As this transcription factor was shown to play a significant role in alfalfa's response to abiotic stress, including heat, drought and flooding (Arshad et al. 2017a; Feyissa et al. 2021; Matthews et al. 2019), as well as in flowering time and biomass yield (Gao et al. 2018b), I attempted to generate knock-out lines using CRISPR-Cas9 gene editing technology, with the long term aim of generating transgene-free mutants for inclusion in alfalfa breeding.

3.1.1 Designing sgRNA for editing *SPL13* in alfalfa

In an attempt to knock-out *SPL13*, I first designed three gRNAs using the online tool CRISPR-P 2.0 (Liu et al. 2017). For this, I analyzed all the putative sgRNAs in *SPL13* based on the reference genome of *M. truncatula*, a close relative of *M. sativa*, *as* the CRISPR-P database does not include *M. sativa* genome sequences (**Figure 3.1A**). Three sgRNAs with the highest scores were selected and separately cloned into the vector pFGC5941-Cas9 (Meng et al. 2017), which expresses *SpCas9* under the *35S* promoter, sgRNA under *MtU6* promoter, and *Basta* gene (selectable marker) under *Bar* promoter (**Figure 3.1B**). The three constructs were used in alfalfa *A. tumefaciens*-mediated

Figure 3.1 CRISPR/Cas9 mutagenesis of *SPL13* in alfalfa

A) Schematic drawing showing the three sgRNA targets relative to the *SPL13* intron-exon structure. **B)** A schematic drawing of the construct used to target *SPL13* using CRISPR/Cas9 system. **C)** PCR analysis of genomic DNA of transgenic alfalfa plants using primers designed to amplify fragments of *SpCas9* (984 bp) from genomic DNA. Each 13-CR number indicates the callus from which each plant was taken. *Bar*, *Bar* resistance gene; sgRNA: single guide RNA; LB, T-DNA left border; M: DNA ladder Marker; *MtU6*: *M. truncatula U6 polymerase III* promotor; *p35S*: constitutive promotor; RB: T- DNA right border; WT: Wild Type.

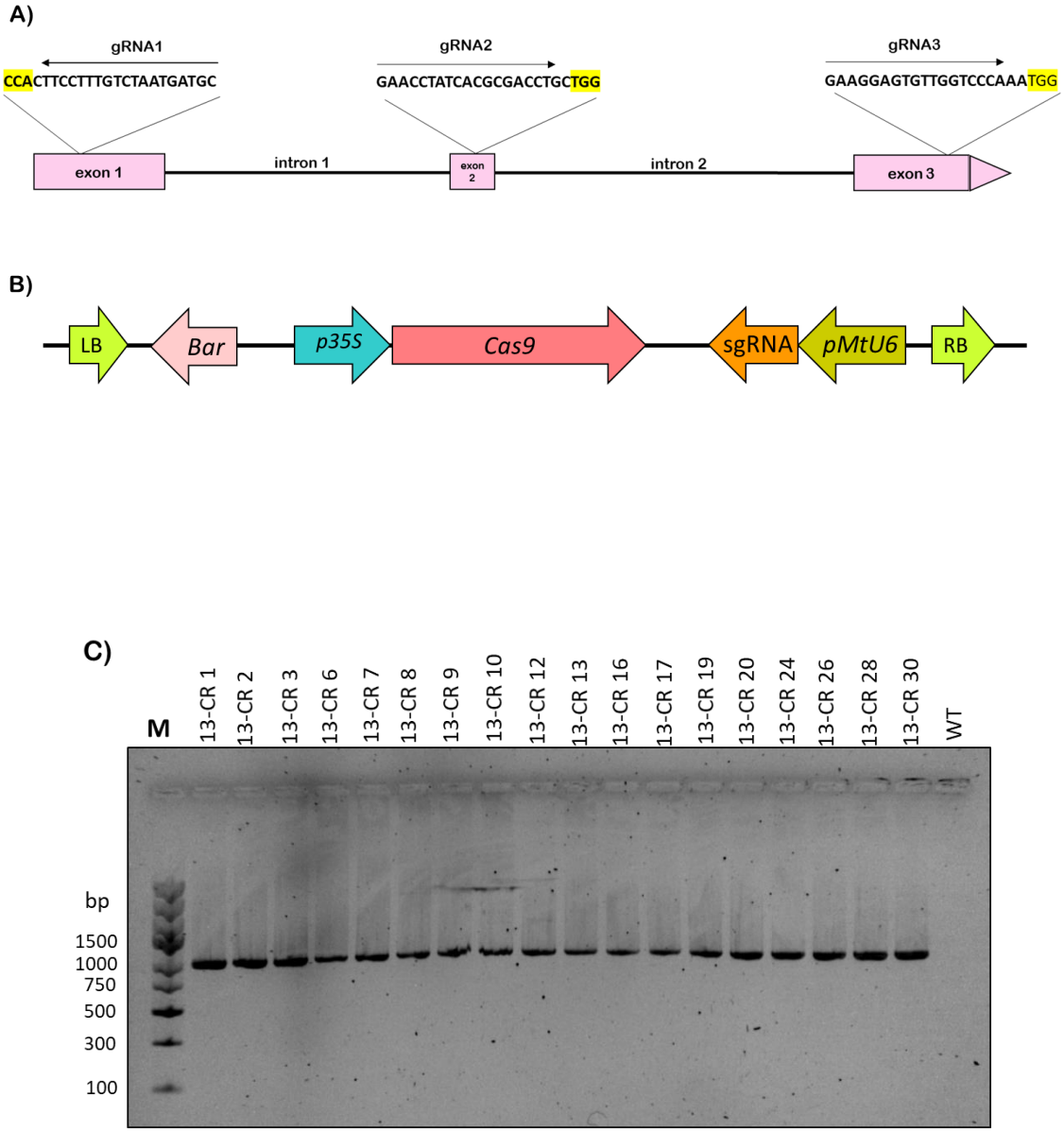
A)
gRNA1
CCACTTCCTTTGTCTAATGATGC
gRNA2
GAACCTATCACGCGACCTGCTGG
gRNA3
GAAGGAGTGTTGGTCCCAAATGG
exon 1
intron 1
exon 2
intron 2
exon 3
B)
LB
Bar
p35S
Cas9
sgRNA
pMtU6
RB
C)
M
13-CR 1
13-CR 2
13-CR 3
13-CR 6
13-CR 7
13-CR 8
13-CR 9
13-CR 10
13-CR 12
13-CR 13
13-CR 16
13-CR 17
13-CR 19
13-CR 20
13-CR 24
13-CR 26
13-CR 28
13-CR 30
WT
bp
1500
1000
750
500
300
100

transformation (Section 2.3) at the same time, and potential transgenic plants harboring the T-DNA inserts were identified by selectable marker screening, and were further analyzed by PCR to confirm the presence of *SpCas9* transgene.

A single expected band of 984 bp was observed after amplification of genomic DNA from 18 different transgenic plants using primers specific to *SpCas9* gene (**Figure 3.1C**).

3.1.2 Screening of CRISPR-modified alfalfa plants by T7 endonuclease 1 digestion

T7 endonuclease I (T7E1) assay (Kim et al. 2009) was used to detect putative mutations in all three targeted *SPL13* sites in the transgenic alfalfa plants. In this assay, fragments containing targeted sites were amplified from genomic DNA, and the amplicons were subjected to the mismatch-sensitive T7E1 digestion after melting and annealing. Cleaved DNA fragments are visible if amplified products contained mutated (mismatched) DNA sequences. DNA extracted from each of the 18 transgenic plants were subjected to the PCR three times in order to amplify the specific gRNA content of each fragment. As shown in **Figure 3.2A**, PCR products including gRNA1 from 13-CR-6 transgenic plant (only one out of 18 plants) yielded two extra bands in addition to the universal band generated from all other samples (data are not shown for other 17 transgenic plants), indicating that a genomic fragment was modified. For gRNA2 and gRNA3, T7E1-digested fragments were detected in all of the samples except in 13-CR-1, 13-CR-17 (gRNA2) and 13-CR-17, 13-CR-26, 13-CR-28 and 13-CR-30 (gRNA3) (**Figure 3.2B,C**).

Figure 3.2 Detection and molecular analysis of CRISPR/Cas9-modified alfalfa plants by T7E1 assay

The DNA regions spanning the gRNA target sites were PCR amplified for the T7E1 assay. PCR amplification was used to screen alfalfa plants containing putative CRISPR/Cas9-mediated genomic modification for **A)** gRNA1 **B)** gRNA2 and **C)** gRNA3 using T7E1 assay.

A)

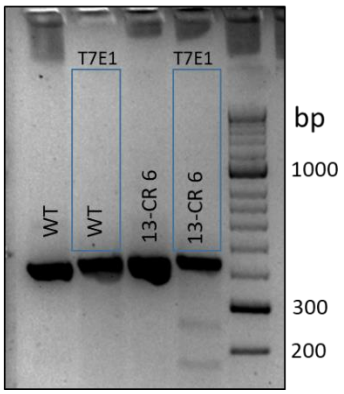
T7E1
T7E1
WT
WT
13-CR 6
13-CR 6
bp
1000
300
200

B)

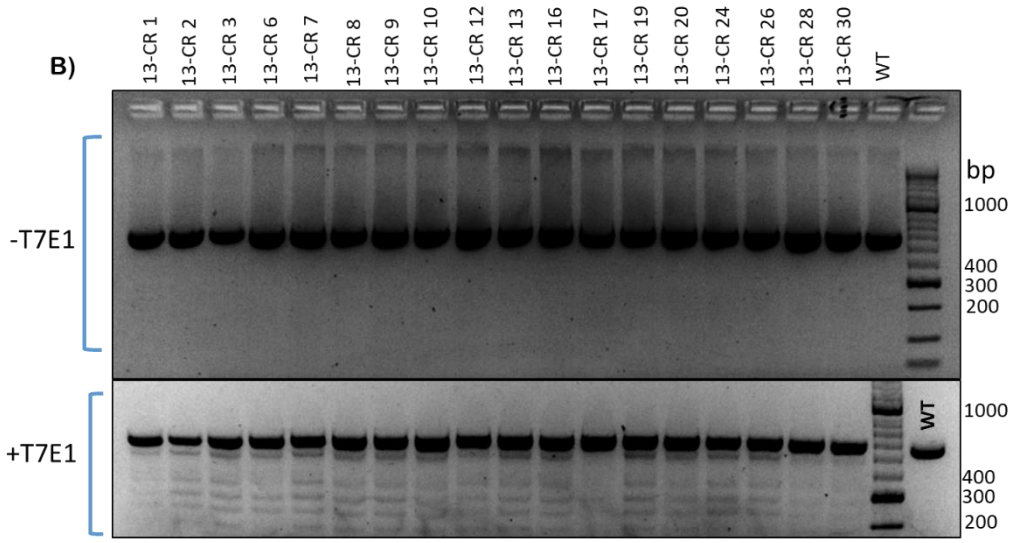
13-CR 1
13-CR 2
13-CR 3
13-CR 6
13-CR 7
13-CR 8
13-CR 9
13-CR 10
13-CR 12
13-CR 13
13-CR 16
13-CR 17
13-CR 19
13-CR 20
13-CR 24
13-CR 26
13-CR 28
13-CR 30
WT
-T7E1
+T7E1
bp
1000
400
300
200
WT

C)

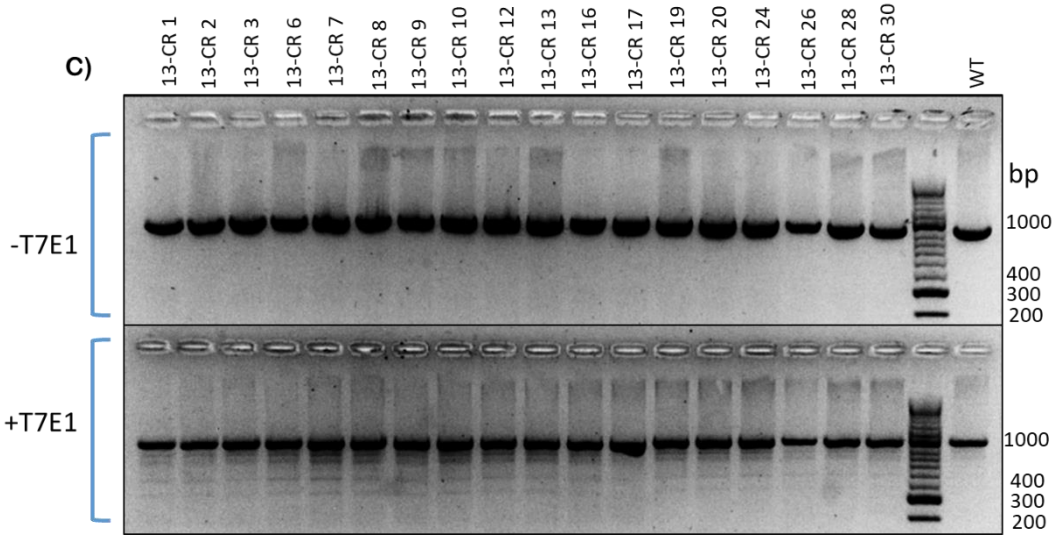
13-CR 1
13-CR 2
13-CR 3
13-CR 6
13-CR 7
13-CR 8
13-CR 9
13-CR 10
13-CR 12
13-CR 13
13-CR 16
13-CR 17
13-CR 19
13-CR 20
13-CR 24
13-CR 26
13-CR 28
13-CR 30
WT
-T7E1
+T7E1
bp
1000
400
300
200

3.1.3 Validation of edited *SPL13* locus by Sanger Sequencing

To further confirm the CRISPR/Cas9 editing of *SPL13*, the three fragments of the *SPL13* coding sequence containing each gRNA's complementary region were cloned into pJET1.2/blunt cloning vector. DNA was extracted from positive clones and subjected to Sanger sequencing. Relative to the WT sequence, sequence of the representative transgenic plant 13-CR-6 (gRNA1) showed a 3-bp deletion in *SPL13* locus corresponding to gRNA1 (**Figure 3.3A**), indicating the successful CRISPR-Cas9 editing of this gene in alfalfa. While the 3-bp deletions would not change the frameshift, it would result in missing proline amino acid just upstream of the SBP domain (**Figure 3.3B**). Given the limited editing frequency of the *SPL13* gene in this study, I decided to focus only on the characterization of SPL12 for the rest of my thesis as will be discussed in the following chapters.

3.2 SPL12 plays a role in root architecture, nodulation and nitrogen fixation

The involvement of miR156 in regulating nodulation and root architecture in alfalfa was previously reported, as overexpressing *miR156* resulted in increased nodulation, improved nitrogen fixation and enhanced root regenerative capacity during vegetative propagation (Aung et al. 2015). As *SPL12* is a target of transcript cleavage by miR156 in alfalfa (Aung et al. 2015), I hypothesized that miR156-mediated regulation of underground organs could be achieved by silencing *SPL12*. The current study aimed to investigate this hypothesis by analyzing transgenic plants with altered transcript levels of *SPL12* and putative downstream genes at the molecular and phenotypic levels.

Figure 3.3 Confirmation of *SPL13* editing in 13-CR-6 genotype with gRNA1.

A) Targeted genome editing of *SPL13* in CRISPR/Cas9-mediated transgenic alfalfa plant. PCR amplicons containing the sgRNA targeting sequence were sub-cloned and sequenced, and a mutation event was detected at the gRNA1 target site. The underlined sequences identify the PAM sequences and the red color letters show the gRNA1. Deletion is indicated by dashed lines. **B)** Amino acid sequences of SPL13 gRNA1 target region from untransformed (WT) and 13-CR-6 genotypes. Deletion is indicated by blue highlighted dashed line, and the red arrow shows the SBP domain.

A)

PAM

WT 5'...CAACAGCATCATTAGACAAAGGAAGTGGTGATTGAT...3'

13-CR 6 5'...CAACAGCATCATTAGACAA------AAGTGGTGATTGAT...3'

B)

gRNA1 edit site

SBP domain

WT ....TDQSPLPLSNDAVVVSKIATPTSSSGSSKRARAMNNATLTVSCLVDGCNSDLSNCRDYHRRHKVCELHSKTPEVTICGL....

13-CR 6 ....TDQSPL-LSNDAVVVSKIATPTSSSGSSKRARAMNNATLTVSCLVDGCNSDLSNCRDYHRRHKVCELHSKTPEVTICGL....

Plants characterized within this study were RNAi-silenced *SPL12* (*SPL12*-RNAi), *SPl12* overexpression (*35S::SPL12*), GFP-tagged SPL12 and RNAi-silenced *AGL6* (*AGL6*-RNAi).

3.2.1 *SPL12* transcript levels in *SPL12*-RNAi and *35S::SPL12* plants

To study the role of SPL12 in various root traits within alfalfa, plants with altered expression of *SPL12* , including *SPL12* overexpression (*35S::SPL12*), *SPL12*-RNAi, and wild-type (WT) plants were used for analysis. First, I determined the relative transcript levels of *SPL12* in *35S::SPL12* genotypes, L1, L5, and L7, all of which were found to overexpress *SPL12* relative to WT (**Figure 3.4A**). As *SPL12* is one of the *SPL* genes that are silenced by miR156 in alfalfa (Aung et al. 2015; Gao et al. 2016), I generated RNAi-silenced *SPL12* (*SPL12*-RNAi) transgenic plants (see Section 2.2.1). Of the 33 plants harboring the *SPL12*-RNAi construct (**Figure 3.4B**), I chose three genotypes (RNAi12-7, RNAi12-24, and RNAi12-29) with the lowest *SPL12* transcript levels (43%, 36% and 32% of WT) (**Figure 3.4C**) for subsequent analyses.

3.2.2 Effect of *SPL12* silencing on root regenerative capacity

To assess root regeneration capacity, transgenic *SPL12*-RNAi genotypes and WT alfalfa were propagated by stem cuttings, and root regeneration from stem nodes was observed in one or more of the *SPL12*-RNAi genotypes as early as 10 days after vegetative propagation. Compared to WT plants, the number of rooted stem propagules was significantly higher in *SPL12*-RNAi transgenic alfalfa genotypes at 13 days post propagation (**Figure 3.5A,B**). Genotype RNAi12-29 showed an increase in root regeneration earlier than the other

Figure 3.4 Relative transcript levels of *SPL12* in different genotypes of alfalfa plants

A) Relative *SPL12* transcript levels in *35S::SPL12* plants. Relative *SPL12* transcript **B)** in all of the generated *SPL12*-RNAi plants, and **C)** in the three of the lowest *SPL12* expressing *SPL12*-RNAi plants. Transcript levels are relative to WT after being normalized to *Cyclo* and *ACTB* reference genes. * and ** indicate significant differences relative to WT using Student's t-test ($n = 3$) $p < 0.05$, $p < 0.01$, respectively. Error bars indicate standard deviation.

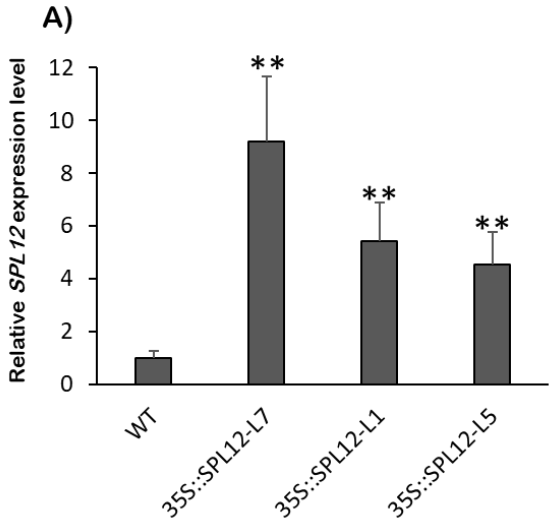
A)
Relative SPL 12 expression level
12
10
8
6
4
2
0
**
**
**
WT
35S::SPL12-L7
35S::SPL12-L1
35S::SPL12-L5

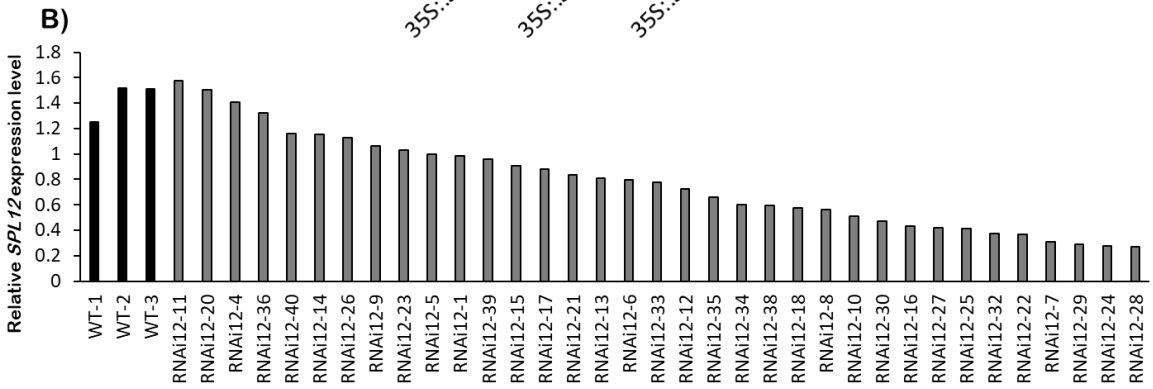
B)
Relative SPL12 expression level
1.8
1.6
1.4
1.2
1
0.8
0.6
0.4
0.2
0
WT-1
WT-2
WT-3
RNAi12-11
RNAi12-20
RNAi12-4
RNAi12-36
RNAi12-40
RNAi12-14
RNAi12-26
RNAi12-9
RNAi12-23
RNAi12-5
RNAi12-1
RNAi12-39
RNAi12-15
RNAi12-17
RNAi12-21
RNAi12-13
RNAi12-6
RNAi12-33
RNAi12-12
RNAi12-35
RNAi12-34
RNAi12-38
RNAi12-18
RNAi12-8
RNAi12-10
RNAi12-30
RNAi12-16
RNAi12-27
RNAi12-25
RNAi12-32
RNAi12-22
RNAi12-7
RNAi12-29
RNAi12-24
RNAi12-28

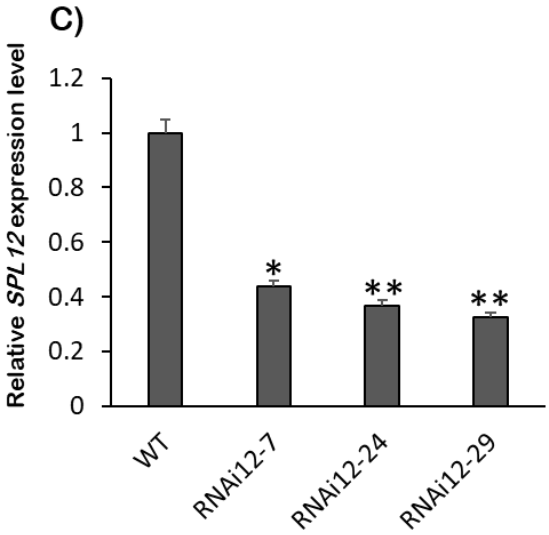
C)
Relative SPL 12 expression level
1.2
1
0.8
0.6
0.4
0.2
0
*
**
**
WT
RNAi12-7
RNAi12-24
RNAi12-29

Figure 3.5 Effect of *SPL12* silencing on root regeneration in alfalfa

A) Typical root regeneration phenotype from stem cuttings at 13 days after vegetative propagation. **B)** Number of rooted stems arising from 14 stems (per replicate) at 13 days after vegetative propagation. * and ** indicate significant differences relative to WT using Student's t-test ($n = 3$) $p < 0.05$, $p < 0.01$, respectively. Error bars indicate standard deviation.

A)

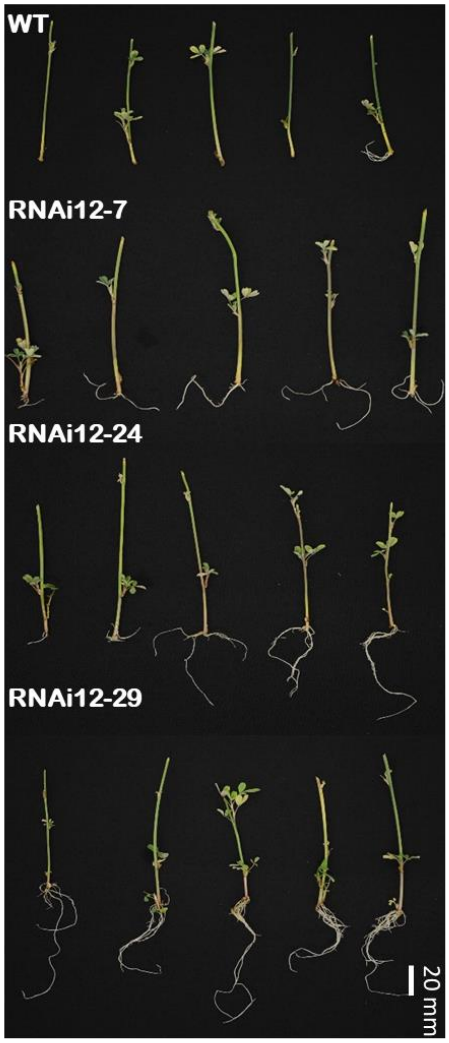
WT
RNAi12-7
RNAi12-24
RNAi12-29
20 mm

B)

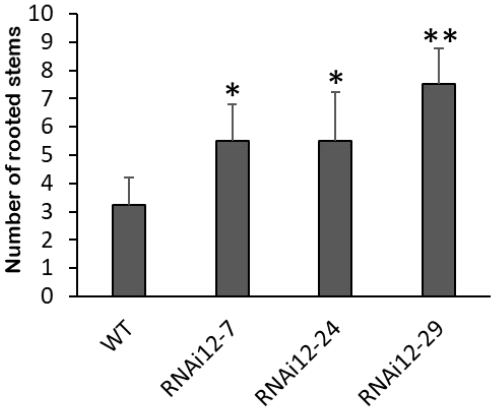
Number of rooted stems
0
1
2
3
4
5
6
7
8
9
10
*
*
**
WT
RNAi12-7
RNAi12-24
RNAi12-29

genotypes tested, but genotypes RNAi12-7 and RNAi12-24 still showed a significantly higher root generation compared to WT at 13 days.

3.2.3 Effect of inoculation with *Sinorhizobium meliloti* on *SPL12* transcript levels

To gain an insight into the role of the *SPL12* gene in the alfalfa-*S. meliloti* symbiosis, I determined *SPL12* transcript levels in inoculated roots of WT alfalfa (**Figure 3.6A**). To analyze *SPL12* regulation at different stages of the symbiosis process, rooted alfalfa WT plants (21 days after cutting) were inoculated with *S. meliloti* Sm1021, and RNA transcript analysis was carried out at 0, 7, 14 and 21 days after inoculation (dai). As shown in **Figure 3.6A**, the relative transcript levels of *SPL12* gradually decreased, with the lowest transcript levels detected at 21 dai.

To investigate if *SPL12* transcript levels correlate with events associated with the rhizobial infection process, I analyzed the RNA transcript levels of some early nodulation genes in inoculated roots (**Figure 3.6B-J**). These genes are *NIN* (Marsh et al. 2007), *NSP2* (Kaló et al. 2005), *IPD3* (Messinese et al. 2007), *DMI1* (Ané et al. 2004), *DMI2* (Bersoult et al. 2005), *DMI3* (Messinese et al. 2007), *DELLA* (Jin et al. 2016), *LysM* (Arrighi et al. 2006), and *CLE13* (Mortier et al. 2010). In general, the transcript levels of all these genes gradually increased over the inoculation period compared to time 0 (**Fig. 3-6B-J**), indicating a clear correlation between *SPL12* and nodulation genes.

Figure 3.6 Relative transcript levels of *SPL12* and early nodulation genes upon rhizobium infection

Transcript levels of *SPL12* **A)**, and early nodulation genes **B-J)** were determined in roots inoculated with *S. meliloti* at the initial time (0), 7, 14 and 21 dai. The alfalfa early nodulation genes include **B)** *NIN*, **C)** *LysM*, **D)** *NSP2*, **E)** *IPD3*, **F)** *CLE13*, **G)** *DMI1*, **H)** *DMI2*, **I)** *DMI3*, and **J)** *DELLA.* Transcript levels are relative to 0 dai after being normalized to *Cyclo* and *ACTB* reference genes. *, ** and *** indicate significant differences relative to 0 dai using Student's t-test (n = 3) $p < 0.05$, $p < 0.01$ and $p < 0.001$ respectively. Error bars indicate standard deviation.

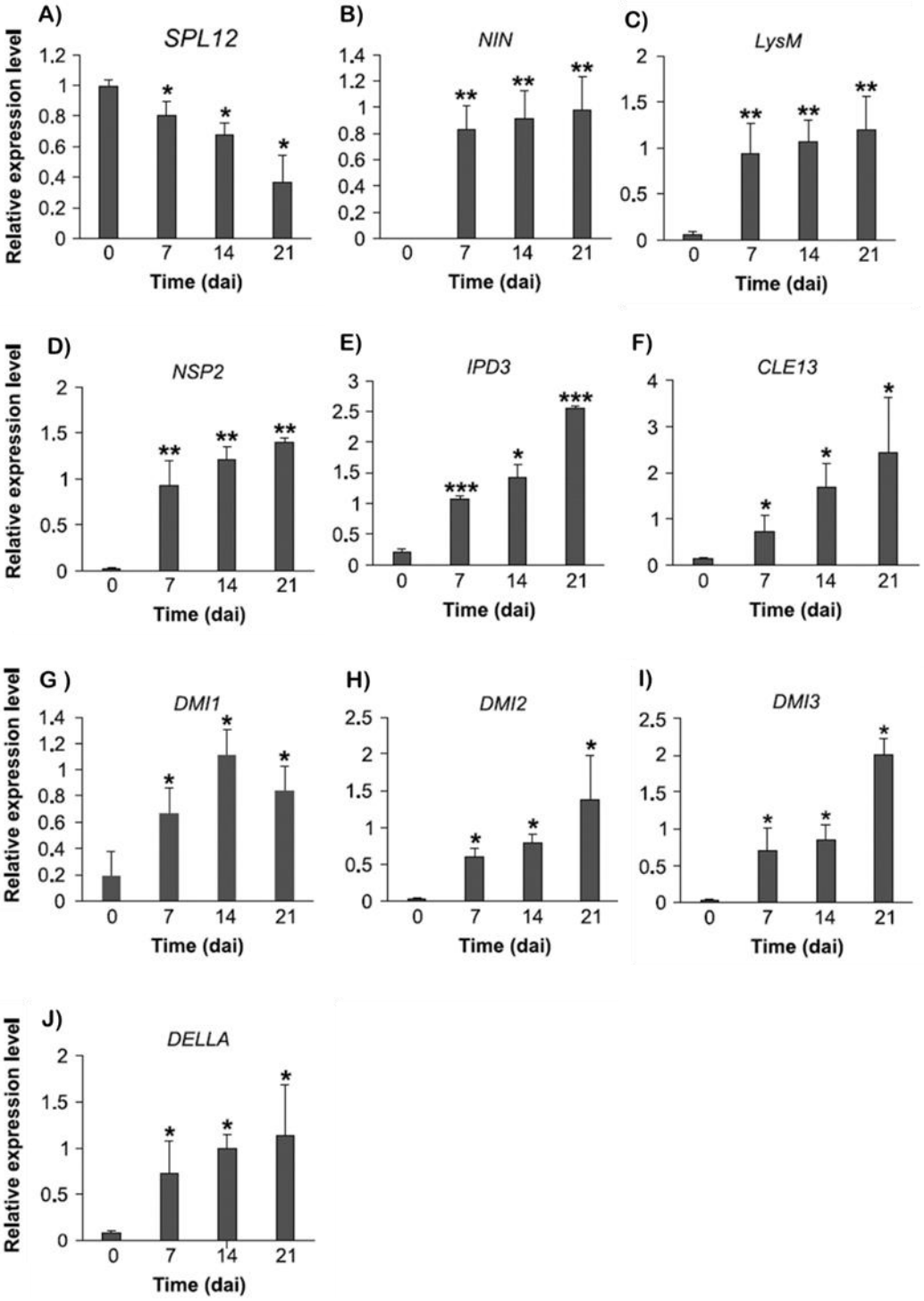
A)
SPL12
B)
NIN
C)
LysM
D)
NSP2
E)
IPD3
F)
CLE13
G)
DMI1
H)
DMI2
I)
DMI3
J)
DELLA
Relative expression level
Time (dai)
0
7
14
21

3.2.4 Role of SPL12 in nodulation

Overexpression of miR156 was previously reported to increase root length and enhance nodulation in transgenic alfalfa genotypes (Aung et al. 2015), so I investigated the root phenotypes in WT and *SPL12*-RNAi plants to determine if SPL12 is involved in root-related traits. To determine the ability of *SPL12*-RNAi transgenic plants to form symbiotic nodules, three-week-old (three weeks post cutting) rooted plants were inoculated with *S. meliloti* for a period of either two (14 dai) or three weeks (21 dai). At 14 dai, *SPL12*-RNAi plants showed an increase in nodulation of 2-, 2.6- and 2.4-fold in RNAi12-7, RNAi12-24 and RNAi12-29, respectively, compared to WT (**Figure 3.7A,B**), however, no significant differences in nodule numbers were observed between *SPL12*-RNAi genotypes and WT at 21 dai (**Figure 3.7C**).

To further investigate the role of SPL12 in nodulation and root regeneration, I analyzed these traits in transgenic alfalfa plants overexpressing *SPL12*. The number of rooted stem propagules was decreased by more than 5.75-fold in *35S::SPL12* plants compared to WT control (**Figure 3.8A**).

To determine the ability of *35S::SPL12* transgenic plants to form symbiotic nodules, three-week-old rooted plants were inoculated with *S. meliloti* for 14 days. Among the *35S::SPL12* genotypes, L7 and L5 had lower total nodule number compared to WT control at this stage (**Figure 3.8B**). These results suggest that the transcript levels of *SPL12* are negatively correlated to nodulation and root regeneration in alfalfa.

Figure 3.7 The effect of *SPL12* silencing on nodulation

A) Nodule phenotypes of WT, and the *SPL12*-RNAi genotypes at 14 dai. **B)** The number of nodules in WT and the *SPL12*-RNAi at 14 dai, and **C)** 21 dai (n = 10-14). ** and *** indicate significant differences relative to WT using Student's t-test $p < 0.01$ and $p < 0.001$ respectively. Error bars indicate standard deviation.

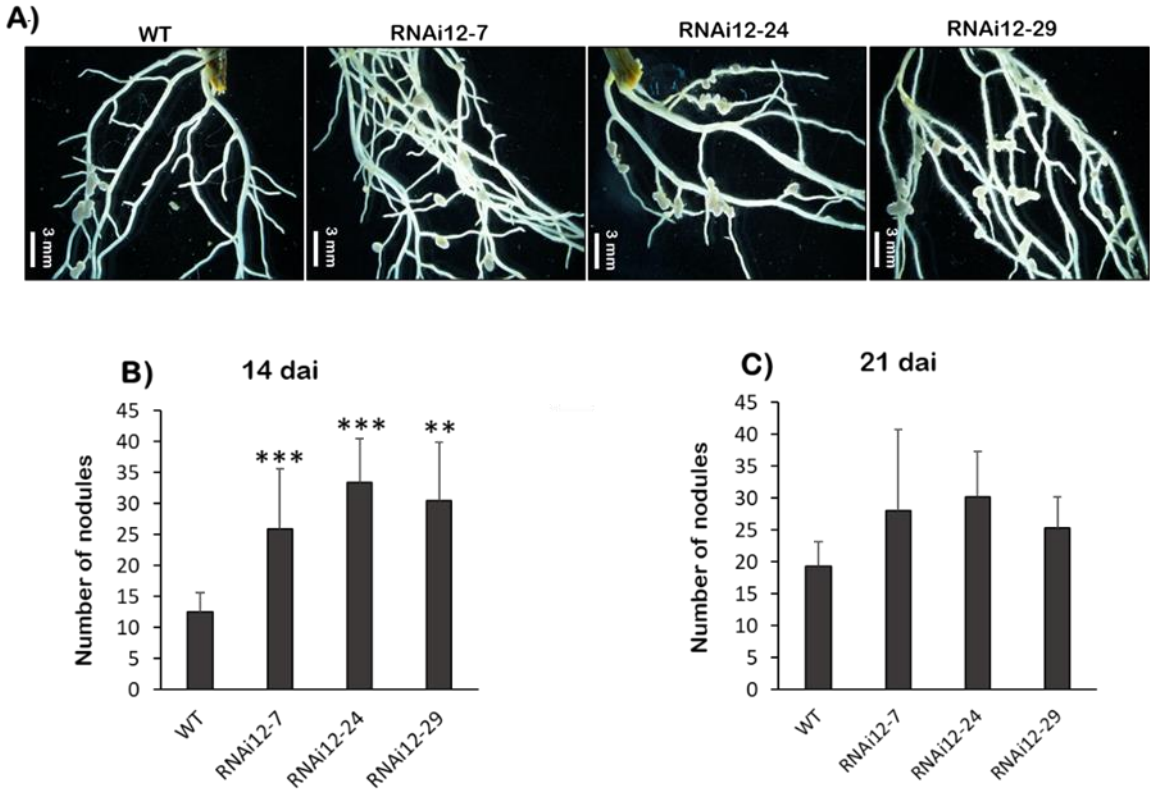
A)
WT
RNAi12-7
RNAi12-24
RNAi12-29
3 mm
B)
14 dai
Number of nodules
45
40
35
30
25
20
15
10
5
0
***
***
**
WT
RNAi12-7
RNAi12-24
RNAi12-29
C)
21 dai
Number of nodules
WT
RNAi12-7
RNAi12-24
RNAi12-29

Figure 3.8 Effect of *SPL12* overexpressing on root regeneration and nodule numbers in alfalfa

A) Number of rooting stems arising from 12 stems (per replicate) at 13 days after vegetative propagation. **B)** The number of nodules in WT and *35S::SPL12* at 14 dai (n = 9-12 plants). * and ** indicate significant differences relative to WT using Student's t-test $p < 0.05$, $p < 0.01$, respectively. Error bars indicate standard deviation.

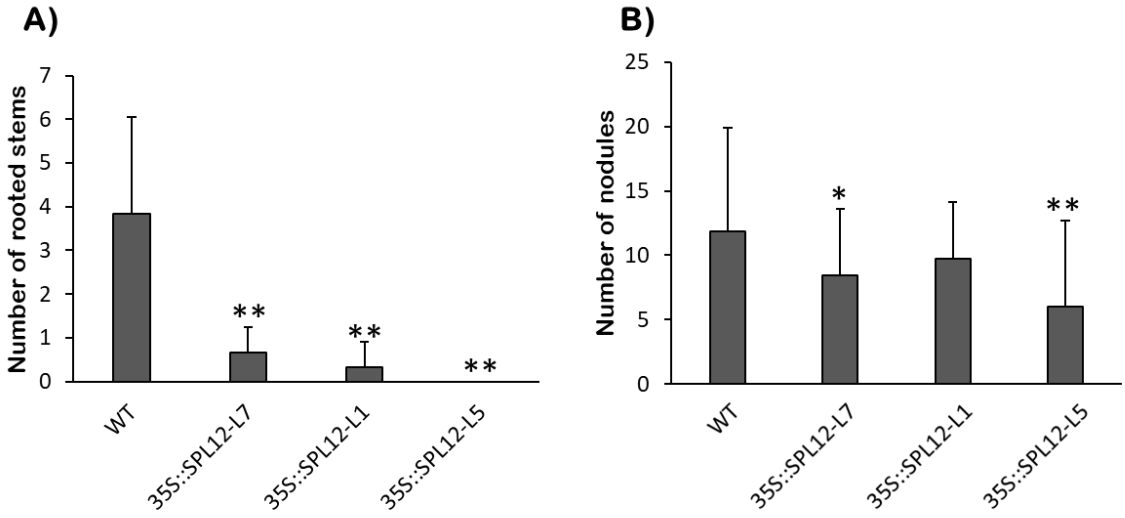
A)
Number of rooted stems
7
6
5
4
3
2
1
0
**
**
**
WT
35S::SPL12-L7
35S::SPL12-L1
35S::SPL12-L5
B)
Number of nodules
25
20
15
10
5
0
*
**
WT
35S::SPL12-L7
35S::SPL12-L1
35S::SPL12-L5

3.2.5 Silencing of *SPL12* enhances nitrogen fixation

To investigate the role of SPL12 in nitrogen fixation, I analyzed the effect of *SPL12* silencing on nitrogenase activity in *S. meliloti*-inoculated roots of alfalfa genotypes. Three-week-old *SPL12*-RNAi plants derived from stem cuttings were inoculated with *S. meliloti* and allowed to grow in the absence of nitrate for an additional two weeks. During this time the mature nodules formed, and I had observed a significant increase in nodulation in genotypes RNAi12-7, RNAi12-24 and RNAi12-29 relative to WT (**Figure 3.7B**). The nitrogenase activity in the nodules was determined using the acetylene reduction assay (ARA; Section 2.6). The nitrogenase activity of the nodulated roots of transgenic alfalfa genotypes RNAi12-7 and RNAi12-29 was significantly higher than that of WT plants (**Figure 3.9A**). The level of ethylene production was the highest from roots of genotype RNAi12-29 (4.64 nmol/plant), whereas the WT control plant showed the lowest level (2.8 nmol/plant). Furthermore, given the increased nirogenase activity of nodules in the *SPL12*-RNAi genotypes, the transcript levels of several rhizobial genes, including *FixK* (induces the expression of genes involved in nodule respiration), *NifA* (induces the expression of genes involved in nitrogen fixation) and *RpoH* (sigma 32 factor for effective nodulation) (Defez et al. 2016; Fischer 1994) were also investigated in alfalfa roots inoculated with *S. meliloti*.

Compared to WT, *SPL12*-RNAi showed increased transcript levels of *NifA*, *FixK* and *RpoH* genes (**Figure 3.9B-D**). Taken together, these findings suggest that *SPL12* silencing enhances nodulation and nitrogen fixation in alfalfa.

Figure 3.9 Analysis of nitrogen fixation activity in alfalfa

A) Nitrogenase activity (ARA; nmol ethylene/hr/plant root) in *SPL12*-RNAi and WT alfalfa plants at two weeks after inoculation with *S. meliloti* (n = 8). Transcript levels of *S. meliloti* **B)** *NifA*, **C)** *FixK* and **D)** *RpoH* genes in alfalfa roots inoculated with *S. meliloti*. Transcript levels in '**B**', '**C**', and '**D**' are shown relative to WT after being normalized to *Cyclo* and *ACTB* reference genes. * and ** indicate significant differences relative to wild type using Student's t-test $p < 0.05$, $p < 0.01$, respectively. Error bars indicate standard deviation.

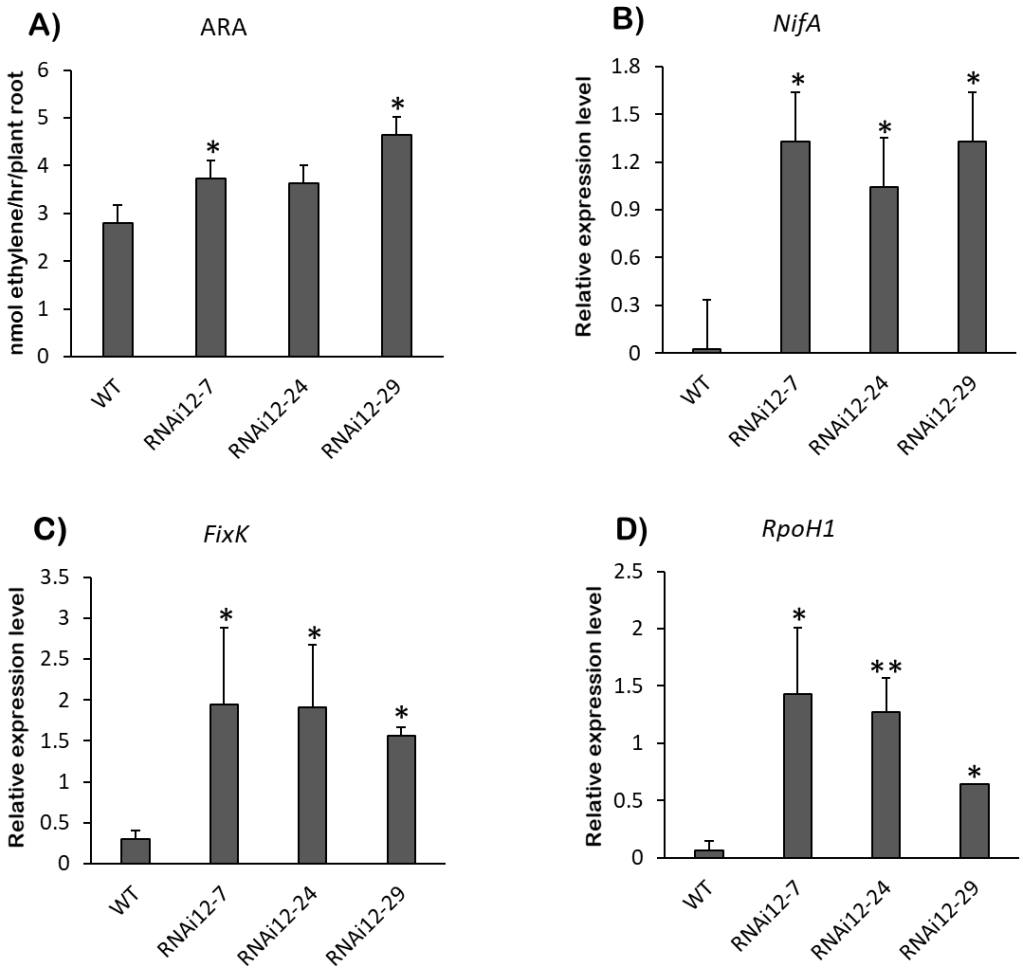
A)
ARA
nmol ethylene/hr/plant root
0
1
2
3
4
5
6
*
*
WT
RNAi12-7
RNAi12-24
RNAi12-29
B)
NifA
Relative expression level
0
0.3
0.6
0.9
1.2
1.5
1.8
*
*
*
WT
RNAi12-7
RNAi12-24
RNAi12-29
C)
FixK
Relative expression level
0
0.5
1
1.5
2
2.5
3
3.5
*
*
*
WT
RNAi12-7
RNAi12-24
RNAi12-29
D)
RpoH1
Relative expression level
0
0.5
1
1.5
2
2.5
*
**
*
WT
RNAi12-7
RNAi12-24
RNAi12-29

3.2.6 *SPL12* silencing affects nodulation-related genes

Given the aforementioned finding that *SPL12*-RNAi alfalfa plants had enhanced nodulation at 14 dai (Section 3.1.4), I examined the transcript levels of several nodulation-related genes in alfalfa plants at 14 dai and 21 dai. I found that *SPL12* silencing differentially regulated the transcript levels of *IPD3* (Messinese et al. 2007), *LysM* (Arrighi et al. 2006), *NOOT1*, *NOOT2* (Magne et al. 2018), *CLE13* (Mortier et al. 2010), *miR172* (Gao et al. 2016; Wang et al. 2019), *NIN* (Marsh et al. 2007), and *ChOMT* (Breakspear et al. 2014; Maxwell et al. 1992) genes in roots of alfalfa at the two time points (**Figure 3.10**). Of the tested genes, *IPD3*, *NOOT1* and *NOOT2* were significantly higher in all of the *SPL12*-RNAi genotypes (RNAi12-7, RNAi12-24 and RNAi12-29) at 14 dai (**Figure 3.10A-C**), but these genes were only higher in two of the lines (RNAi12-24 and RNAi12-29) at 21 dai (**Figure 3.10I-K**). *LysM* was at a lower level in all of *SPL12*-RNAi plants at 14 dai compared to WT (**Figure 3.10D**), but no significant changes were observed at 21 dai (**Figure 3.10L**).

Consistent with the differential nodulation responses at 14 dai and at 21 dai, *SPL12*-RNAi plants showed reduced transcript levels of *CLE13* (**Figure 3.10E**) with enhanced transcript levels of *miR172* in only two of *SPL12*-RNAi plants (RNAi12-7 and RNAi12-24) at 14 dai (**Figure 3.10F**). However, at 21 dai, *CLE13* was significantly upregulated in the three *SPL12*-RNAi plants, whereas *miR172* did not show any significant difference (**Figure 3.10M,N**). Moreover, significant effects of *SPL12* silencing on *NIN* and *ChOMT* transcript levels were observed in all of the *SPL12*-RNAi roots at 14 dai (**Figure 3.10G,H**), but were

Figure 3.10 Effect of *SPL12* silencing on the nodulation-related gene transcription level

Relative transcript levels of nodulation-related genes in *SPL12*-RNAi genotypes at 14 dai (**A**-**H**) and 21 dai (**I**-**P**). **A**) *IPD3,* **B**) *NOOT1,* **C**) *NOOT2,* **D**) *LysM,* **E**) *CLE13,* **F**) *miR172,* **G**) *NIN,* **H**) *ChOMT,* **I**) *IPD3,* **J**) *NOOT1,* **K**) *NOOT2,* **L**) *LysM,* **M**) *CLE13,* **N**) *miR172,* **O**) *NIN,* and **P**) *ChOMT*. Transcript levels are shown relative to WT after being normalized to *Cyclo* and *ACTB* reference genes. *, ** and *** indicate significant differences relative to WT using Student's t-test (n = 3) $p < 0.05$, $p < 0.01$ and $p < 0.001$ respectively. Error bars indicate standard deviation.

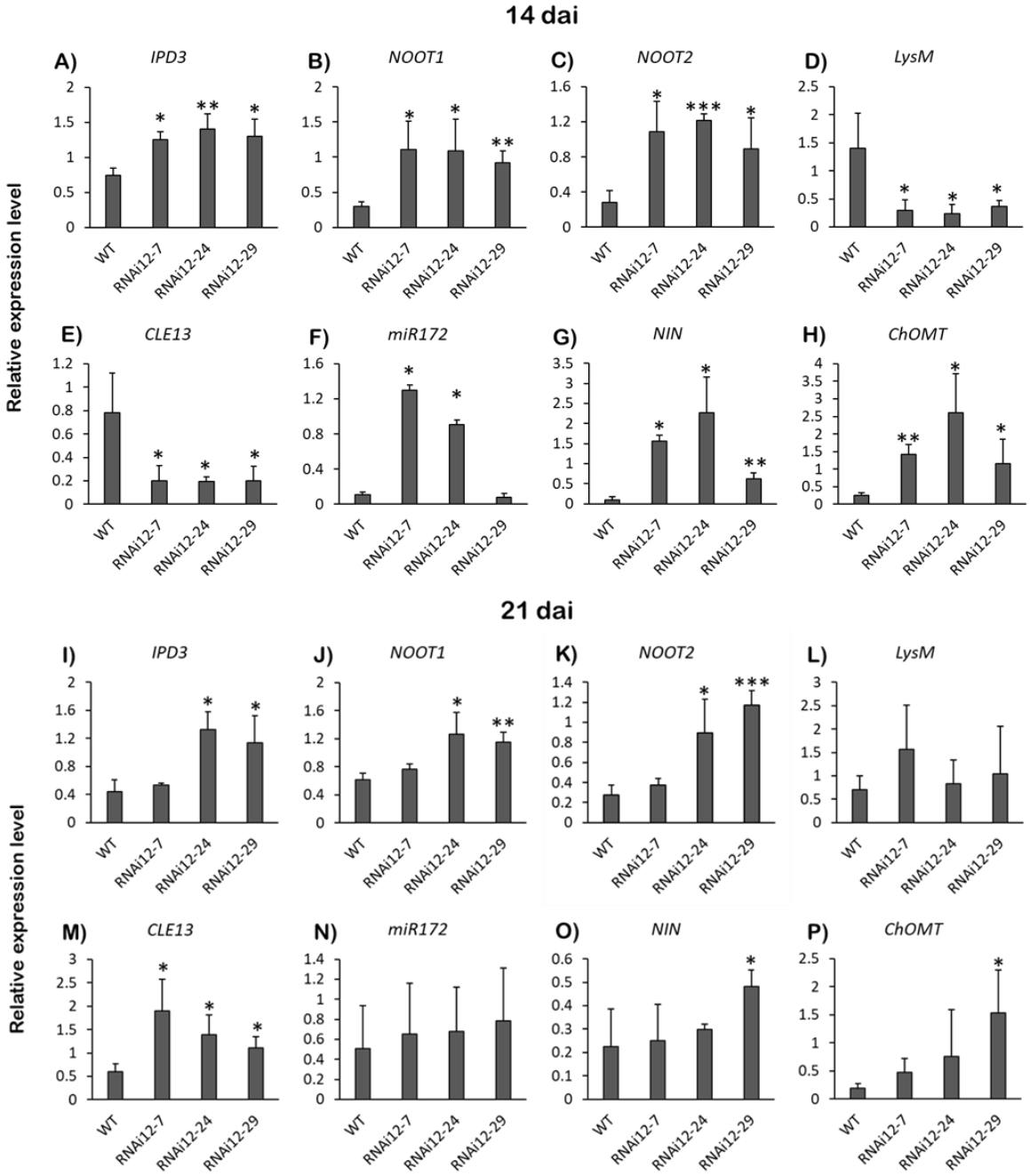
14 dai
21 dai
Relative expression level
A) IPD3
B) NOOT1
C) NOOT2
D) LysM
E) CLE13
F) miR172
G) NIN
H) ChOMT
I) IPD3
J) NOOT1
K) NOOT2
L) LysM
M) CLE13
N) miR172
O) NIN
P) ChOMT
WT
RNAi12-7
RNAi12-24
RNAi12-29

higher in only RNAi12-29 at 21 dai (**Figure 3.10O-P**). These findings suggest a potential role for SPL12 in autoregulation of nodulation (AON) in alfalfa symbiosis.

3.3 Effect of *SPL12* silencing on root transcriptome

Given the potential role of SPL12 in regulating nodulation and root emergence capacity, Next Generation Sequencing (NGS)-based transcriptomic analysis (RNA-Seq) was carried out on the root tissues of WT and *SPL12*-RNAi (RNAi12-24 and RNAi12-29) alfalfa plants to identify genes that are potentially differentially regulated by SPL12.

3.3.1 Differentially expressed genes between *SPL12*-RNAi and WT alfalfa plants

Root architecture is the basis of plant growth as it controls the uptake and utilization of nutrients, and affects the plant's growth and biomass (Zhao et al. 2018). Investigating the molecular mechanism underpinning the role of SPL12 in this trait is important as this knowledge can be useful in marker-assisted breeding programs for crop improvement. In the earlier sections (3.1.2 - 3.1.5), I investigated the role of the miR156/SPL12 module in alfalfa root architecture and nodulation. Here, I compared the global transcriptomic profiles of root tissues of RNAi-silenced *SPL12* and WT plants. The observed phenotypic traits in *SPL12*-RNAi plants in root emergence capacity, nodulation and nitrogen fixation were investigated to determine if they can be linked to differential gene expression. A total of 1710 and 840 DEGs were found in RNAi12-29 and RNAi12-24, respectively, relative to WT (**Table S5, S6**). Of these DEGs, 84 transcripts were commonly increased in root tissues of both *SPL12*-RNAi lines, while 85 transcripts were commonly decreased (**Table S7, S8**).

Among the genes increased in both *SPL12*-RNAi lines, genes related to nodulation, nitrogen uptake and assimilation, root development, and stress response were observed, indicating these DEGs may be regulated by SPL12 to affect root architecture and nodulation under different conditions. The nodulation- and nitrogen-related genes such as leguminosin group 485 secreted peptide (Medtr2g009450), a receptor-like kinase (Medtr3g102450), oxidoreductase/ferric-chelate reductase (Medtr8g028780), a caffeic acid O-methyltransferase (Medtr3g021430), nitrate reductase NADH-like protein 1 (Medtr5g059820), nitrate reductase NADH-like protein 2 (Medtr3g073180), peptide/nitrate transporter (Medtr7g065080), and component of high affinity nitrate transporter (Medtr4g104700) were upregulated in *SPL12*-RNAi genotypes compared to WT (**Table S7**). Of the commonly increased root development-related genes in *SPL12*-RNAi plants, transcripts encoding a KDEL-tailed cysteine endopeptidase CEP1 (Medtr3g075390), a FAD-binding berberine family protein (Medtr4g091150), and extensin-like region protein (Medtr4g065113) showed increased levels (**Table S7**).

Moreover, transcript analysis showed higher levels of several abiotic stress-related genes such as a cytochrome P450 family 94 protein (Medtr8g030590), a peroxidase family protein (Medtr5g049280), a transducin/WD40 repeat protein (Medtr3g074070), F-box plant-like protein (Medtr7g089640), and WRKY family transcription factor (Medtr7g079010) (**Table S7**). These findings indicate that SPL12 may be involved in the regulation of these DEGs to control root architecture and nodulation in alfalfa.

3.3.2 Gene ontology enrichment analysis of DEGs

Gene ontology (GO) enrichment analysis of DEGs was carried out to identify pathways that may be affected in *SPL12*-RNAi plants. This analysis revealed that DEGs belong to these categories, molecular function (65%), biological process (26%), and cellular components (9%) (**Figure 3.11A**). Graphical representation of the components of GO-term analysis is provided in **Figure 3.11B-D**. In the molecular function category, catalytic activity, hydrolase activity, nucleotide binding, metal ion binding, and oxidoreductase activity are highly represented (**Figure 3.11B; Table S9**). Among the 40 functions classified as biological processes, metabolic processes, primary metabolic processes, cellular biosynthetic processes, and cellular aromatic compound metabolic processes are the major representation of GO-terms (**Figure 3.11C; Table S9**). The full list of the components for the three fractions (molecular function, biological process, and cellular component) is shown in **Table S9**.

3.3.3 RNA-Seq data validation by quantitative real time PCR

To validate the findings of the RNA-Seq data using RT-qPCR, a total of 14 genes (upregulated and downregulated) were randomly selected and analyzed by RT-qPCR (**Table 3.1**). For most of the genes, the trends between the RNA-seq and RT-qPCR analyses were similar. A total of 13 of the 14 transcripts (92%) showed similar levels of transcript change (**Table 3.1**), suggesting the reproducibility of the RNA-Seq results.

Figure 3.11 Gene Ontology enrichment analysis of DEGs between *SPL12*-RNAi and WT

A) Gene Ontology (GO-term) –based percent representation of DEGs in cellular components, biological process, and molecular functions between WT and *SPL12*-RNAi in alfalfa roots. Go frequency of **B)** Molecular function, **C)** Biological process **D)** Cellular component and.

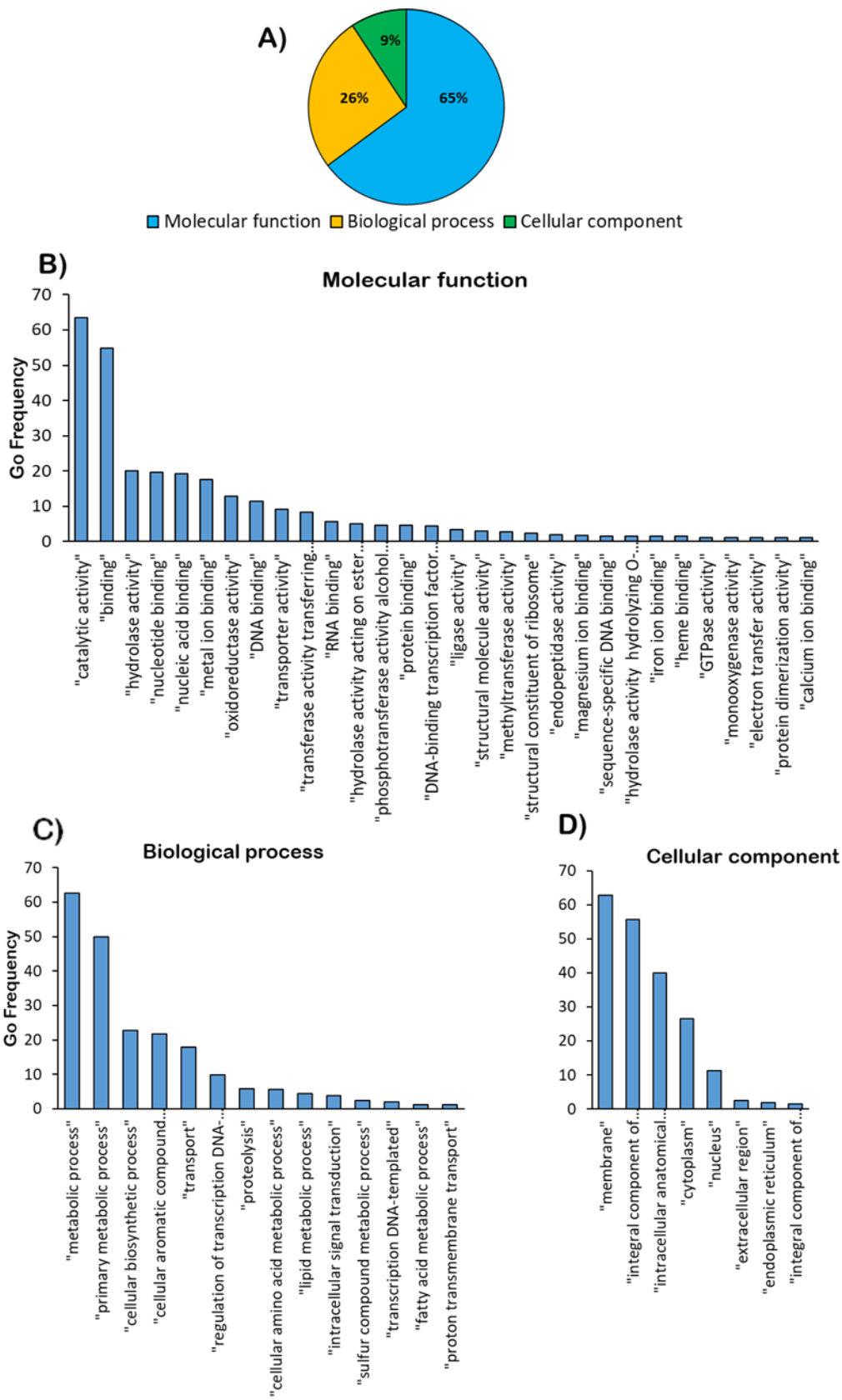
A)
9%
26%
65%
Molecular function
Biological process
Cellular component
B)
Molecular function
Go Frequency
70
60
50
40
30
20
10
0
"catalytic activity"
"binding"
"hydrolase activity"
"nucleotide binding"
"nucleic acid binding"
"metal ion binding"
"oxidoreductase activity"
"DNA binding"
"transporter activity"
"transferase activity transferring...
"RNA binding"
"hydrolase activity acting on ester...
"phosphotransferase activity alcohol...
"protein binding"
"DNA-binding transcription factor...
"ligase activity"
"structural molecule activity"
"methyltransferase activity"
"structural constituent of ribosome"
"endopeptidase activity"
"magnesium ion binding"
"sequence-specific DNA binding"
"hydrolase activity hydrolyzing O-...
"iron ion binding"
"heme binding"
"GTPase activity"
"monooxygenase activity"
"electron transfer activity"
"protein dimerization activity"
"calcium ion binding"
C)
Biological process
Go Frequency
70
60
50
40
30
20
10
0
"metabolic process"
"primary metabolic process"
"cellular biosynthetic process"
"cellular aromatic compound...
"transport"
"regulation of transcription DNA-...
"proteolysis"
"cellular amino acid metabolic process"
"lipid metabolic process"
"intracellular signal transduction"
"sulfur compound metabolic process"
"transcription DNA-templated"
"fatty acid metabolic process"
"proton transmembrane transport"
D)
Cellular component
70
60
50
40
30
20
10
0
"membrane"
"integral component of...
"intracellular anatomical...
"cytoplasm"
"nucleus"
"extracellular region"
"endoplasmic reticulum"
"integral component of...

Table 3. 1 Validation of RNA-Seq data using RT-qPCR.

	RNAi12-24/WT*		RNAi12-29/WT*	
Gene name	**RNA-Seq**	**RT-qPCR**	**RNA-Seq**	**RT-qPCR**
ABA/WDS induced protein	--	0.73	0.07	0.88
GRAS family transcription factor	0.53	0.53	0.41	0.28
WRKY family transcription factor 41	0.2	0.7	0.27	0.51
lateral organ boundaries (LOB) domain protein	0.57	0.89	0.47	0.23
Nod26 MIP family transporter	5.52	1.56	3.57	1.27
peptide/nitrate transporter	3.98	1.53	2.14	2.33
two-component response regulator ARR3-like protein	2.52	77.39	3.85	4.39
sulfate/bicarbonate/oxalate exchanger and transporter sat-1	4.53	2.22	2.54	1.81
high affinity sulfate transporter type 1	4.37	4.9	1.87	2.1
nitrate reductase [NADH]-like protein 1	8.15	1.24	2.50	1.09
nitrate reductase [NADH]-like protein 2	6.29	4.14	1.99	1.01
high affinity sulfate transporter type 1	1.95	2.36	1.74	2.78
component of high affinity nitrate transporter	2.02	0.43	1.52	0.77
caffeic acid O-methyltransferase	6.52	2.96	5.12	3.12

* Fold change (*SPL12*-RNAi/WT)

3.3.4 Comparison of differentially expressed genes between the two *SPL12*-RNAi genotypes

Analysis of RNA-seq data revealed a total of 1710 and 840 DEGs detected in RNAi12-29 and RNAi12-24 genotypes, respectively, relative to WT (**Figure 3.12A; Table S5, S6**). Of the total DEGs in RNAi12-29, 1032 genes were upregulated and 678 were downregulated. RNAi12-24, on the other hand, had a total of 274 upregulated genes and 566 downregulated. Of the total DEGs, only 169 were differentially expressed in both RNAi12-29 and RNAi12-24 genotypes (**Figure 3.12A**), indicating that these genes may be specifically regulated by SPL12, while others might be the result of secondary effects due to copy number in transgenic plants, gene positional effects, and gene insertion effects of T-DNA in the genome.

To investigate if there is a variation in the T-DNA insertion profiles, I carried out a Southern blot analysis using genomic DNA from RNAi12-24 and RNAi12-29 and a T-DNA specific probe. The analysis revealed that these two lines are the result of two independent transgenic events with distinct T-DNA insertion profiles (**Figure 3.12E**), resulting in different DEG profiles.

3.3.5 SPL12 regulation of *AGL6* and *AGL21*

Previous transcriptomic analysis of miR156-OE plant A17 (Aung et al. 2017), revealed 8373 differentially expressed genes between roots of WT and miR156-OE. Of the many genes differentially expressed in miR156-OE plant A17 relative to WT, *AGL6* (MS.gene052964, MS.gene071001 and MS.gene34431), a gene that encodes a yet to be

Figure 3.12 Numbers of DEGs based on RNA-Seq of WT and *SPL12*-RNAi plants

The Venn diagrams show statistically significant DEGs in **(A)** total, **(B)** upregulated, and **(C)** downregulated, in RNAi12-29 and RNAi12-24 compared to WT. **D)** Southern blot analysis of transgenic and WT plants. Total DNA was prepared from the leaf tissues of two *SPL12*-RNAi plants (RNAi12-24 and RNAi12-29) and WT. Genomic DNA was digested with the restriction enzyme *Eco*RI and probed using a labeled *35S*-specific promotor sequence.

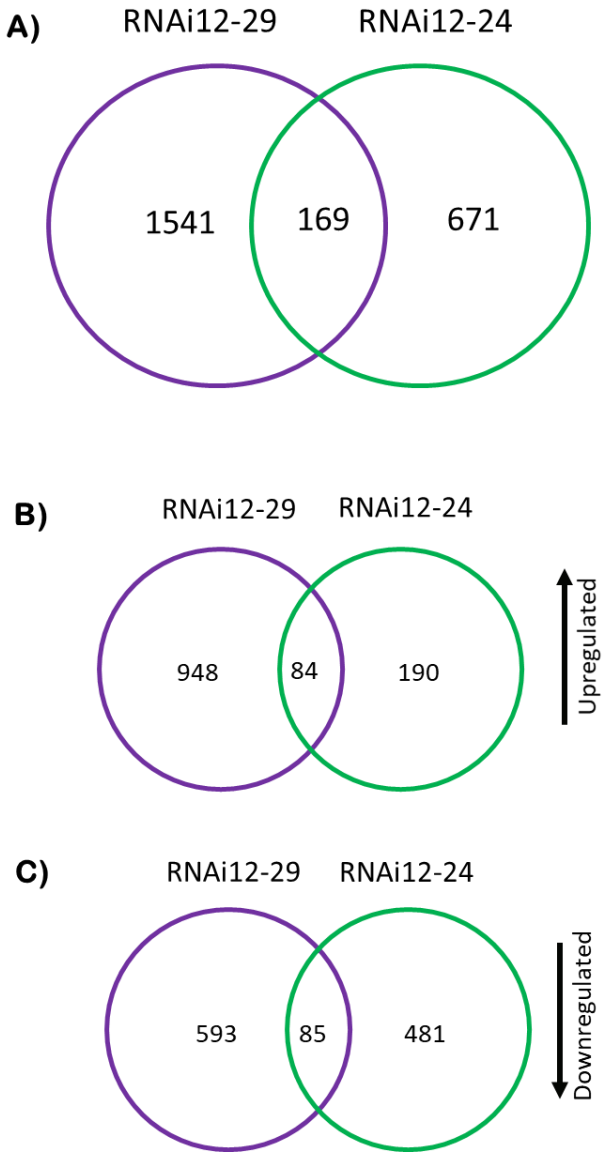
A)
RNAi12-29
RNAi12-24
1541
169
671
B)
RNAi12-29
RNAi12-24
948
84
190
Upregulated
C)
RNAi12-29
RNAi12-24
593
85
481
Downregulated

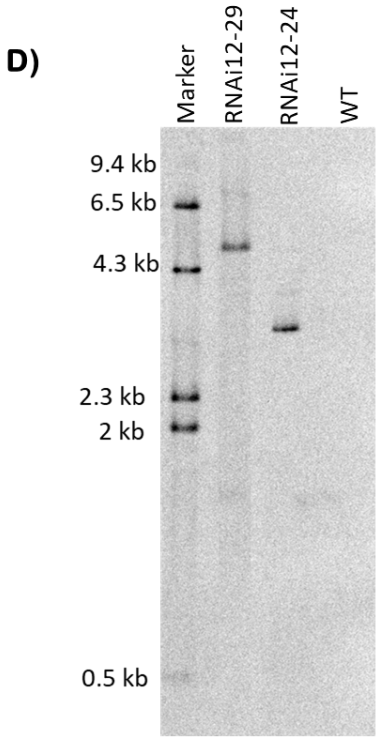
D)
Marker
RNAi12-29
RNAi12-24
WT
9.4 kb
6.5 kb
4.3 kb
2.3 kb
2 kb
0.5 kb

characterized alfalfa MADS box protein, was significantly downregulated in A17 (Aung et al. 2017). This gene is closely related to the Arabidopsis *AtAGL79* gene that is regulated by *At*SPL10. In Arabidopsis, miR156/SPL10 regulatory pathway targets *AGL79* to regulate plant lateral root development (Gao et al. 2018c). Another uncharacterized transcription factor gene, *AGL21* (MS.gene069166, MS.gene068633, MS.gene70086 and MS.gene027842); a MADS-box gene closely related to the Arabidopsis *NITRATE REGULATED1* (*ANR1*) clade, was significantly upregulated in *SPL12*-RNAi (**Figure 3.13A,B**) and as it was already shown in miR156-OE plants (Aung et al. 2017).

3.3.6 Expression profiles of *SPL12*, *AGL6* and *AGL21* genes in alfalfa

To investigate the expression profile of *SPL12* in alfalfa, I measured its transcript levels in various organs of 21-day-old WT alfalfa plants (leaf, stem, and root). The transcript levels of *SPL12* were detected at similar levels in all three tissues (**Figure 3.14A**). The transcript levels of *AGL6* and *AGL21* were also determined in the same tissues (**Figure 3.14B,C**). *AGL6* transcripts were detected in all the tissues (**Figure 3.14B**), and were highly expressed in roots with much lower levels in leaves. Transcript analysis of *AGL21* revealed that it was nearly undetectable in leaf and stem tissues and highly expressed in roots (**Figure 3.14C**). This low leaf transcript levels of *AGL21* is consistent with previous reports which found that the Arabidopsis *ANR1-like* genes were expressed primarily in roots (Burgeff et al. 2002). *AGL79* expression was also nearly undetectable in leaf tissues in Arabidopsis (Gao et al. 2018c). In roots, *AGL6* transcript levels were higher in *SPL12* overexpressing genotypes (**Figure 3.14D**), and lower in miR156-OE genotypes (A11 and

Figure 3.13 SPL12 regulation of *AGL21* in alfalfa

Relative *AGL21* expression in roots of WT and *SPL12*-RNAi alfalfa plants by **A)** RT-qPCR and **B)** NGS. Transcript abundance in '**B**' is relative to WT after being normalized to *Cyclo* and *ACTB* reference genes. * and ** indicate significant differences relative to WT using Student's t-test ($n = 3$) $p < 0.05$, $p < 0.01$, respectively. Error bars indicate standard deviation.

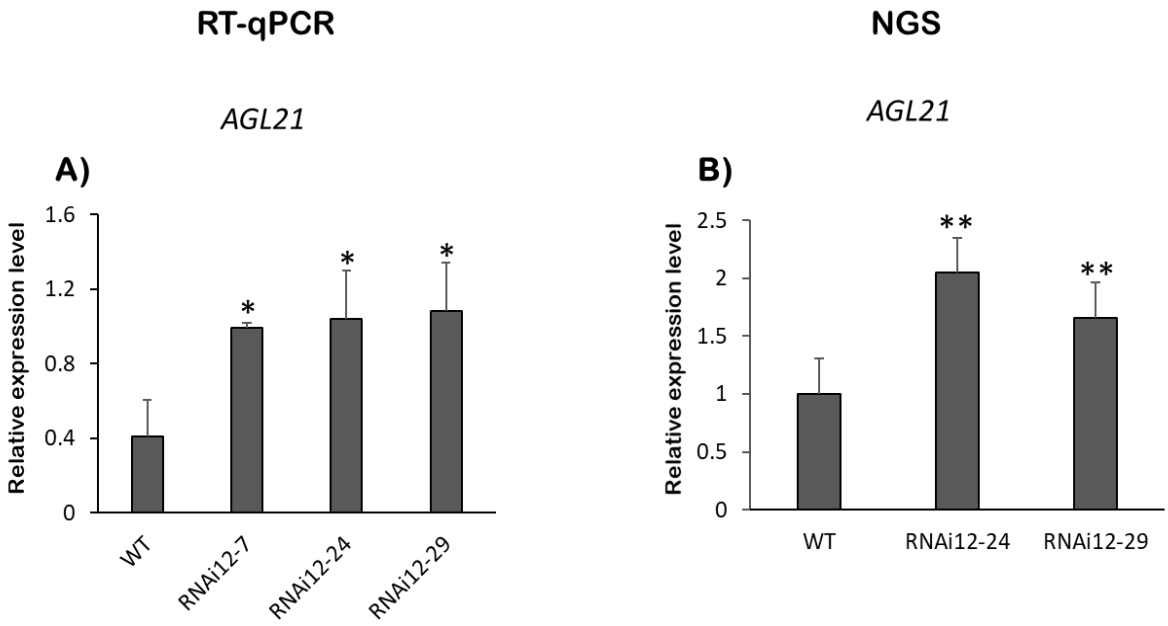
RT-qPCR
AGL21
A)
Relative expression level
1.6
1.2
0.8
0.4
0
*
*
*
WT
RNAi12-7
RNAi12-24
RNAi12-29
NGS
AGL21
B)
Relative expression level
2.5
2
1.5
1
0.5
0
**
**
WT
RNAi12-24
RNAi12-29

Figure 3.14 Tissue-specific transcript profiles of *SPL12*, *AGL6*, and *AGL21*

Relative transcript levels of **A)** *SPL12*, **B)** *AGL6*, and **C)** *AGL2*1 in leaf, stem and root of WT plants. Transcript levels in '**A**', '**B**' and '**C**' are normalized to *Cyclo* and *ACTB* reference genes. Significant difference from ANOVA was followed by *Post hoc* Tukey ($P<0.05$) multiple comparisons test indicated with different letters. *AGL6* transcript analysis in **D)** *35S::SPL12* and **E)** miR156-OE relative to WT. Transcript levels in **'D'** and '**E**' are shown relative to WT after being normalized to *Cyclo* and *ACTB* reference genes. * and ** indicate significant differences relative to WT using Student's t-test ($n = 3$) $p < 0.05$, $p < 0.01$, respectively. Error bars indicate standard deviation.

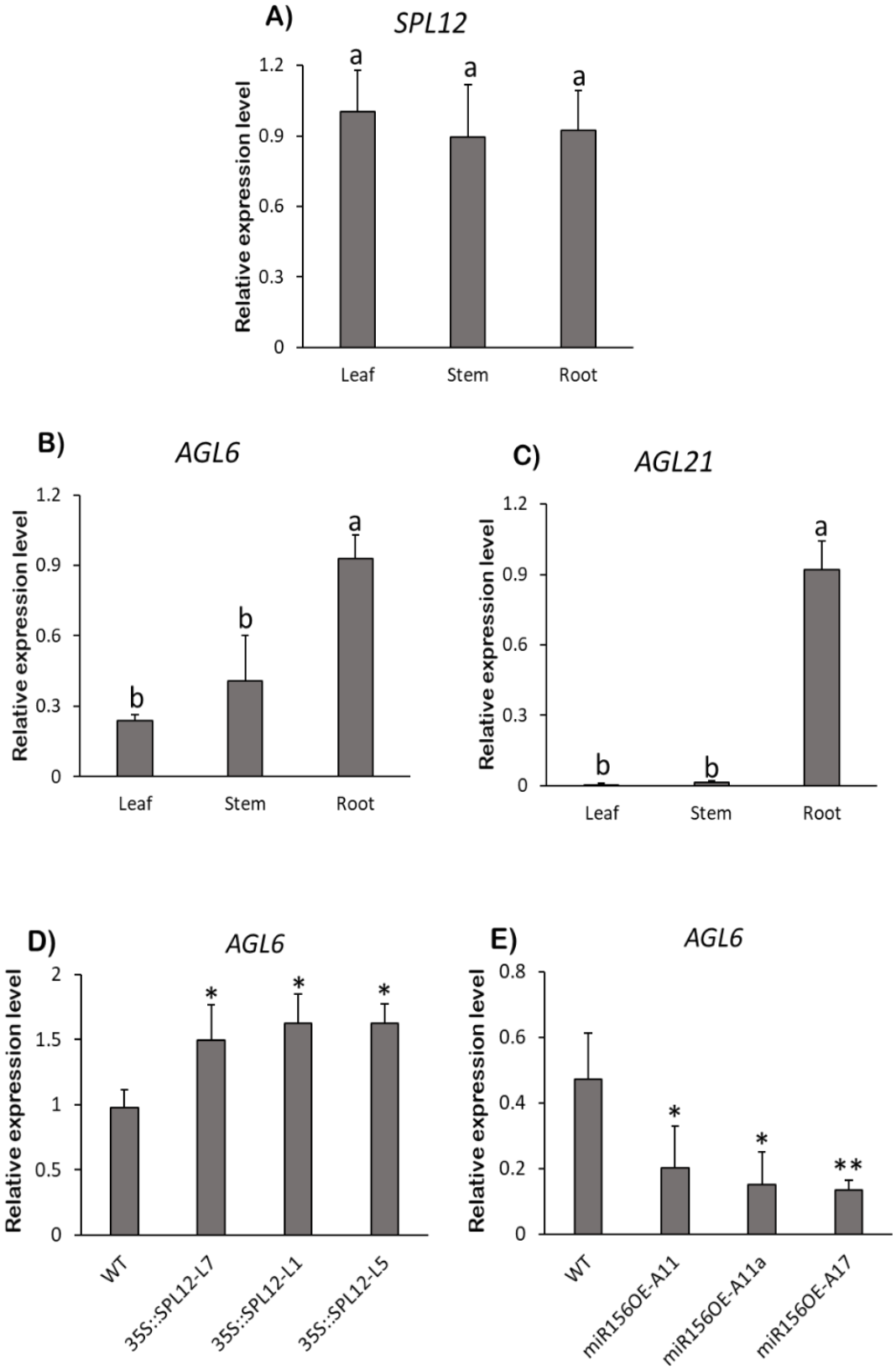
A)
SPL12
Relative expression level
1.2
0.9
0.6
0.3
0
a
a
a
Leaf
Stem
Root
B)
AGL6
Relative expression level
1.2
0.9
0.6
0.3
0
b
b
a
Leaf
Stem
Root
C)
AGL21
Relative expression level
1.2
0.9
0.6
0.3
0
b
b
a
Leaf
Stem
Root
D)
AGL6
Relative expression level
2
1.5
1
0.5
0
*
*
*
WT
35S::SPL12-L7
35S::SPL12-L1
35S::SPL12-L5
E)
AGL6
Relative expression level
0.8
0.6
0.4
0.2
0
*
*
**
WT
miR156OE-A11
miR156OE-A11a
miR156OE-A17

A11a and A17) compared to WT (**Figure 3.14E**), suggesting that *AGL6* is positively regulated by SPL12.

3.3.7 SPL12 is a direct regulator of *AGL6*

In this study, *AGL6* was found to be expressed significantly at higher levels under *SPL12* overexpression in L7, L1 and L5 plants (**Figure 3.14D**). Given the fact that *AGL6* was also expressed at lower levels in miR156-OE alfalfa (**Figure 3.14E**), further characterization was carried out using alfalfa plants expressing the SPL12-GFP fusion protein to determine if *AGL6* is a direct target of SPL12. For that, plants expressing the SPL12m-GFP fusion protein (*35S::SPL12m-GFP*) were analyzed by Western blotting, where a band (~75 kDa) corresponding to SPL12-GFP fusion was detected in *35S::SPL12m-GFP* plants, but not in WT (**Figure 3.15A**). There are at least five core GTAC sequences in three sites (I, II, and III) within 2000 bp upstream of the translation start codon of *AGL6* (**Figure S2**), which could act as potential SPL12 binding sites (**Figure 3.15B**). These three sites (I, II, and III) were tested for SPL12 occupancy on *AGL6* promoter. A relatively strong binding capacity of SPL12 to the *AGL6* promoter at all three sites was detected by ChIP-qPCR in the *35S::SPL12m-GFP* transgenic alfalfa plants (**Figure 3.15C**).

Occupancy in these three sites was significantly higher than that in the WT and *LOB1* (Shuai et al. 2002) controls, indicating that SPL12 protein could bind directly to multiple sites in *AGL6* promoter to regulate its expression.

Figure 3.15 Detection of SPL12 binding to *AGL6* promoter

A) Detection of SPL12m-GFP fusion protein (~75 kDa) in transgenic alfalfa plants using Western blotting. **B)** Schematic representation of the promoter region of *AGL6*. Black box: coding sequences; asterisks: locations of putative SPL binding elements within *AGL6* promoter. Roman numerals (I, II and III): sites that were tested by qPCR. **C)** Chromatin Immunoprecipitation-qPCR (ChIP-qPCR) based fold enrichment analysis of SPL12 in *35S::SPL12m-GFP* and WT plants from means of n = three individual plants where *LATERAL ORGAN BOUNDARES-1*, *LOB1*, is used as a negative control. * and ** indicate significant differences relative to WT in each potential SPL12 binding sites (I, II and III) using Student's t-test (n = 3) $p < 0.05$, $p < 0.01$, respectively. Error bars indicate standard deviation.

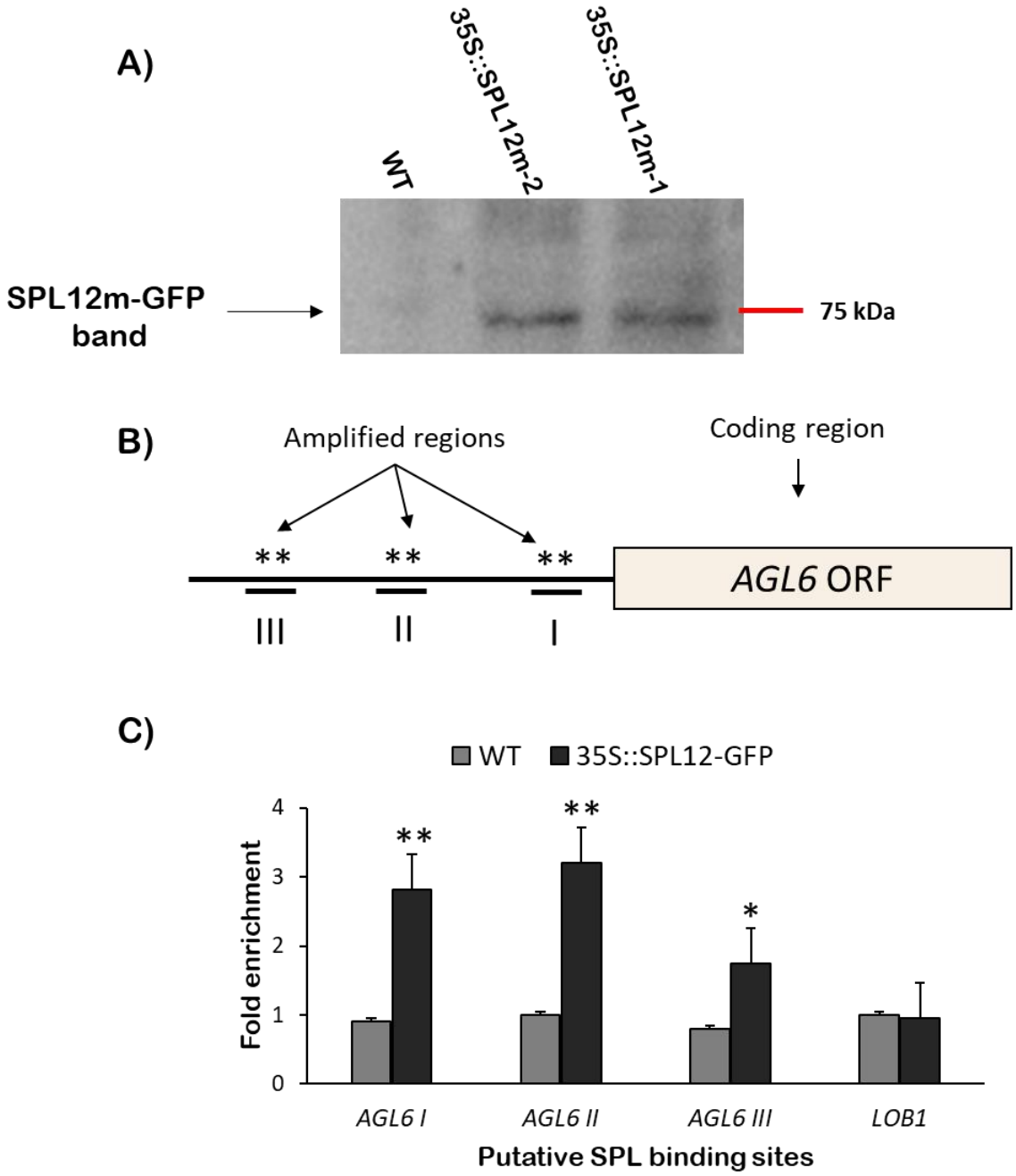
A)
WT
35S::SPL12m-2
35S::SPL12m-1
SPL12m-GFP band
75 kDa
B)
Amplified regions
Coding region
**
**
**
AGL6 ORF
III
II
I
C)
WT
35S::SPL12-GFP
Fold enrichment
0
1
2
3
4
**
**
*
AGL6 I
AGL6 II
AGL6 III
LOB1
Putative SPL binding sites

3.3.8 *AGL6* silencing enhances nodulation

Given the role of SPL12 in nodulation and in regulating *AGL6*, I used *AGL6*-RNAi transgenic alfalfa plants to further investigate the role of *AGL6* in nodulation traits in this plant. Of the 19 transgenic plants harboring the *AGL6*-RNAi construct I selected three genotypes (L9, L13A and L13B) that exhibited the lowest *AGL6* transcript levels (**Figure 3.16A**) for phenotypic comparison following inoculation with *S. meliloti*.

At 14 dai, the three *AGL6*-RNAi plants had approximately double the number of nodules compared to WT (**Figure 3.16B,C**), thus confirming the likely involvement of *AGL6* in regulating nodulation in alfalfa.

3.4 SPL12 and AGL6 affect nodulation in alfalfa under osmotic stress and nitrate application

The involvement of miR156 in regulating drought responses was previously demonstrated in alfalfa (Arshad et al. 2017a; Feyissa et al. 2019). Given the finding that *AGL6* is a direct target of SPL12 (**Figure 3.15**), a confirmed target of miR156 (Aung et al. 2015), I used *SPL12*-RNAi and *AGL6*-RNAi plants in subsequent experiments to determine if SPL12 and AGL6 affect nodulation under osmotic stress and nitrate treatment.

3.4.1 Effect of *SPL12* silencing on response to osmotic stress

To determine whether *SPL12* is regulated in response to osmotic stress, the *SPL12* transcript levels were assessed in six-week-old WT alfalfa plants treated with 400 mM mannitol (to mimic osmotic stress) (Vera-Estrella et al. 2004) for three weeks. The transcript

Figure 3.16 Effect of the *AGL6* silencing on nodulation

A) Relative *AGL6* transcript levels in *AGL6*-RNAi plants. Transcript levels are relative to WT after being normalized to *Cyclo* and *ADF* reference genes. **B)** Nodule phenotypes of WT and *AGL6*-RNAi genotypes at 14 dai. **C)** The number of nodules in WT and *AGL6*-RNAi at 14 dai (n = 9-11). * and ** indicate significant differences relative to WT using Student's t-test $p < 0.05$, $p < 0.01$, respectively. Error bars indicate standard deviation.

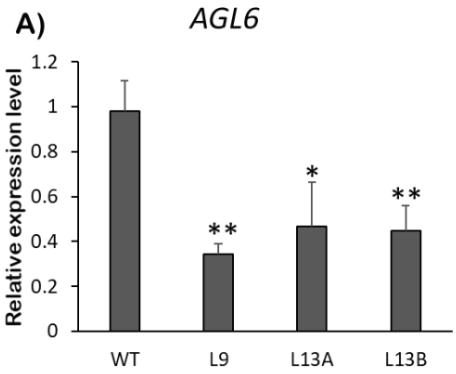
A)
AGL6
Relative expression level
1.2
1
0.8
0.6
0.4
0.2
0
**
*
**
WT
L9
L13A
L13B

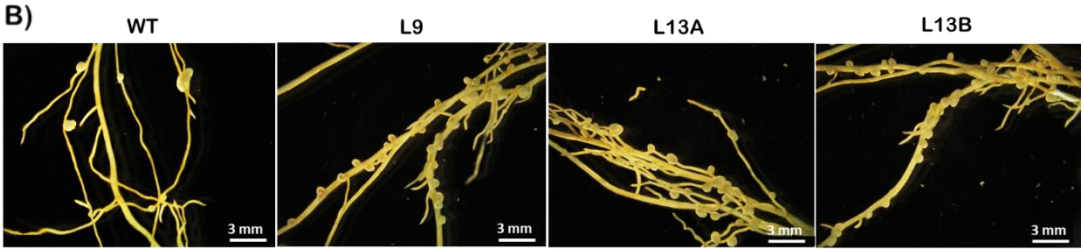
B)
WT
L9
L13A
L13B
3 mm
3 mm
3 mm
3 mm

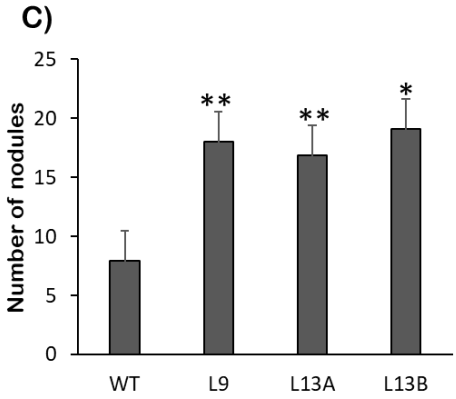
C)
Number of nodules
25
20
15
10
5
0
**
**
*
WT
L9
L13A
L13B

abundance of *SPL12* was significantly increased (1.4 fold) under osmotic stress compared to well-watered control treatment (**Figure 3.17A**). *SPL12*-RNAi plants appeared to tolerate stress better than WT plants because, after three weeks of stress, viable green leaves were observed in *SPL12*-RNAi plants but not in WT plants (**Figure 3.17B**).

To understand the role of *SPL12* in osmotic tolerance response, additional experiments were performed on *SPL12*-RNAi and WT alfalfa plants, where phenotypic parameters of plants were recorded. After three weeks of osmotic treatment, *SPL12*-RNAi root length, and both lateral and main root numbers were affected by osmotic stress to various degrees depending on the genotype (**Figure 3.17C,D,E**). Only WT showed a decrease in root length due to osmotic stress, whereas the *SPL12*-RNAi plants maintained root growth (**Figure 3.17C**). Maintenance of root growth by *SPL12*-RNAi also included the number of adventitious roots regenerated from the stems under osmotic stress, while WT plants showed a reduction over the three weeks of stress (**Figure 3.17D**). Furthermore, an increase in lateral root numbers was observed in one of the *SPL12*-RNAi genotypes (RNAi12-7) relative to WT under control condition, and in all of the *SPL12*-RNAi transgenic plants under stress conditions (**Figure 3.17E**).

3.4.2 *SPL12* silencing mitigates nodulation inhibition under osmotic stress

To gain an insight into the function of SPL12 in nodulation under osmotic stress, three weeks after cutting, the rooted *SPL12*-RNAi transgenic plants were inoculated with *S. meliloti* and also treated with mannitol (400 mM) for three weeks (21 dai).

Figure 3.17 Effect of *SPL12* silencing on response to osmotic stress

A) Relative *SPL12* transcript levels in WT alfalfa exposed to control and osmotic stress (400 mM mannitol) conditions after normalizing to *Cyclo* and *ACTB* reference genes. * indicates significant differences between conditions using Student's t-test $p < 0.05$. **B)** Representative WT and *SPL12*-RNAi plants that were exposed to osmotic stress (400 mM mannitol) for three weeks (n = 11-14). **C)** Root length; **D)** Number of main roots; and **E)** Number of lateral roots of WT and *SPL12*-RNAi alfalfa under control and osmotic stress (400 mM mannitol) conditions (n = 11-14). * and ** indicate significant differences within conditions between WT and *SPL12*-RNAi plants and bars indicate significant differences between conditions using Student's t-test $p < 0.05$, $p < 0.01$, respectively. Error bars indicate standard deviation.

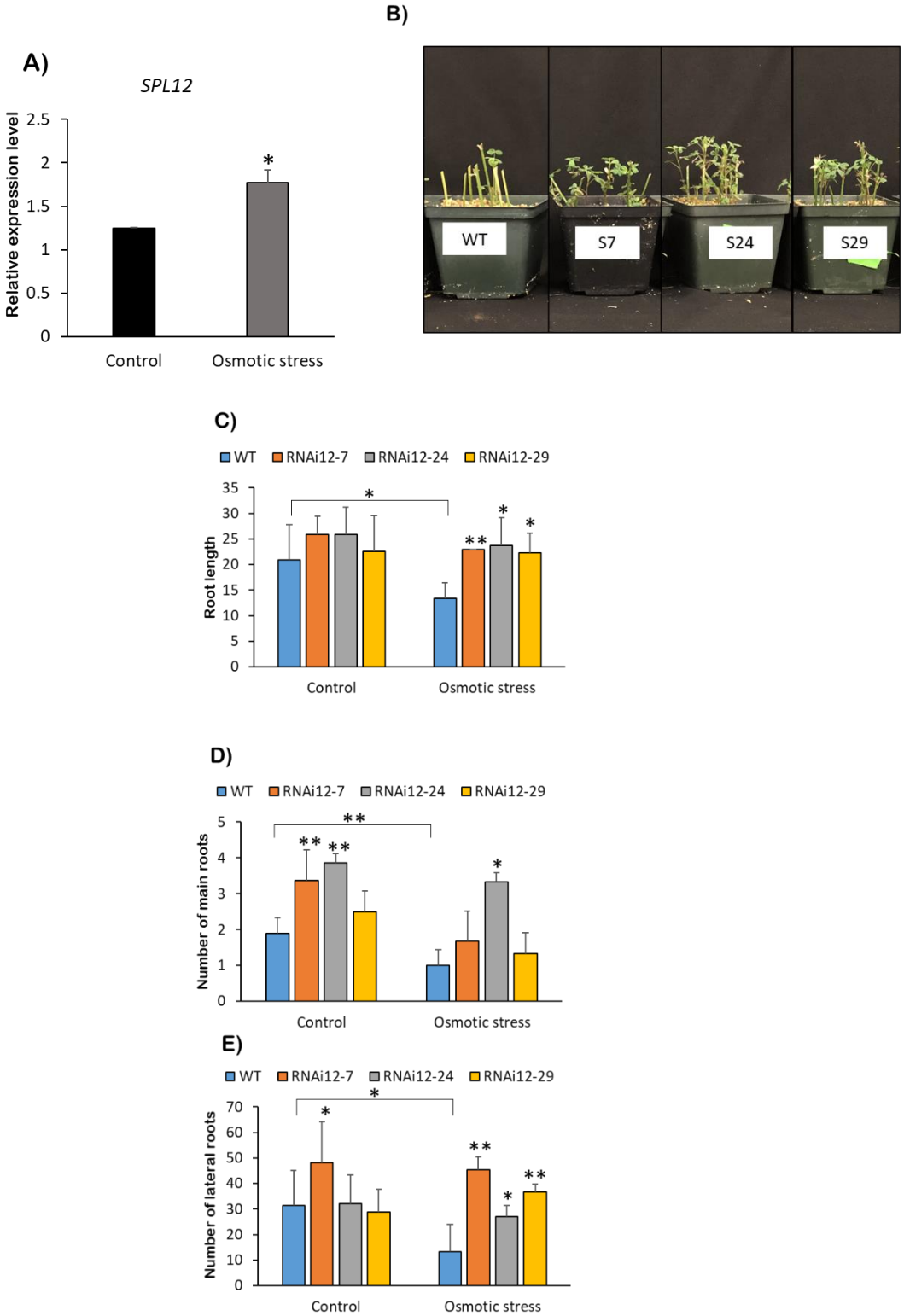
A)
SPL12
Relative expression level
2.5
2
1.5
1
0.5
0
*
Control
Osmotic stress
B)
WT
S7
S24
S29
C)
WT
RNAi12-7
RNAi12-24
RNAi12-29
Root length
35
30
25
20
15
10
5
0
*
**
*
*
Control
Osmotic stress
D)
WT
RNAi12-7
RNAi12-24
RNAi12-29
Number of main roots
5
4
3
2
1
0
**
**
**
*
Control
Osmotic stress
E)
WT
RNAi12-7
RNAi12-24
RNAi12-29
Number of lateral roots
70
60
50
40
30
20
10
0
*
*
**
*
**
Control
Osmotic stress

When comparing the number of nodules in well-watered (treated with distilled water) and mannitol-treated plants (**Figure 3.18A**), WT plants showed a decrease in nodulation, while *SPL12*-RNAi genotypes maintained nodulation after three weeks of osmotic stress (**Figure 3.18B**). Considering the increased nodule numbers in *SPL12*-RNAi plants at 14 dai (**Section 3.2.4, Figure 3.7B**), I also tested the nodulation capacity of *SPL12*-RNAi plants at 14 dai under osmotic stress (**Figure 3.18**). In line with this, under well-watered conditions, *SPL12*-RNAi transgenic plants produced significantly more nodules compared to WT. Following 400 mM mannitol treatment, the nodule number was reduced in WT compared to well-watered condition at 14 dai (**Figure 3.18C**), but the transgenic *SPL12*-RNAi plants maintained nodulation after two weeks of osmotic stress (**Figure 3.18C**).

3.4.3 Changes in the transcript levels of *AGL21* and *AGL6* in *SPL12*-RNAi alfalfa under osmotic stress

To shed light on the molecular events associated with SPL12 function under osmotic stress conditions, I investigated the effect of mannitol treatment on the transcript levels of *AGL6*, *AGL21* (regulated by SPL12) and *CLE13* (which negatively regulates nodulation) in WT and *SPL12*-RNAi alfalfa. The results showed that there were significant differences of transcript levels between plants under stress and control conditions (**Figure 3.19**). As expected, the transcript level of *AGL21* was significantly higher in all of the *SPL12*-RNAi plants compared to WT under control condition (**Figure 3.19A**). Under stress, *AGL21* was also significantly higher in *SPL12*-RNAi genotypes compared to WT, except for RNAi12-7, but was downregulated in WT. Two of the *SPL12*-RNAi genotypes (RNAi12-24 and RNAi12-29) showed no significant differences between the two

Figure 3.18 Effect of *SPL12* silencing on nodulation under osmotic stress

A) Phenotypes of nodules of WT and *SPL12*-RNAi plants that were exposed to osmotic stress (400 mM mannitol) at 21 dai. **B)** The number of nodules in WT and *SPL12*-RNAi alfalfa plants under control and osmotic stress (400 mM mannitol) conditions (n = 12-14) at 21 dai and **C)** at 14 dai (n = 10-12 plants). * and ** indicate significant differences within conditions between WT and *SPL12*-RNAi plants and bars indicate significant differences between conditions using Student's t-test $p < 0.05$, $p < 0.01$, respectively. Error bars indicate standard deviation.

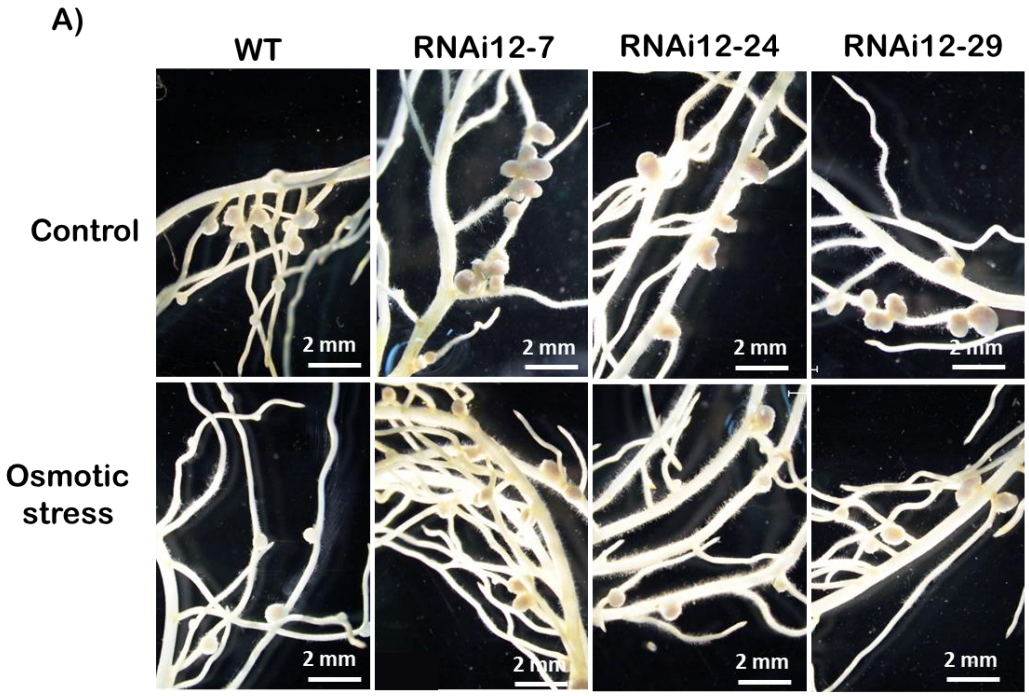
A)
WT
RNAi12-7
RNAi12-24
RNAi12-29
Control
Osmotic stress
2 mm

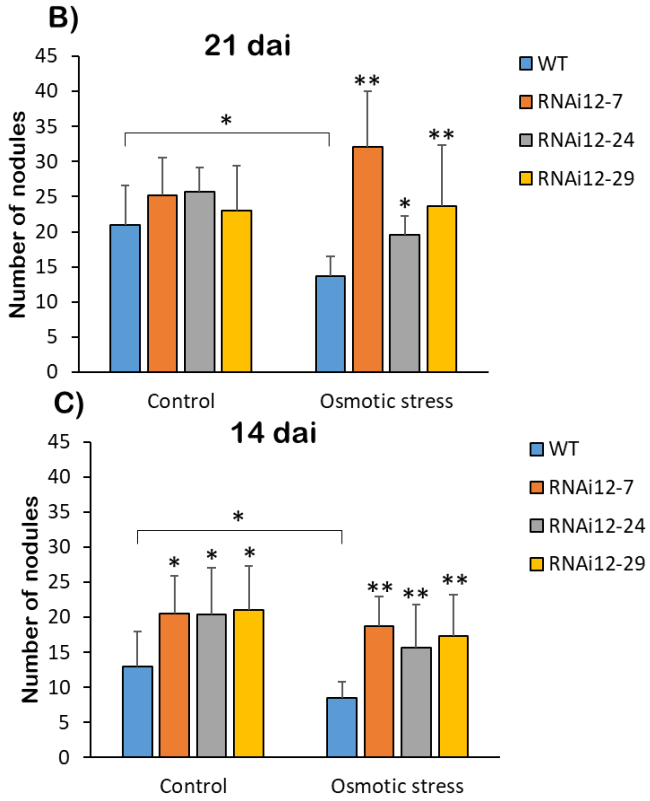
B)
21 dai
Number of nodules
Control
Osmotic stress
WT
RNAi12-7
RNAi12-24
RNAi12-29
C)
14 dai
Number of nodules
Control
Osmotic stress
WT
RNAi12-7
RNAi12-24
RNAi12-29

Figure 3.19 Transcript levels of *AGL21*, *AGL6* and *CLE13* in *SPL12*-RNAi and WT alfalfa under osmotic stress

Relative transcript levels of **A)** *AGL21*, **B)** *AGL6* and **C)** *CLE13* in WT and *SPL12*-RNAi alfalfa exposed to three weeks of osmotic stress (400 mM mannitol). Transcript levels are shown relative to WT after being normalized to *Cyclo* and *ACTB* reference genes. * and ** indicate significant differences within conditions between WT and *SPL12*-RNAi plants and bars indicate significant differences between conditions using Student's t-test $p < 0.05$, $p < 0.01$, respectively and $n = 3$. Error bars indicate standard deviation.

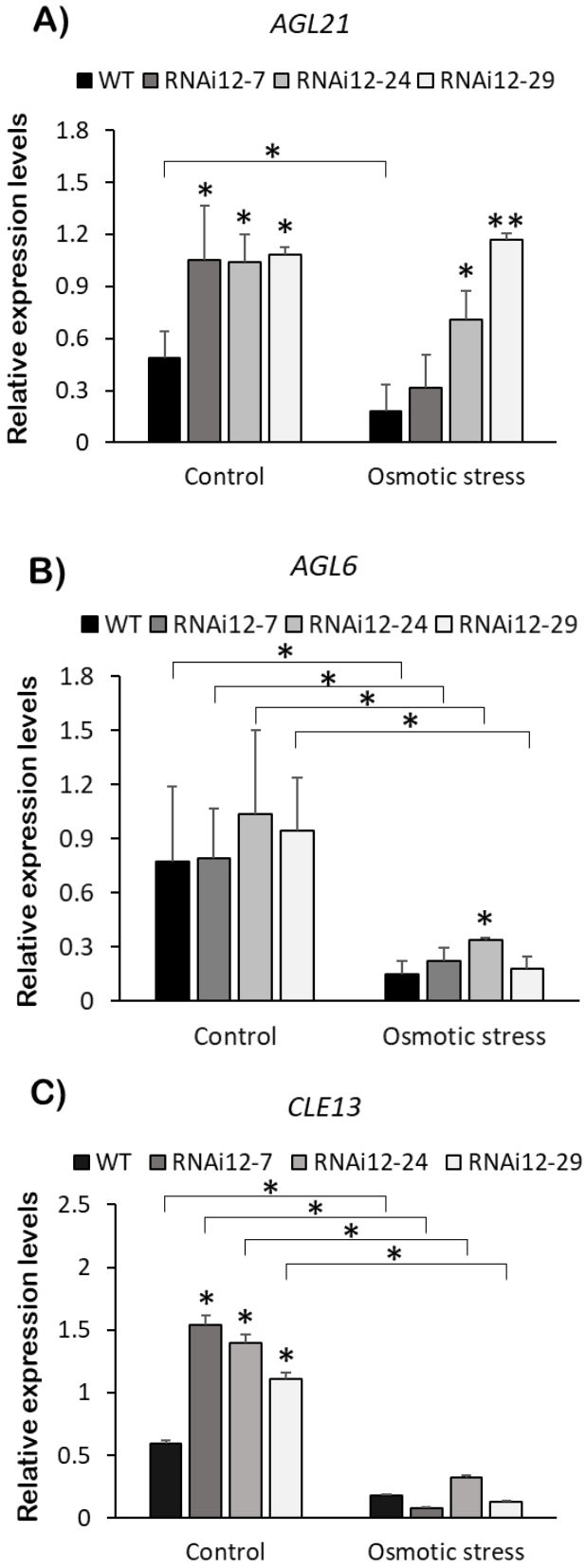
A)
AGL21
WT RNAi12-7 RNAi12-24 RNAi12-29
Relative expression levels
1.8
1.5
1.2
0.9
0.6
0.3
0
Control
Osmotic stress
B)
AGL6
WT RNAi12-7 RNAi12-24 RNAi12-29
Relative expression levels
1.8
1.5
1.2
0.9
0.6
0.3
0
Control
Osmotic stress
C)
CLE13
WT RNAi12-7 RNAi12-24 RNAi12-29
Relative expression levels
2.5
2
1.5
1
0.5
0
Control
Osmotic stress

conditions (**Figure 3.19A**). For *AGL6*, significantly lower transcript levels were detected in WT and *SPL12*-RNAi transgenic plants under stress condition compared to counterpart plants grown under control condition (**Figure 3.19B**). However, no significant changes in *AGL6* transcript levels were detected in *SPL12*-RNAi genotypes compared to WT under neither control nor osmotic stress conditions except for RNAi12-24 under osmotic stress (**Figure 3.19B**).

Given that, under osmotic stress, *SPL12*-RNAi plants at 21 dai produced more nodules compared to WT, I analyzed the transcript levels of *CLE13* (which inhibits nodulation), and found a decrease in transcript levels under osmotic stress in all genotypes relative to control condition (**Figure 3.19C**). Under control condition, *CLE13* transcript levels were higher in *SPL12*-RNAi plants relative to WT, while under stress condition there was no significant change (**Figure 3.19C**), which is consistent with results of nodulation in *SPL12*-RNAi and WT at 21 dai (**Figure 3.7C**).

3.4.4 Sulfate transporters are enhanced in *SPL12*-silenced plants

There is a high demand for sulfur in nodulating legumes, and nitrogen fixation is more sensitive to sulfur deficiency than to nitrate uptake (Varin et al. 2010). A good supply of sulfur enhances nodulation and nitrogen fixation (Anderson and Spencer 1950; Varin et al. 2010). RNA-seq analysis in RNAi12-24 and RNAi12-29 revealed that two Group3 *SULTR* genes, *SULTR3.4* and *SULTR3.5*, were significantly upregulated in *SPL12*-RNAi plants (**Figure 3.20A,B**); a finding that was confirmed by RT-qPCR (**Figure 3.20C,D**). Since, *SULTR3.4* and *SULTR3.5* are members of Group3 *SULTRs* which are strongly regulated by abiotic stress in plant roots (Gallardo et al. 2014), I decided to investigate their transcript

Figure 3.20 Relative transcript levels of sulfate transporter genes based on NGS and RT-qPCR in WT and *SPL12*-RNAi alfalfa plants

Relative transcript levels of **A)** *SULTR3.4* and **B)** *SULTR3.5* in WT and *SPL12*-RNAi plants as determined by NGS. ** indicates a significant difference between WT and *SPL12*-RNAi plants. Relative transcript levels of **C)** *SULTR3.4* and **D)** *SULTR3.5* in WT and *SPL12*-RNAi plants as determined by RT-qPCR. In '**C**' and '**D**' transcript levels are shown relative to WT after being normalized to *Cyclo* and *ACTB* reference genes, and * and ** indicate significant differences between WT and *SPL12*-RNAi plants using Student's t-test $p < 0.05$, $p < 0.01$, respectively and $n = 3$. Relative transcript levels of **E)** *SULTR3.4* and **F)** *SULTR3.5* in WT and *SPL12*-RNAi alfalfa exposed to three weeks of osmotic stress. Transcript levels in '**E**' and '**F**' are shown relative to WT after being normalized to *Cyclo* and *ACTB* reference genes. * and ** indicate significant differences within conditions between WT and *SPL12*-RNAi plants and bars indicate significant differences between conditions using Student's t-test $p < 0.05$, $p < 0.01$, respectively and $n = 3$. Error bars indicate standard deviation.

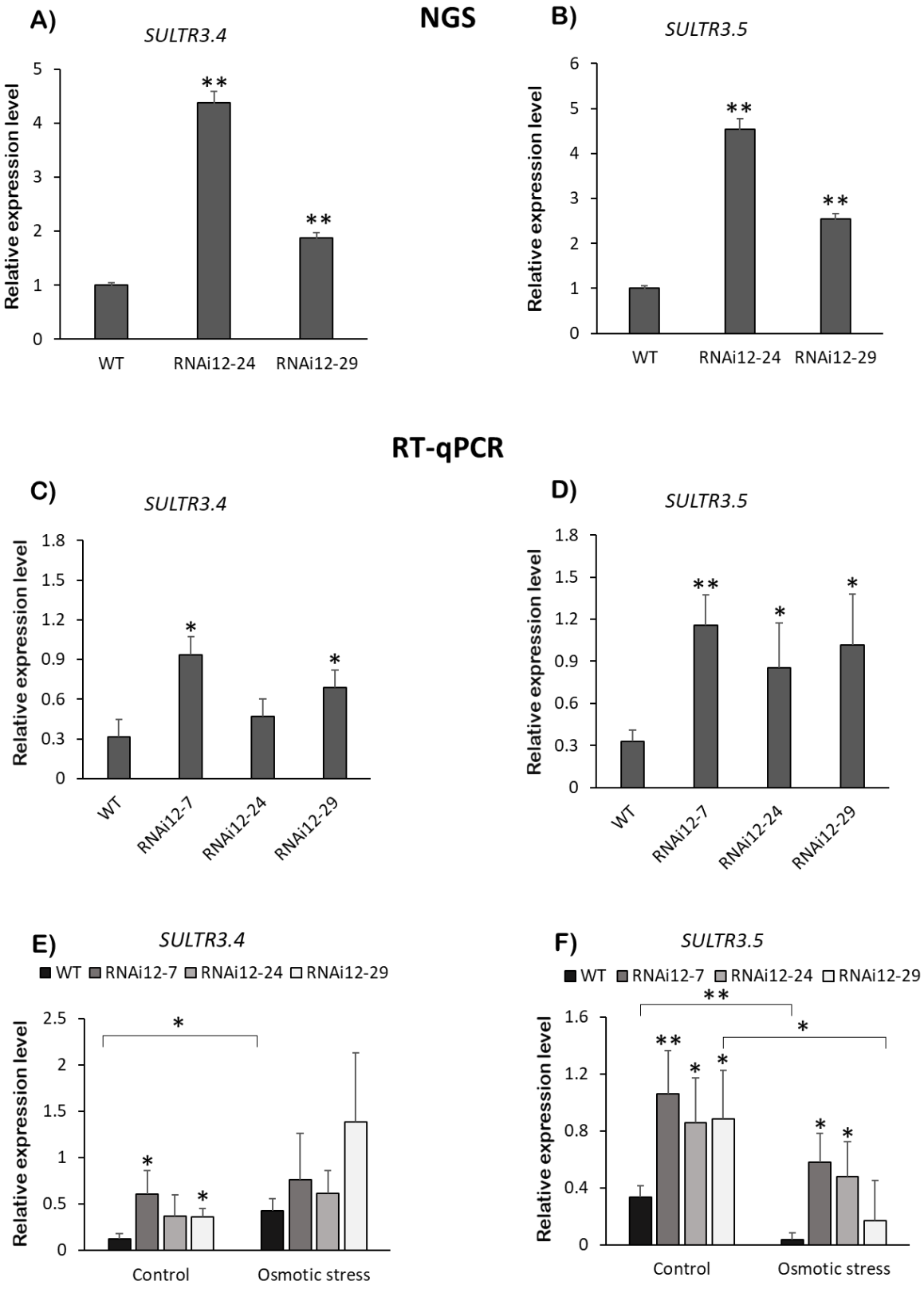
NGS
A)
SULTR3.4
Relative expression level
WT
RNAi12-24
RNAi12-29
B)
SULTR3.5
Relative expression level
WT
RNAi12-24
RNAi12-29
RT-qPCR
C)
SULTR3.4
Relative expression level
WT
RNAi12-7
RNAi12-24
RNAi12-29
D)
SULTR3.5
Relative expression level
WT
RNAi12-7
RNAi12-24
RNAi12-29
E)
SULTR3.4
WT RNAi12-7 RNAi12-24 RNAi12-29
Relative expression level
Control
Osmotic stress
F)
SULTR3.5
WT RNAi12-7 RNAi12-24 RNAi12-29
Relative expression level
Control
Osmotic stress

levels under osmotic stress. WT alfalfa plants had higher *SULTR3.4* levels under osmotic stress compared to WT plant under control condition, but *SULTR3.4* abundance in *SPL12*-RNAi plants did not change between treatments (**Figure 3.20E**). It was noted that *SULTR3.4* expression in RNAi12-7 and RNAi12-29 was higher than in WT under control conditions. WT and RNAi12-29 plants showed a decrease in *SULTR3.5* abundance in response to osmotic stress, whereas RNAi12-7 and RNAi12-24 plants were able to maintain their levels of *SULTR3.5* (**Figure 3.20F**).

When considering the plants under the stress condition only, RNAi12-7 and RNAi12-24 had an enhanced *SULTR3.5* transcript level compared to WT. *SULTR3.5* expression in well-watered *SPL12*-RNAi plants was higher than in WT (**Figure 3.20F**).

3.4.5 Effect of *SPL12* silencing on expression of stress-related genes under mannitol treatment

The effect of drought on expression of antioxidant-related *glutathione synthase* (*GSH*) (Innocenti et al. 2007) and the stress responsive transcription factor *WD40–1* (Pang et al. 2009) was previously reported in alfalfa. Enhanced levels of *GSH* and *WD40-1* in miR156-OE alfalfa under drought stress in leaves and roots, respectively, were also reported by Arshad et al. (2017a) and Feyissa et al. (2019). In the current study, I examined the transcript abundance of *GSH* and *WD40–1* to determine whether SPL12 serves to maintain the transcript levels of these genes in alfalfa exposed to osmotic stress. While the transcript levels of *GSH* increased in well-watered RNAi12-7 and RNAi12-24 compared to WT plants (**Figure 3.21A**), it did not show a change in *SPL12*-RNAi and WT plants between

Figure 3.21 Relative transcript levels of stress-related genes in response to osmotic stress

Transcript levels of **A)** *GSH* and **B)** *WD40-1* in WT and *SPL12*-RNAi roots under osmotic and control conditions. Transcript levels are shown relative to WT after being normalized to *Cyclo* and *ACTB* reference genes. * and ** indicate significant differences within conditions between WT and *SPL12*-RNAi plants and bars indicate significant differences between conditions using Student's t-test $p < 0.05$, $p < 0.01$, respectively and $n = 3$. Error bars indicate standard deviation.

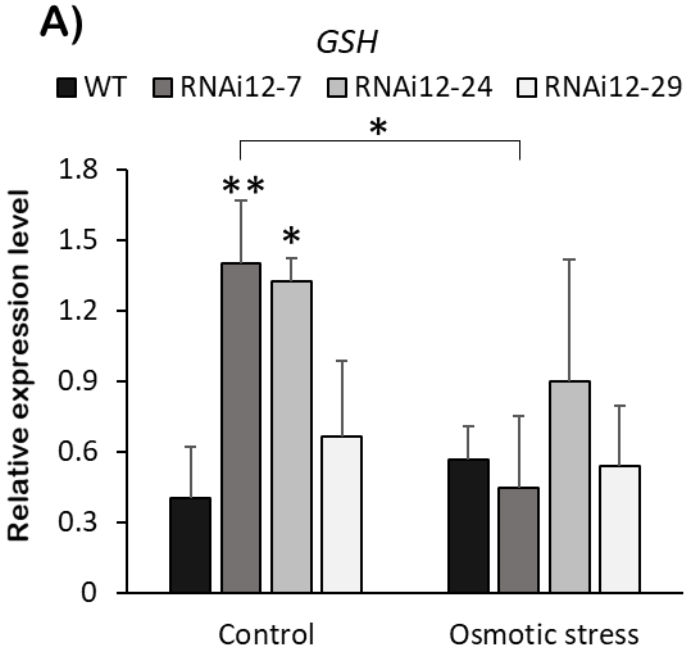
A)
GSH
WT
RNAi12-7
RNAi12-24
RNAi12-29
Relative expression level
1.8
1.5
1.2
0.9
0.6
0.3
0
Control
Osmotic stress

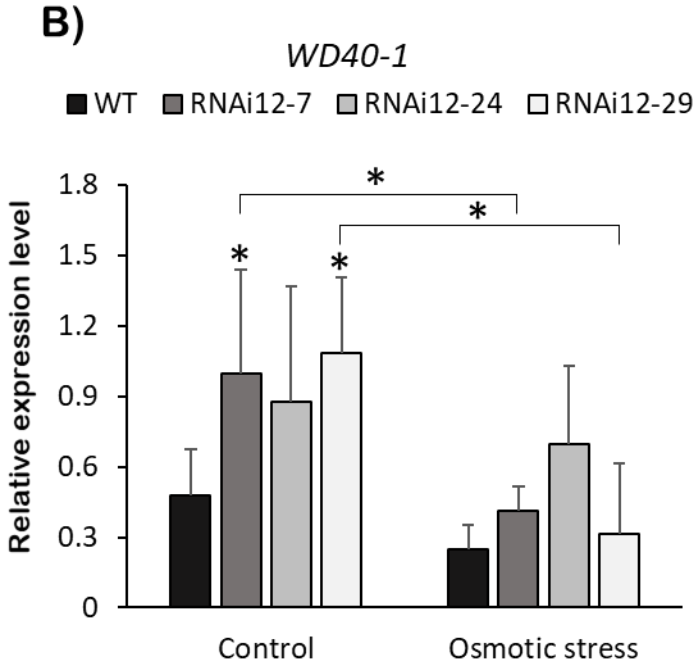
B)
WD40-1
WT
RNAi12-7
RNAi12-24
RNAi12-29
Relative expression level
1.8
1.5
1.2
0.9
0.6
0.3
0
Control
Osmotic stress

the two conditions. In fact, *GSH* was decreased in RNAi12-7 under stress relative to control (**Figure 3.21A**). Similarly, for *WD40-1* transcript levels, RNAi12-7 and RNAi12-29 showed an increase under control treatment compared to WT plants (**Figure 3.21B**), but there was no change between *SPL12*-RNAi and WT plants under osmotic stress, with *WD40-1* showing even a decrease in RNAi12-7 and RNAi12-29 under stress relative to control (**Figure 3.21B**).

3.4.6 *AGL6* silencing maintains nodulation under osmotic stress

With the observed lower transcript levels of *AGL6* in WT and *SPL12*-RNAi plants during osmotic stress (**Figure 3.22B**), and considering the direct regulation of *AGL6* by SPL12 (**Figure 3.15**), I set out to investigate the potential role of AGL6 in alfalfa's response to this stress. Three-week-old rooted *AGL6*-RNAi and WT plants were inoculated with *S. meliloti* and treated with mannitol (400 mM) for two weeks (14 dai) or three weeks (21 dai). The number of nodules was compared in control and mannitol-treated plants 21 dai (**Figure 3.22A**). At 14 dai, *AGL6*-RNAi transgenic plants produced significantly more nodules compared to WT under well-watered condition (**Figure 3.22B**). Upon treatment with 400 mM mannitol, the nodule number was reduced in WT, but there was no change in nodule numbers in *AGL6*-RNAi between the two conditions, showing that *AGL6*-RNAi plants maintained nodulation after two weeks of osmotic stress (**Figure 3.22B**). At 21 dai, stressed WT plants had a lower nodule number when compared to well-watered WT and stressed *AGL6*-RNAi plants, while *AGL6*-RNAi genotypes maintained nodulation after three weeks of stress (**Figure 3.22C**), thus confirming the likely involvement of *AGL6* in regulating nodulation under osmotic stress.

Figure 3.22 The effect of *AGL6* silencing on nodulation under osmotic stress

A) Nodule phenotypes of WT and *AGL6*-RNAi genotypes that were exposed to osmotic stress at 21 dai. **B)** Number of nodules in WT and the *AGL6*-RNAi alfalfa under control and osmotic stress (400 mM mannitol) conditions (n = 12-15) at 14 dai, and **C)** 21 dai (n = 8-11 plants). * and ** indicate significant differences relative to WT within conditions and bars indicate significant differences between conditions using Student's t-test $p < 0.05$, $p < 0.01$, respectively. Error bars indicate standard deviation.

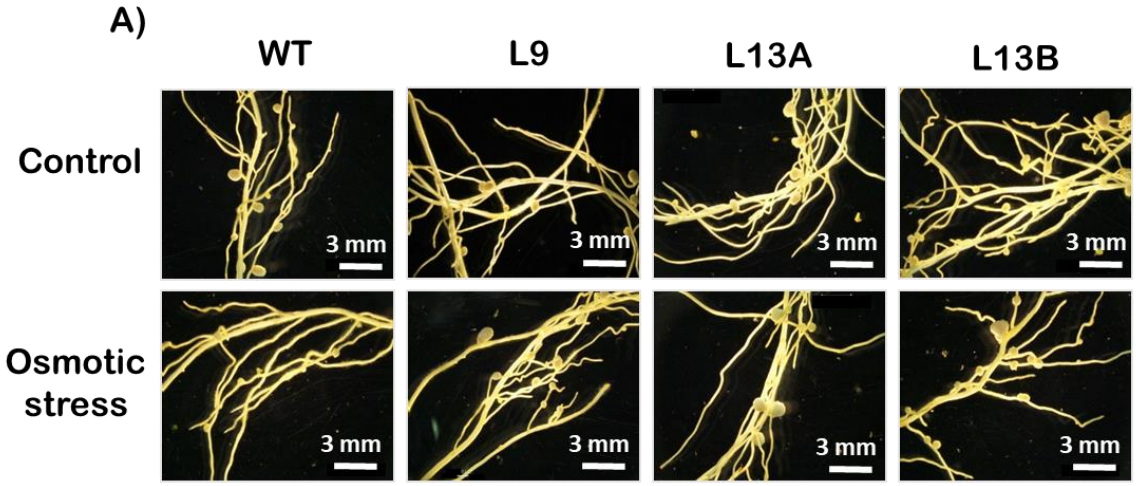
A)
WT
L9
L13A
L13B
Control
Osmotic stress
3 mm

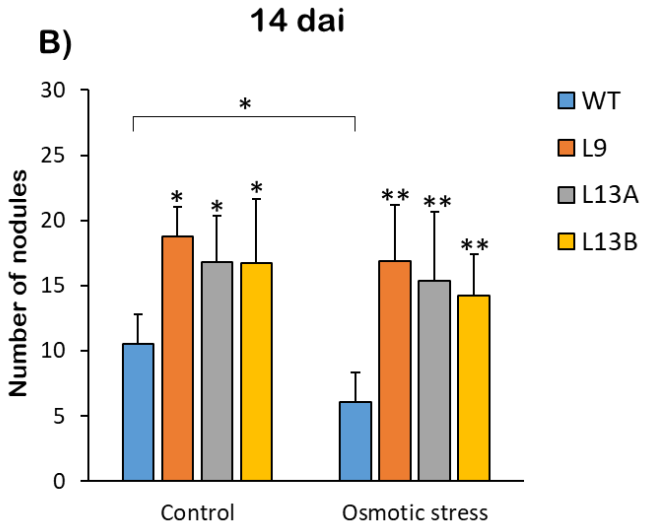
B)
14 dai
Number of nodules
30
25
20
15
10
5
0
*
**
Control
Osmotic stress
WT
L9
L13A
L13B

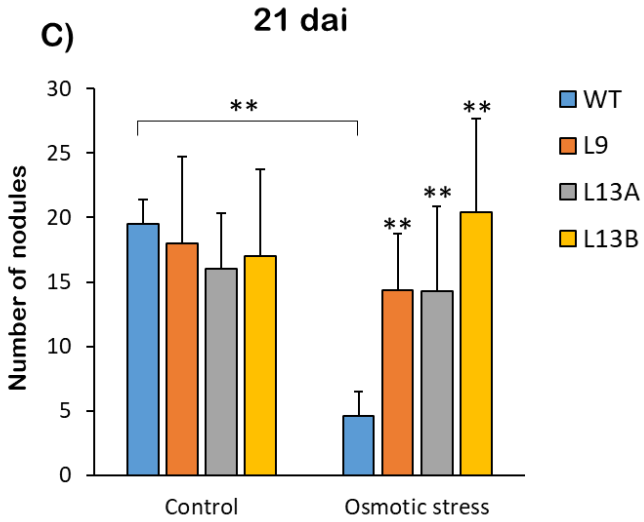
C)
21 dai
Number of nodules
30
25
20
15
10
5
0
**
Control
Osmotic stress
WT
L9
L13A
L13B

3.4.7 *SPL12* silencing reduces effect of nitrate on nodulation

Nitrogen abundance in the soil inhibits nodulation, and this regulatory process is a part of the AON pathway (Moreau et al. 2021; Streeter and Wong 1988). Given the effects of SPL12 on nodulation (**Figure 3.7**), I assessed if the number of nodules in *SPL12*-RNAi plants was affected by nitrate treatment. The number of nodules was compared between WT and *SPL12*-RNAi plants treated with 3 mM, 8 mM and 20 mM KNO_3 or KCl, at 21 dai. There were no significant changes in nodulation between the plants that were watered with 3 mM KCl or KNO_3 (**Figure S3**). All plants that were watered with KCl (8 mM and 20 mM) formed active nitrogen-fixing nodules that were pink-colored (containing leghaemoglobin) (**Figure 3.23A; Figure 3.24A**), with no significant difference in the number of either white (nodules not active in fixing nitrogen) or pink nodules between *SPL12*-RNAi and WT plants (**Figure 3.23B; Figure 3.24B**). When watered with 8 mM KNO_3, all *SPL12*-RNAi plants formed significantly more mature pink nodules relative to WT (**Figure 3.23C**). When treating with 20 mM KNO_3, WT plants formed only small white nodules, while RNAi12-24 and RNAi12-29 plants produced significantly more pink nodules (**Figure 3.24C**). These results suggest that SPL12 may be involved in preventing nitrate inhibition of nodulation in alfalfa.

3.4.8 Effect of nitrate on expression of *SPL12* and *AGL21*

To shed light on the possible role of SPL12 in nitrate inhibition of nodulation, I determined whether the transcript levels of *SPL12* and *AGL21* were regulated by nitrate. *AGL21* in alfalfa is closely related to ANR1 clade in Arabidopsis (**Figure 3.25A**). *At*ANR1, a

Figure 3.23 Effect of 8 mM nitrate on nodulation phenotype in *SPL12*-RNAi roots

A) Nodule phenotypes in WT and *SPL12*-RNAi genotypes at 21 dai growing in nitrate-starved media and watered with 8 mM KCl or KNO_3. The average numbers of pink and white nodules in WT and the *SPL12*-RNAi at 21 dai (n = 15-22 plants) under 8 mM **B)** KCl and **C)** KNO_3. * indicates significant differences in the number of pink nodules (active nodules) in *SPL12*-RNAi plants relative to WT using Student's t-test $p < 0.05$. Error bars indicate standard deviation.

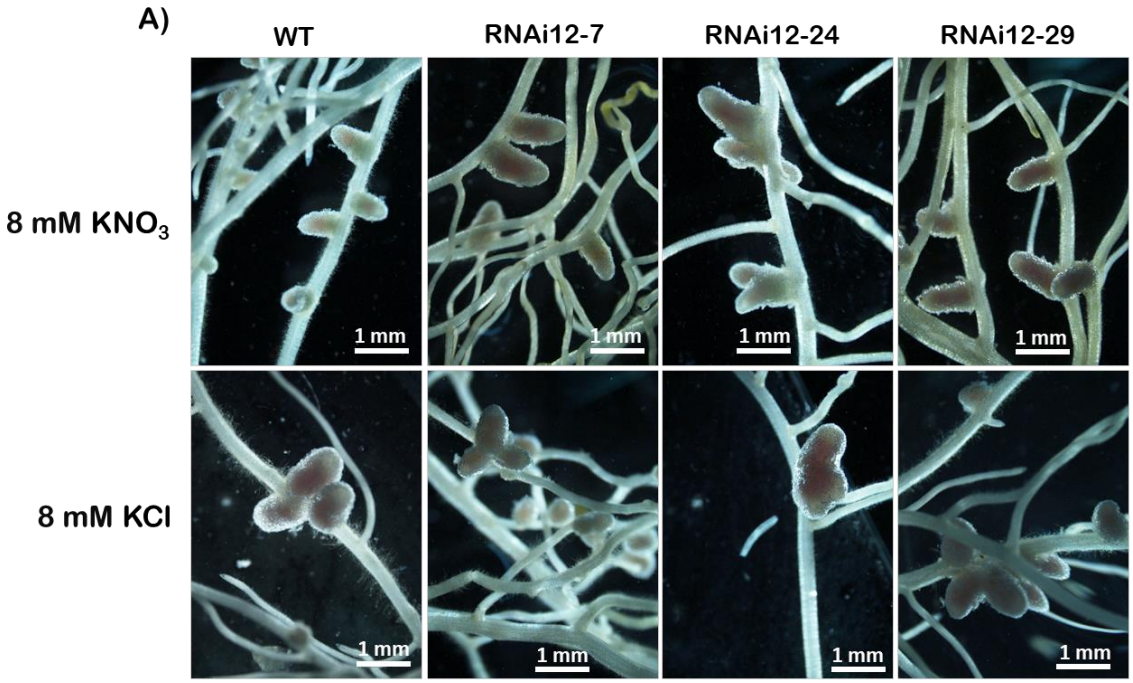
A)
WT
RNAi12-7
RNAi12-24
RNAi12-29
8 mM KNO3
8 mM KCl
1 mm

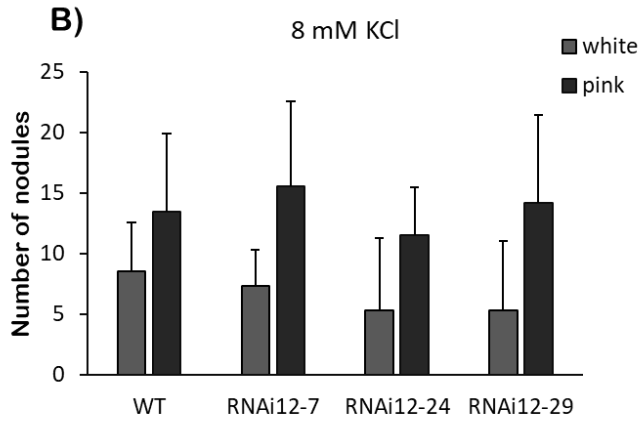
B)
8 mM KCl
white
pink
Number of nodules
0
5
10
15
20
25
WT
RNAi12-7
RNAi12-24
RNAi12-29

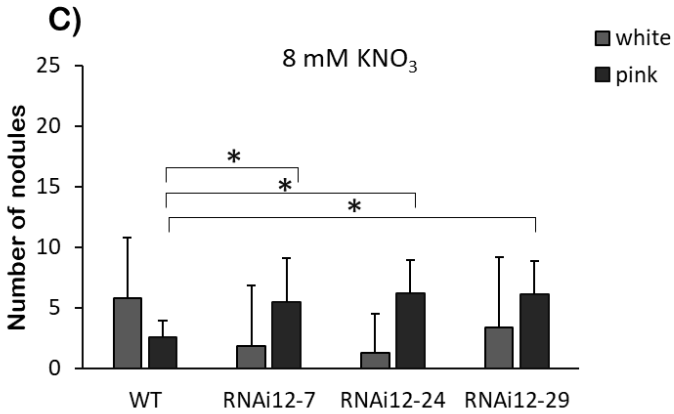
C)
8 mM KNO3
white
pink
Number of nodules
0
5
10
15
20
25
*
*
*
WT
RNAi12-7
RNAi12-24
RNAi12-29

Figure 3.24 Effect of 20 mM nitrate on nodulation phenotype in *SPL12*-RNAi roots

A) Nodule phenotypes of WT and the *SPL12*-RNAi genotypes at 21 dai growing in nitrate-starved substrate and watered with 20 mM KCl or KNO_3,. The average numbers of pink and white nodules in WT and the *SPL12*-RNAi at 21 dai (n = 14-25 plants) under 20 mM **B)** KCl and **C)** KNO_3. * indicates significant differences in the number of pink nodules (active nodules) in *SPL12*-RNAi plants relative to WT using Student's t-test $p < 0.05$. Error bars indicate standard deviation.

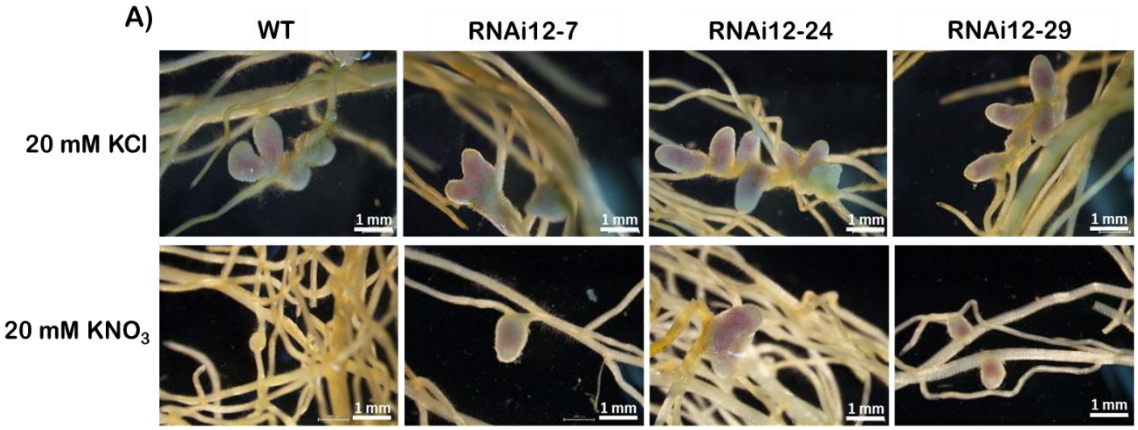
A)
WT
RNAi12-7
RNAi12-24
RNAi12-29
20 mM KCl
20 mM KNO3
1 mm

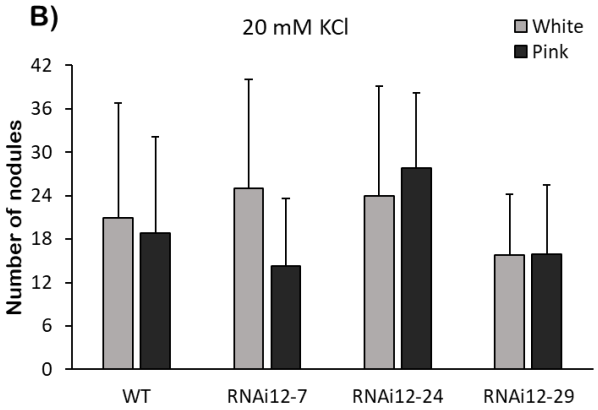
B)
20 mM KCl
White
Pink
Number of nodules
0
6
12
18
24
30
36
42
WT
RNAi12-7
RNAi12-24
RNAi12-29

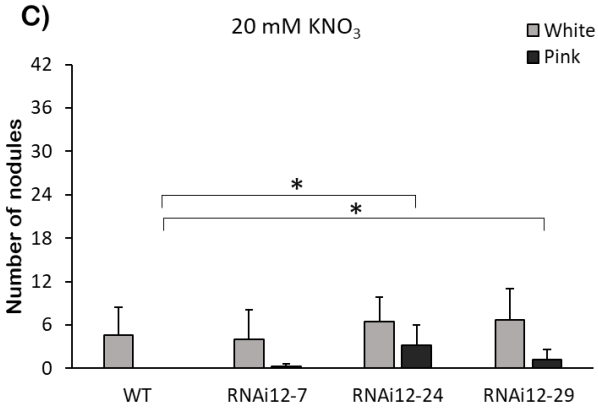
C)
20 mM KNO3
White
Pink
Number of nodules
0
6
12
18
24
30
36
42
*
*
WT
RNAi12-7
RNAi12-24
RNAi12-29

Figure 3.25 Phylogenetic tree of *M. truncatula* and Arabidopsis MADS-box proteins

A) Phylogenetic tree based on an alignment of the MADS-box domain and using publicly available sequences of *M. sativa*, *M. truncatula* and Arabidopsis. **B)** Relative transcript levels of *SPL12* and *AGL21* were analyzed in WT by RT-qPCR at 0, 5 and 24 hrs after 20 mM nitrate treatment. Transcript levels are normalized to *Cyclo* and *ACTB* reference genes. Significant difference from ANOVA was followed by *Post hoc* Tukey ($P<0.05$) multiple comparisons test indicated with different letters, and have been determined separately for *SPL12* and *AGL21* transcriptome abundance. Green box: ANR1 clade; Pink box: AGL21 in alfalfa.

A)

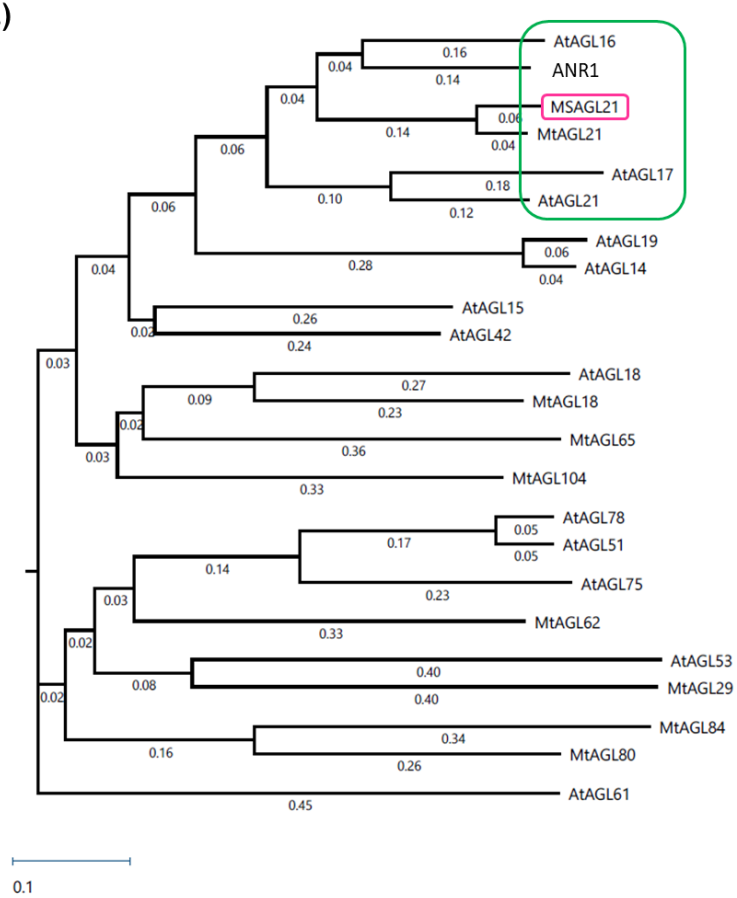
AtAGL16
ANR1
MSAGL21
MtAGL21
AtAGL17
AtAGL21
AtAGL19
AtAGL14
AtAGL15
AtAGL42
AtAGL18
MtAGL18
MtAGL65
MtAGL104
AtAGL78
AtAGL51
AtAGL75
MtAGL62
AtAGL53
MtAGL29
MtAGL84
MtAGL80
AtAGL61
0.1

B)

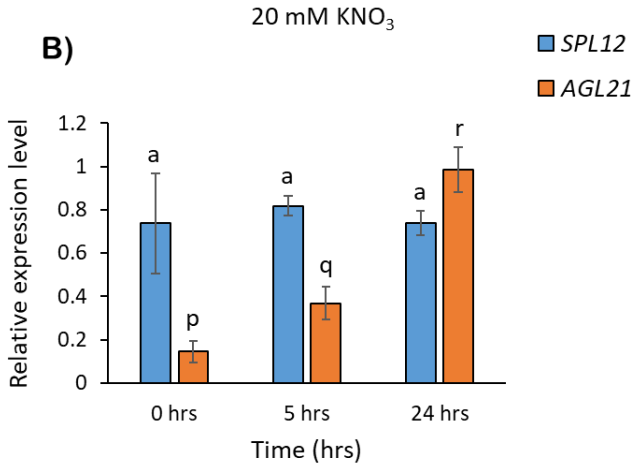
20 mM KNO3
SPL12
AGL21
Relative expression level
1.2
1
0.8
0.6
0.4
0.2
0
a
p
a
q
a
r
0 hrs
5 hrs
24 hrs
Time (hrs)

member of ANR1 clade, plays a role in the nitrate regulation of root development in Arabidopsis (Gan et al. 2012; Zhang and Forde 1998). Also, *AtAGL21*, another member of this clade is upregulated by nitrogen deprivation in Arabidopsis (Yu et al. 2014). Based on these findings, I hypothesized that AGL21 might be involved in the nitrate regulation of nodulation in alfalfa. To test this hypothesis, I investigated changes in the transcript levels of *AGL21* and *SPL12* under nitrate treatment (**Figure 3.25B**). The results showed that *AGL21* was increased at 5 hrs and 24 hrs of nitrate treatment in WT plants, but *SPL12* level did not change in response to KNO_3 treatment. Given that *AGL21* was increased in *SPL12*-RNAi plants (**Figure 3.13**), I propose that SPL12 is involved in regulating nitrate inhibition of nodulation in alfalfa by targeting *AGL21*.

3.4.9 SPL12 is a direct regulator of *AGL21*

As the results in section 3.2.5 suggested that *AGL21* might be regulated by SPL12, further characterization was carried out by ChIP-qPCR to determine if *AGL21* is a direct target of SPL12. The promoter region (2000 bp) of alfalfa *AGL21* has four putative SPL binding sequences with the core GTAC SBP binding consensus sequence that are distributed in three sites (I, II, III) (**Figure 3.26A**), and three of them (in sites I and III) possess the typical NNGTACR SBP binding consensus sequence (**Figure S4**). I tested these three sites for SPL12 occupancy using ChIP-qPCR analysis of *35S::SPL12m-GFP* plants. Compared to WT, *35S::SPL12m-GFP* plants showed significantly higher SPL12 binding at the listed sites (**Figure 3.26B**), and occupancy at the three sites was substantially higher than that in the negative control *LOB1* (**Figure 3.26B**), indicating that SPL12 is able to bind to multiple sites in the *AGL21* promoter to regulate its expression.

Figure 3.26 Detection of *SPL12* binding to *AGL21* promoter

A) Schematic representation of the promoter region of *AGL21*. Black box: coding sequences; asterisks: locations of putative SPL binding sites on *AGL21* promoter (amplified sites). Roman numerals (I, II and III): sites that were tested by qPCR. **B)** ChIP-qPCR-based fold enrichment analysis of SPL12 in *35S::SPL12m-GFP* and WT plants from means of n = three individual plants where *LATERAL ORGAN BOUNDARES-1* (*LOB1*) is used as a negative control. * and ** indicate significant differences relative to WT in each potential SPL12 binding sites (I, II and III) using Student's t-test (n = 3) $p < 0.05$, $p < 0.01$, respectively. Error bars indicate standard deviation.

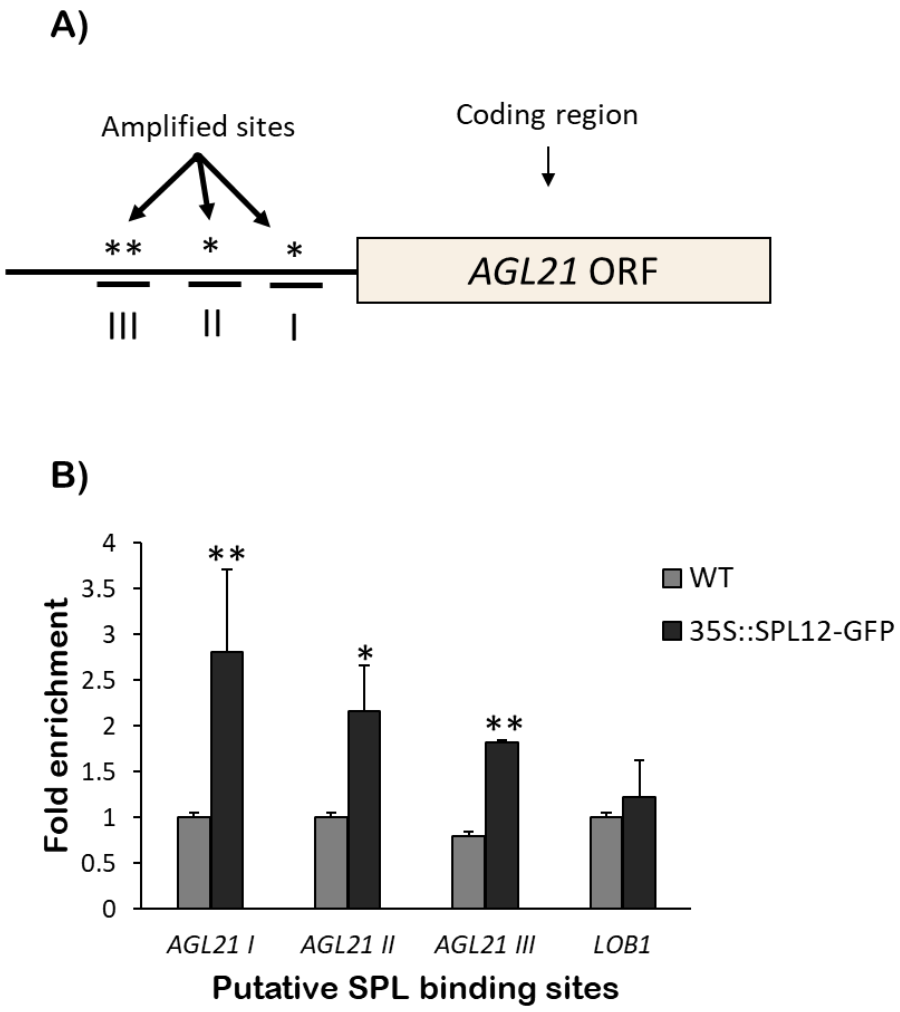
A)
Amplified sites
Coding region
**
*
*
AGL21 ORF
III
II
I
B)
Fold enrichment
4
3.5
3
2.5
2
1.5
1
0.5
0
**
*
**
WT
35S::SPL12-GFP
AGL21 I
AGL21 II
AGL21 III
LOB1
Putative SPL binding sites

3.5 Characterization of *Lotus japonicus spl12* mutants

To determine whether the role of SPL12 in nodulation in alfalfa is conserved in other legume species, I also investigated the function of its ortholog, *Lj*SPL12, in the model legume *L. japonicus*. For that, I made use of the *L. japonicus* retrotransposon (LORE1) mutation tool (Madsen et al. 2005). LORE1 is a long terminal repeat retrotransposon that amplifies in the *L. japonicus* genome by a copy-and-paste mechanism (Małolepszy et al. 2016). The presence of the 5.041-kb LORE1 sequence in coding (exonic) regions introduces multiple premature, translational stop codons (Urbański et al. 2012), which in many cases inactivate the genes and generate strong, null mutant alleles (Hossain et al. 2016; Madsen et al. 2005).

To begin addressing the functional relevance of *Lj*SPL12 during nodulation, the LORE1 retrotransposon insertion population (Małolepszy et al. 2016; Mun et al. 2016) was surveyed to identify mutant *spl12* alleles. Screening of the LORE1 insertion population (http://users-mb.au.dk/pmgrp/) allowed for the isolation of two candidate lines carrying insertions of LORE1 in exonic regions that were identified to disrupt *SPL12* by genotyping. The alleles were designated as *spl12-1* and *spl12-2* (**Figure 3.27A**). The genotype of the seedlings was confirmed using PCR-based genotyping (see section 2.4) for LORE1 insertion and the homozygous plants were identified. The genotyping results proved that the *spl12-1* and *spl12-2* seedlings were homozygous for both mutant alleles **(Figure 3.27B)**.

Figure 3.27 PCR genotyping of LORE1 insertions in *Lotus japonicus*

A) The intron-exon structure of the *spl12* gene is shown. Blue boxes represent predicted exons while lines denote 5' and 3' UTRs and introns. Red boxes show *spl12 L. japonicu*s LORE1 retrotransposon insertion with allele identification. The black arrows represent forward, reverse and P2 primer used for genotyping. **B)** Two combinations of primers were used to characterize a locus for WT or LORE1 insertion alleles. Primers “Forward” and “Reverse” are used to detect WT alleles, whereas “Forward” and “P2” for alleles with an insertion (Heterozygote and Homozygote).

A)

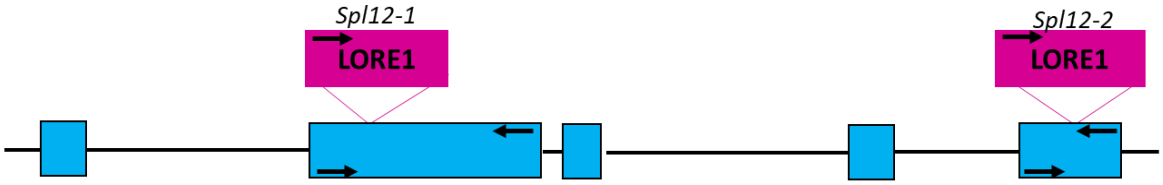
Spl12-1
LORE1
Spl12-2
LORE1

B)

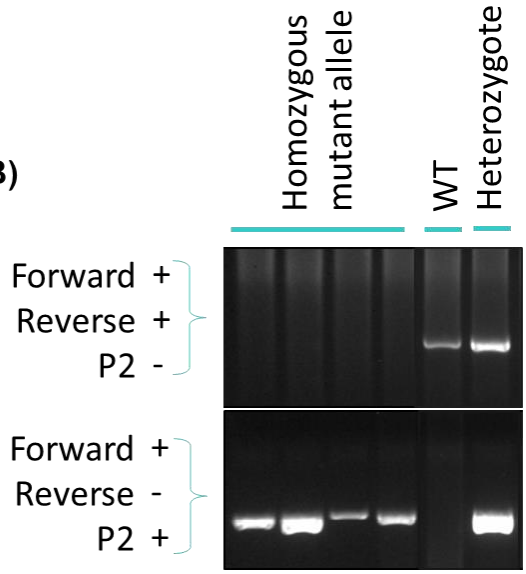
Homozygous mutant allele
WT
Heterozygote
Forward +
Reverse +
P2 -
Forward +
Reverse -
P2 +

3.5.1 Nodulation is enhanced in *spl12* mutant of *L. japonicus*

The progeny of the *L. japonicus* plants homozygous for the LORE1-containing alleles (*spl12-1* and s*pl12-2*) were used to evaluate the symbiotic relationship with *M. loti*, namely the number of mature nodules at 14, 21 and 30 dai. As shown in **Figure 3.28**, nodulation was significantly higher in *spl12-1* and *spl12-2* relative to WT at 14 dai (**Figure 3.28A**). At 21 and 30 dai, on the other hand, no significant differences in nodule numbers could be observed between WT and *spl12* mutants (**Figure 3.28B,C**). These results are consistent with findings on SPL12 function in alfalfa, where *SPL12*-RNAi plants showed more nodules compared to WT at 14 dai but not at 21 dai (**Figure 3.7**), and suggests that SPL12 function in nodulation may be maintained in other leguminous plants as well.

Figure 3.28 Analysis of nodulation in spl12 *L. japonicus* mutant

Number of nodules in *spl12* mutant lines was scored at **A)** 14 dai, **B)** 21 dai and **C)** 30 dai (n = 20). * and ** indicate significant differences relative to WT using Student's t-test $p < 0.05$, $p < 0.01$, respectively. Error bars indicate standard deviation.

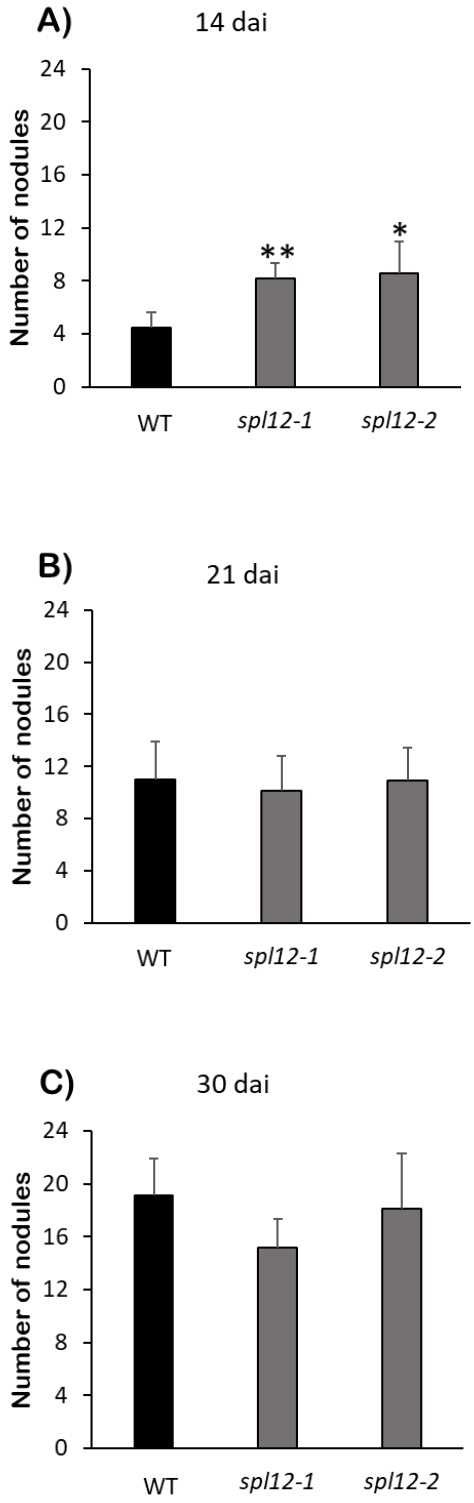
A)
14 dai
Number of nodules
24
20
16
12
8
4
0
**
*
WT
spl12-1
spl12-2
B)
21 dai
Number of nodules
24
20
16
12
8
4
0
WT
spl12-1
spl12-2
C)
30 dai
Number of nodules
24
20
16
12
8
4
0
WT
spl12-1
spl12-2

Chapter 4

4 Discussion

The small RNA, miR156, is a master regulator of plant development, playing a fundamental role in the regulation of a range of plant growth and development processes, such as transition from vegetative to reproductive stages, fertility, and response to stress (Cardon et al. 1999; Wang and Wang 2015; Xu et al. 2016). Previously, it was shown that overexpression of *miR156* in alfalfa (miR156-OE) resulted in increased nodulation, improved nitrogen fixation and enhanced root regenerative capacity during vegetative propagation (Aung et al. 2017). It was also reported that miR156 targets 11 *SPL* genes, including *SPL12*, for silencing by transcript cleavage (Aung et al. 2015; Feyissa et al. 2021; Gao et al. 2016). Whereas the role of some of the targeted SPL transcription factors, such as SPL13 and SPL9, have been well characterized in alfalfa (Arshad et al. 2017a; Feyissa et al. 2019; Gao et al. 2018b; Hanly et al. 2020; Matthews et al. 2019), the specific functions of SPL12 remain elusive, as no functional studies have been conducted for this transcription factor in alfalfa. In the present study, I analyzed transgenic plants with altered expression of *SPL12* and *AGL6*, including *SPL12*-RNAi, *35S::SPL12*, GFP-tagged SPL12 and *AGL6*-RNAi to investigate the role of SPL12 in root architecture.

4.1 Role of SPL12 in root regeneration capacity

Whereas alfalfa plants with reduced *SPL12* transcript levels (*SPL12*-RNAi) showed an enhanced root regenerative capacity during vegetative propagation (**Figure 3.2**), the

number of rooted stem propagules was significantly decreased in *35S::SPL12* plants compared with the WT control (**Figure 3.5A**). The increase in root emergence in *SPL12*-RNAi was observed as early as 13 days after initiation of vegetative propagation from stem nodes, but no significant improvement in root length or root biomass were observed in *SPL12*-RNAi genotypes at the early stages of root development (3-week-old roots). Aung et al. (2015) previously reported that while overexpression of miR156 significantly increased root regenerative capacity in alfalfa, the root biomass was not significantly changed during the early stages of root development (3-week-old roots). In Arabidopsis, it was suggested that at least one group of SPLs (SPL3, SPL9, and SPL10) are involved in the regulation of Arabidopsis lateral root development, with SPL10 playing the most dominant role (Yu et al. 2015b). Moreover, the miR156/SPL module has been shown to play a role in lateral root development through its response to growth hormone signals, and that plants with reduced miR156 levels exhibited fewer lateral and adventitious roots (Yu et al. 2015b). Taken together, these findings corroborate the results that the miR156-SPL12 module regulates root regeneration capacity at least during the early stages of plant development.

4.2 Role of SPL12 in nodulation and nitrogen fixation

Symbiotic nodulation is a complex process that governs the mutually beneficial relationship between leguminous plants and their compatible rhizobia, and includes the downstream components of signaling pathways that trigger changes in gene expression in both partners. The signals that provide bacterial access to the plant and eventually nodule organogenesis have been well studied in legume species (Mergaert et al. 2020; Roy et al.

2020). miR156/SPL was shown to play a role in nodulation in legume plants, including alfalfa, where overexpression of miR156 increased the number of root nodules (Aung et al. 2015). However, the role of miR156/SPL in nodulation may be species-specific, as a reduction in nodulation was reported in other studies involving miR156 overexpression in plants. For example, when *Lj*miR156 was overexpressed in *L. japonicus* it reduced nodule numbers (Wang et al. 2015). Similarly, in soybean, *Gm*miR156 was found to inhibit nodulation through its negative regulation of miR172 (Yan et al. 2013). More recently, Yun et al. (2022) reported that the miR156-SPL9 regulatory system in soybean acts as an upstream master regulator of nodulation by targeting and regulating the expression of nodulation genes in soybean. *Gm*SPL9 is a positive regulator of soybean nodulation which directly binds to the miR172c promoter and activates its expression (Yun et al. 2022). *Gm*SPL9 also directly targets *GmNINa* and *GmENOD40*, which are the nodulation master regulator and nodulation marker genes, respectively, during nodule formation and development (Yun et al. 2022).

In the current study, SPL12 was demonstrated to have a negative effect on nodulation in alfalfa, as the expression level of *SPL12* decreased gradually after 7, 14 and 21 days (a nodulation period) in *S. meliloti*-inoculated roots (**Figure 3.3A**). Decreasing of *SPL12* was concomitant with increasing of genes known for their involvement in nodulation, including *NIN*, *NSP2*, *IPD3*, *DMI1*, *DMI2*, *DMI3*, *DELLA*, *LysM*, and *CLE13*. The expression of these genes was increased after the rhizobial inoculation of alfalfa roots, indicating a possible function for *SPL12* in nodulation. While overexpression of *SPL12* in alfalfa resulted in reduced nodulation in at least two genotypes (L7 and L5) (**Figure 3.5B**), silencing of this gene produced plants (*SPL12*-RNAi) with increased nodulation at 14 dai,

but the exponential increase in the number of nodules in these plants ceased to occur by 21 dai (**Figure 3.4**).

To balance the costs and benefits associated with root nodule symbiosis and to maintain an optimal number of nodules, plants use the AON pathway; a systemic long-range signaling pathway between roots and shoots. Once nodulation is initiated, two nodulation-inhibiting peptides of the CLE family, *Mt*CLE12 and *Mt*CLE13, are normally produced in nodulated roots (Mortier et al. 2010). These peptides are likely translocated to the shoot (Okamoto et al. 2013), and act through the SUNN receptor, where shoot-derived inhibitors are delivered to the roots to inhibit nodulation (Mortier et al. 2012). It has been reported that the negative effect of these CLE peptides on nodulation is due to the downregulation of *ENOD11*, an early epidermal infection marker, and NF perception genes (Gautrat et al. 2019; Mortier et al. 2010). Here I show that the expression of *CLE13* was reduced in *SPL12*-RNAi plants at 14 dai compared to WT, while at 21 dai, *CLE13* was significantly upregulated in the three *SPL12*-RNAi plants (**Figure 3.7E,M**). This is consistent with the increased number of nodules at 14 dai and no change at 21 dai, suggesting the potential existence of a regulatory relationship between *SPL12* and *CLE13*, and the involvement of SPL12 in regulating nodulation.

To show whether the function of SPL12 is conserved in other legume species, I set out to investigate the role of a *L. japonicus* homolog of alfalfa SPL12 (*Lj*SPL12) in nodulation in this model legume. In *L. japonicus spl12-1* and *spl12-2* mutants, nodulation was significantly increased at 14 dai, whereas no significant differences in nodulation between WT and the *spl12* mutant lines was found at 21 dai (**Figure 3.25**). These results are

consistent with the nodulation test results in *SPL12*-RNAi and *AGL6*-RNAi plants in alfalfa, indicating that SPL12 may perform similar functions in both alfalfa and *L. japonicus*. However, further studies are required to understand exactly how *SPL12* is involved in nodulation in alfalfa and *L. japonicus*. It has been shown that *Lj*miR156 and *Gm*miR156 both negatively regulate nodulation in *L. japonicus* and soybean, respectively (Wang et al. 2015; Yan et al. 2013), whereas another conserved miRNA, miR172, positively regulates nodulation in both soybean and common bean (Wang et al. 2014; Yan et al. 2013).

Aung et al. (2017) reported that overexpression of miR156 increased nodule numbers, nitrogenase activity, and the transcript levels of bacterial genes *FixK* (induces the expression of genes involved in nodule respiration), *NifA* (induces the expression of genes involved in nitrogen fixation) and *RpoH* (sigma 32 factor for effective nodulation) (Defez et al. 2016; Fischer 1994) in alfalfa roots inoculated with *S. meliloti*. Similarly, our study indicated that at 14 dai, silencing *SPL12* stimulates nitrogenase activity in RNAi12-7 and RNAi12-29 (**Figure 3.6A**). RT-qPCR expression analysis also showed that silencing of *SPL12* enhanced the expression of *S. meliloti*'s *RpoH*, *FixK* and *nifA* in alfalfa (**Figure 3.6B-D**). Although, it is estimated that mature alfalfa plants can obtain up to 80% of their total nitrogen requirements through biological nitrogen fixation (Provorov and Tikhonovich 2003), emerging seedlings and those grown under abiotic stress (e.g. cold, drought and salinity) still require nitrogen fertilizers, and thus enhancing nodulation and nitrogen fixation at the early stages of plant development should have agronomic and economic benefits to farmers.

4.3 Genes and pathways affected by *SPL12* silencing

To identify genes that may be regulated by SPL12, two *SPL12*-RNAi genotypes, RNAi12-24 and RNAi12-29, were used for transcriptomic analysis using RNA-Seq. This analysis revealed that SPL12 affects expression of a range of genes in both genotypes, as well as in a genotype-specific manner. In this study, there was a total of 169 DEGs between WT and both *SPL12*-RNAi genotypes (RNAi12-24 and RNAi12-29), whereas the rest were genotype-specific (**Figure 3.9A**). Southern blot analysis revealed that RNAi12-24 and RNAi12-29 are independent transgenic lines containing different T-DNA insertion sites in the genome. This suggests that the 169 common DEGs are due to silencing of SPL12, whereas other DEGs may be the result of differing insertion events leading to other transcriptomic effects triggered by disruption of different genomic sites or genes.

Based on the DEG list, GO-enrichment analysis revealed a number of pathways that are affected in *SPL12*-RNAi plants. These pathways can be classified in three functional categories; biological process, molecular function and cellular component. The GO terms such as effect of metal ion binding, oxidoreductase activity, intracellular signal transduction, and sulfur compound metabolic process are related to *SPL12*-RNAi alfalfa phenotypes, such as increased nodule number and nitrogen fixation (Zou et al. 2020; Fonseca-García et al. 2022; Popp and Ott 2011; Kalloniati et al. 2015), which involve a large number of biological pathways. For example, metallothioneins (MTs), the metal ion binding proteins, are involved in symbiotic associations in legume. Downregulation of *PvMT1A* reduces the number of infection events, nodules and nitrogen fixation rate in common bean (Fonseca-García et al. 2022).

Moreover, oxidoreductases are a large class of enzymes catalyzing biological oxidation/reduction reactions, which are important in redox processes, transferring electrons from a reductant to an oxidant (Hollmann and Schmid 2004; Jeelani et al. 2010). *M. loti*, the *L. japonicus* symbiosis partner, expresses a malate oxidoreductase, and it was reported that the nodules induced by *M. loti* mutants deficient in malate oxidoreductase were unable to fix nitrogen (Thapanapongworakul et al. 2010). Zou et al. (2020) showed the role of an oxidoreductase, GMCA, in symbiotic nitrogen fixation, whereby the *gmcA* mutant of *Rhizobium leguminosarum*, the *Pisum sativum* (pea) symbiotic partner, induced an abnormal nodulation phenotype in pea with reduced nitrogen fixation capacity.

In addition, the symbiotic relationship between the plant and rhizobia is regulated through signal transduction pathways, including the intracellular signaling cascade in the nucleus that results in the initiation of calcium oscillation (reviewed by Roy et al. 2020). Simultaneously, calcium spiking activates expression of *NIN* and subsequently *ENOD* to facilitate nodule infection thread formation (reviewed by Chaulagain and Frugoli 2021). In nodulated legumes, sulfur supply plays an important role in symbiotic nitrogen fixation, as the key symbiotic nitrogen fixation enzyme, nitrogenase, is exceptionally rich in sulfur, which suggests that sulfur may become limiting in nitrogen fixation (Becana et al. 2018). This is corroborated by the finding that sulfur uptake, assimilation, and metabolism were enhanced in both symbiotic partners during nitrogen fixation in *L. japonicus* (Kalloniati et al. 2015).

An increased number of genes belonging to the metal ion binding, oxidoreductase activity, intracellular signal transduction, and sulfur compound metabolic process, in both

SPL12-RNAi genotypes (RNAi12-24 and RNAi12-29) suggests a pronounced role for SPL12 in alfalfa nodulation and nitrogen fixation.

4.4 Direct regulatory interaction between SPL12 and *AGL6* to control nodulation

Among the differentially expressed genes, I hypothesized that AGL6, an ortholog of the Arabidopsis AGL79 (*At*AGL79), performs similar functions in alfalfa to the latter's in Arabidopsis, where the miR156/SPL10 module targets *AtAGL79* to regulate plant lateral root development (Gao et al. 2018c). In a previous transcriptomic study, both *SPL12* and *AGL6* were shown to be downregulated in roots of miR156-OE alfalfa (Aung et al. 2017; Gao et al. 2016). In the current study, the highest *AGL6* transcript levels were detected in roots of *SPL12* overexpression genotypes, and further analysis revealed that *AGL6* was under the regulation of SPL12 (**Figure 3.12**). *AGL6* belongs to the MADS-box protein family of transcription factors that has a conserved MADS-box domain (Shore and Sharrocks 1995; Theißen and Gramzow 2016). In Arabidopsis, *AtAGL79* is regulated by *At*SPL10 and is involved in regulating lateral root development through the miR156-SPL pathway (Gao et al. 2018c). Although the MADS-box proteins have been well characterized in many plants (Puig et al. 2013; Schilling et al. 2018; Zhang et al. 2019), information on their role in regulating legume-rhizobia interactions is still in its infancy. In soybean, the MADS-box protein, *Gm*NMHC5, positively regulates root development and nodulation (Liu et al. 2015), while *Gm*NMH7 is a negative regulator of nodulation (Wei et al. 2019). In common bean, AGLs have been proposed as new protagonists in the regulation of nodulation (Íñiguez et al. 2015). Here, the finding that *SPL12*-RNAi and *AGL*6-RNAi

plants have increased nodulation suggests that SPL12 controls nodulation in alfalfa by regulating *AGL*6.

4.5 The role of SPL12 and AGL6 in regulating nodulation under osmotic stress in alfalfa

Legume crops can adjust their root architecture in response to environmental conditions, not only by branching out, but also by forming a symbiosis with rhizobial bacteria to form nitrogen-fixing nodules (De Zélicourt et al. 2012). Drought is a major abiotic stress that causes nutrients to be unavailable to plants and it leads to a nutrient-deprived situation or nutrient stress, affecting plant yield and root growth (reviewed by Zia et al. 2021). Not only does miR156 regulate nodulation in alfalfa, its role in plant response to abiotic stress (e.g. drought, heat, and salinity) was previously demonstrated in alfalfa (Arshad et al. 2017a; Feyissa et al. 2019; Matthews et al. 2019). miR156 targets a number of *SPL* genes for silencing by transcript cleavage in alfalfa (Aung et al. 2015; Feyissa et al. 2021; Gao et al. 2016). Specifically, *SPL13*, *SPL9*, and *SPL8* have been investigated for their role in drought tolerance in alfalfa (Arshad et al. 2017a; Feyissa et al. 2019; Gou et al. 2018; Hanly et al. 2020). Down-regulating *SPL13*, *SPL9* and *SPL8* in transgenic plants resulted in alfalfa plants that were less susceptible to drought (Arshad et al. 2017a; Feyissa et al. 2019; Gou et al. 2018; Hanly et al. 2020). *SPL12* was shown to be upregulated in response to mild and severe salinity stress conditions in alfalfa, but was suppressed in all miR156-OE genotypes, compared to unstressed control (Arshad et al. 2017b). In the current study, I observed a significant increase in the transcript levels of *SPL12* in WT under osmotic stress as opposed to control conditions. The upregulation of *SPL12* under osmotic stress is

consistent with a previous report that showed an increase in *SPL13* transcript levels in WT alfalfa plants under drought conditions (Arshad et al. 2017a).

The roots are the first plant organ to encounter changes in response to water deficit in the soil. Studies in Arabidopsis showed initiation and elongation of lateral roots in drought tolerant genotypes lead to improved water uptake and drought adaptation (Chen et al. 2012; Xiong et al. 2006). In this study, a significant increase in root length accompanied by higher lateral root numbers was observed in alfalfa *SPL12*-RNAi plants under osmotic stress (**Figure 3.14C,E**). Also in a previous study, Arshad et al. (2017a) showed increased root length in miR156-OE and *SPL13*-RNAi alfalfa genotypes under drought stress. Moreover, the miR156-SPL10 module was reported to be involved in root development by silencing *AtAGL79* to control root length and lateral root numbers in Arabidopsis (Gao et al. 2018c). Therefore, it appears that improved root architecture is regulated at least in part through the miR156-SPL network, and helps plants, including alfalfa, to better access water from deeper soil surface under water scarcity conditions.

The symbiotic interaction between legume plants and rhizobacteria can be negatively impacted by drought, resulting in reduced nodule numbers and diminished nitrogenase activity (Ashraf and Iram 2005; Kibido et al. 2020; Mouradi et al. 2018). Nitrogenase activity in root nodules of *M. truncatula* was decreased by 18% and 66% after two and four days of water withdrawal, respectively (Sańko-Sawczenko et al. 2019). It was shown that in *M. truncatula*, both symbiotic plant components and *S. meliloti* bacteria residing in the root nodules adjust their gene expression profiles in response to drought stress (Sańko-Sawczenko et al. 2019). My results showed a decrease in the nodule numbers in WT plants

under osmotic stress condition, while *SPL12*-RNAi genotypes maintained nodulation under this stress (**Figure 3.15**). The transcript levels of *CLE13* decreased under osmotic stress in all genotypes, while it increased in *SPL12*-RNAi plants under control conditions. This is consistent with increasing nodulation under osmotic stress in *SPL12*-RNAi genotypes. In addition, *AGL6* transcript levels were also lower under osmotic stress, and consequently *AGL6*-RNAi genotypes maintained nodulation under osmotic stress. These results showing that stressed *SPL12*-RNAi and *AGL*6-RNAi plants maintained nodulation suggest a role for SPL12 and AGL6 in the control of nodulation in alfalfa under osmotic stress.

In nodulating legumes, sulfur supply plays an important role in symbiotic nitrogen fixation, as sulfur deficiency causes a decrease in nodulation, inhibition of nitrogen fixation, and a slowing down of nodule metabolism (Becana et al. 2018). Accordingly, sulfate transport and metabolism also positively affect nitrogen fixation and nodulation (Becana et al. 2018). A sulfate transporter in the symbiosomal membrane of *L. japonicus*, *LjSST1*, was the first indication of sulfate exchange between the two symbiotic partners (Krusell et al. 2005). *LjSST1* is specifically and highly expressed in nodules, suggesting a crucial role for this protein in the transport of sulfate from the plant to the bacteroids (Krusell et al. 2005). The *sst1* mutants developed smaller nodules and displayed symptoms of nitrogen deficiency only under symbiotic conditions. The nodules of the *sst1* mutant plants showed a reduction of approximately 90% in the rate of nitrogen fixation (Krusell et al. 2005). In the current study, two of the Group3 *SULTR* genes, *SULTR3.4* and *SULTR3.5*, were significantly upregulated in roots of *SPL12*-RNAi plants (**Figure 3.17**). *MtSULTR3.5* in *M. truncatula*, a homolog of *LjSST1*, is strongly expressed in nodules (Roux et al. 2014).

Other studies showed that *MtSULTR3.5* expression is strongly up-regulated in *M. truncatu*la roots subjected to salt stress (Gallardo et al. 2014; Li et al. 2009). Of the sulfate transporters, Group3 *SULTRs* specifically operate under abiotic stress conditions, and they are responsive to salt and drought in both Arabidopsis and *M. truncatula* (Gallardo et al. 2014; Hyung et al. 2014). Interestingly, *SULTR3.1* and *SULTR3.4* are up-regulated in roots of both Arabidopsis and *M. truncatula* plants subjected to drought stress (Gallardo et al. 2014). Given the above findings, I measured the transcript levels of *SULTR3.4* and *SULTR3.5* in alfalfa root tissues under osmotic stress (**Figure 3.17E,F**). The maintenance of the transcript levels of these genes under osmotic and control conditions in *SPL12*-RNAi roots indicates that SPL12 must be involved in *SULTR3.4* and *SULTR3.5* regulation. Although, the five *At*SULTR3 transporters have been functionally characterized in Arabidopsis (Chen et al. 2019), an understanding of their contribution to salt and drought stress response in legumes remains elusive, and thus further studies are needed to address this gap in knowledge.

4.6 How nitrate availability affects nodulation through SPL12-*AGL21* regulatory pathway

To conserve energy, plants inhibit nodulation under conditions of nitrate abundance in the rhizosphere (Streeter and Wong 1988), resulting in a decrease in nodule numbers, nodule mass, and nitrogen fixation, as well as an acceleration of nodule senescence. This regulation of nodulation by nitrate is a part of the AON signaling pathway (Lin et al. 2018; Moreau et al. 2021). As the *SPL12*-RNAi and *AGL6*-RNAi plants showed an increase in nodulation, I tested the relationship between nitrate and the miR156/SPL12 regulatory

system. Under nitrate sufficient conditions, rhizobia-inoculated roots of *SPL12*-RNAi plants developed more active nodules relative to WT (**Figure 3.20; Figure 3.21**), demonstrating the role of miR156/SPL12-mediated system in controlling rhizobia-alfalfa symbiosis. In common bean, Nova-Franco et al. (2015) showed that miR172c is a signaling component of the nitrate-dependent AON, and that it decreased the sensitivity of nodulation to inhibition by nitrate. Common bean plants overexpressing miR172 showed more active nodules in the presence of nitrate (Nova-Franco et al. 2015). *At*SPL9 was shown to be a potential nitrate regulatory hub in Arabidopsis where it may target the primary nitrate-responsive genes (Krouk et al. 2010). *At*SPL9 expression is affected by nitrate, and the transcript levels of *AtNRT1.1*, *AtNR2*, and *AtNiR* significantly increased in response to nitrate in *AtSPL9* overexpression Arabidopsis plants (Krouk et al. 2010). In tomato (*Solanum lycopersicum*), it was reported that an SPL transcription factor, LeSPL-CNR, directly binds to the promoter of *SlNR* (nitrate reductase), resulting in repressing its expression and activity (Chen et al. 2018). It has been shown that LeSPL-CNR negatively regulates *SlNR* transcription levels in response to cadmium (cd) stress in tomato (Chen et al. 2018).

Based on the findings in the current research, I propose that SPL12 regulates nodulation under nitrate treatment in alfalfa by downregulating *AGL21*. Here, RNAseq followed by gene ontology analysis revealed that *AGL21* is upregulated in *SPL12*-RNAi alfalfa plants. *AGL21* is an ANR1 MADS box protein-coding gene. *At*ANR1 MADS box proteins were previously shown to mediate the effect of externally applied nitrate on lateral root development in Arabidopsis (Gan et al. 2012; Zhang and Forde 1998). In rice, two MADS box genes, *OsMADS25* and *OsMADS27*, are involved in the regulation of root development

in response to nitrate (Puig et al. 2013). In Arabidopsis, *AtAGL21* is expressed in different tissues, but most strongly in roots, where *At*AGL21 plays an important role in lateral root development under nitrogen deficiency conditions (Yu et al. 2014). In common bean, *PvAGL21* is expressed in nodules, and its expression is higher in roots compared to pods, seeds and stems (Íñiguez et al. 2015). These results are consistent with the finding that alfalfa *AGL21* is highly expressed in roots (**Figure 3.11C**) and that its expression is induced by nitrate (**Figure 3.22B**). Future research should focus on generating and analyzing *AGL21*-silencing and -overexpressing alfalfa plants to determine AGL21 effect on root architecture, nodulation and nitrogen fixation.

In the current research, the findings suggest that SPL12 differentially regulates *AGL6* and *AGL21* by activating the expression of *AGL6*, and inhibiting *AGL21* in alfalfa. Transcription factors performing dual roles have been reported in the literature. For example, in regulating anthocyanin biosynthesis in Arabidopsis, a ternary WD40-bHLH-MYB (WBM) transcription factor complex can bind to either positive (NAC, WRKY, MADS-box) or negative (MYB4, MYBL2, SPL) regulators, to activate or repress the expression of the late biosynthetic genes (*DFR*, *ANS*/*LDOX*, *UFGT*), respectively, in the anthocyanin biosynthesis pathway (Gonzalez et al. 2008; Shi and Xie 2014; Xu et al. 2015).

4.7 Efficiency of *SPL13* mutagenesis by CRISPR-Cas9 in alfalfa

Modern genome editing technologies use cutting-edge tools to edit the genetic sequence of an organism in a precise and predictable manner. These technologies which include meganucleases, zinc-finger nucleases (ZFNs), transcription activator–like effector nucleases (TALENs) and lately clustered regularly interspaced short palindromic repeats-

CRISPR associated 9 nuclease (CRISPR-Cas9), are important tools in plant research that allow for the development of crops to respond to future market demands and predicted climate changes (Sander and Joung 2014; Voytas and Gao 2014). CRISPR-Cas9 has become a leading-edge technology, providing an opportunity for genome editing in many important crops, including wheat (Wang et al. 2016), sorghum (Jiang et al. 2013), soybean (Cai et al. 2018; Duan et al. 2021) and maize (Jiang et al. 2020). Of the many genome editing technologies, application of the CRISPR-Cas9 system has increased rapidly, proving to be the most efficient genome editing platform of late. This novel editing platform has superseded previous editing tools with its reliance on an RNA-based approach, which is characterized by simple design of targeting multiple genes, high mutagenesis success rate, greater specificity, lower cost and the ability to generate genetically modified organism (GMO)-free edited plants (Deb et al. 2022; Zimny et al. 2019).

My results showed the successful *A. tumefaciens*-mediated transformation of alfalfa, as indicated by the presence of the exogenous *SpCas9* gene that was expected to be transferred as part of the single gRNA CRISPR/Cas9 construct to target *SPL13* for editing. T7E1 assay revealed potentially high mutagenesis frequency in all three gRNA target sites, but Sanger sequencing revealed otherwise, as only a single mutated plant using gRNA1 was confirmed (**Figure 3.28A**). The T7E1 nuclease is a structure-selective enzyme that is sensitive to the mismatch sequences of heteroduplexed DNA (Shan et al. 2014) and can be used to detect CRISPR-Cas9-mediated gene editing (Shan et al. 2020). T7E1 assay has been used to report genome editing frequencies in different plants such as tomato (Pan et al. 2016), wheat (Zong et al. 2017), rice (Zong et al. 2017), and Arabidopsis (Woo et al. 2015). T7E1

has also been used in alfalfa to provide further confirmation of gene editing introduced by CRISPR in *MsSPL8* alleles (Singer et al. 2021). While T7E1 digestion analysis can be used to detect CRISPR-Cas9 editing frequency, its reliability has been questioned (Sentmanat et al. 2018). In a study, Sentmanat et al. (2018) found that indel estimates with T7E1 assay were lower than the average activity of sgRNAs assayed by NGS, consequently this assay often does not accurately identify the actual sgRNA activities.

In the current study, Sanger sequencing revealed a mutagenesis efficiency of 5.5% for gRNA1 (only one plant out of eighteen), 0% for gRNA2 (no plants), and 0% for gRNA3 (no plants), which is relatively low compared to other plant species (Meng et al. 2017). Regardless of important successes in other crops, the application of the CRISPR/Cas9 system in alfalfa has been challenging. Previously, Gao et al. (2018a) used a single gRNA CRISPR/Cas9 to edit *SPL9* in alfalfa, but genome editing efficiency was low (2.2%), close to the mutagenesis efficiency of only 2.5% (34 out of 1531) in alfalfa, using single gRNA CRISPR/Cas9 (Wolabu et al. 2020). However, the single gRNA CRISPR/Cas9 system performed well in *M. truncatula* (Meng et al. 2017), and other monocot species, including rice and switchgrass (Park et al. 2017).

In this study, the alfalfa plants with silenced *SPL13* had no visible phenotype relative to WT control; a result similar to the report by Gao et al. (2018a) and Wolabu et al. (2020), where they used single gRNA CRISPR/Cas9, and in which no mutant phenotype was observed in the edited alfalfa plants. In the related species *M. truncatula,* Meng et al. (2017) successfully mutated target genes by using a modified CRISPR/Cas9 system where a *M. truncatula U6* (*MtU6*) promoter drove the expression of a specific gRNA, and a total of

10.4% (32 out of 309) of transgenic plants showed an obvious phenotypic change. Although, the *MtU6* promoter from the related *M. truncatula* species was used in the current study to improve the effectiveness of CRISPR/Cas9 genome editing system, the editing frequency was still low; observed in only for one of the gRNAs. This may be due to the presence of four allelic gene copies in alfalfa and incomplete knockout of the target gene, which results in the absence of a mutant phenotype. Most recently, it has been shown that, a modified editing system could successfully mutate target genes with an increased genome editing efficiency in alfalfa using a multiplex CRISPR/Cas9 system targeting different alleles of the gene (Wolabu et al. 2020). The mutated alfalfa plants showed the expected phenotype, indicating a complete knockout mutation, with 75% genotypic efficiency; which is 30 times more efficient than the single gRNA CRISPR/Cas9 system (Wolabu et al. 2020). In alfalfa, Singer et al. (2021) could also successfully mutate *MsSPL8* gene using the single gRNA CRISPR/Cas9 system. They were able to achieve high frequencies of indels in *MsSPL8* alleles, displaying transgenic plants with up to three of four alleles mutated. Moreover, Chen et al. (2020) also could mutate target genes in alfalfa by an efficient CRISPR-Cas9-based genome editing protocol, and a total of 0.57% (5 out of 880) of transgenic plants displayed tetra-allelic mutations into null mutants that showed the mutant phenotypes. Furthermore, multi-generation analysis revealed that the mutation and phenotypes of null alfalfa mutants were specifically inherited by the next generations in a transgene-free manner by cross-pollination (Chen et al. 2020). Production of transgene-free mutants in specifically targeted gene-edited plants is important for regulatory approval of the genetically modified plants. Additionally, with this type of

approach further genome editing events will be minimized, and genetic heritability and trait stability will be properly assessed.

Compared to the various methods of gene modification, such as RNA interference (RNAi), the CRISPR system provides a platform to precisely edit a gene, without randomly disturbing the rest of the genome. This is perceived more positively by the public relative to the products of traditional genetic engineering technologies (Ahmad et al. 2021). Nevertheless, RNAi is a proven, efficient technique for gene silencing, and both RNAi and CRISPR have been used to knock-out or knock-down genes for functional characterization (Arshad et al. 2017a; Feyissa et al. 2019; Gao et al. 2018b).

In summary, while I successfully used CRISPR/Cas9 to elicit a mutation in *SPL13* gene in alfalfa, mutagenesis efficiency was low. In the future, the use of the three gRNAs in a multiplex CRISPR/Cas9 system may result in higher efficiency of *SPL13* editing in this plant.

Conclusion and future research directions

Understanding the molecular mechanisms underpinning the nodule symbiosis pathway in legumes is of great importance for both agricultural and environmental conservation. New plant improvement strategies use molecular marker-assisted breeding tools to produce cultivars of agriculturally significant traits, such as resistance to different biotic and abiotic stresses (Khan et al. 2017). As a potential molecular marker, miR156 has not only been demonstrated to play a role in the regulation of abiotic stress tolerance (Arshad et al. 2017a; Feyissa et al. 2019; Hanly et al. 2020; Matthews et al. 2019), but it has also been proven to increase nodulation, nitrogen fixation, and root regeneration capacity in alfalfa (Aung et al. 2017). miR156 functions by downregulating downstream genes including *SPLs* to control different plant growth and development processes (Cardon et al. 1999; Feyissa et al. 2021; Gao et al. 2016; Wang and Wang 2015; Xu et al. 2016; Yun et al. 2022). These downstream genes have not been fully characterized in alfalfa, and present an opportunity to determine the biochemical and molecular mechanisms underpinning these effects.

miR156 targets a number of *SPL* genes for post-transcriptional silencing in alfalfa (Aung et al. 2015; Feyissa et al. 2021; Gao et al. 2016) and some SPLs, like SPL12, are largely uncharacterized in this plant. In the current research, the role of miR156-targeted *SPL12* and its downstream targets, *AGL6* and *AGL21*, was investigated in alfalfa root architecture and nodulation.

Symbiotic nodulation is a complex process between legumes and compatible rhizobia, including the downstream components of signaling pathways that trigger changes in gene

expression in both partners. The signals that provide bacterial access to the plant and eventually nodule organogenesis have been well studied in legume species (Mergaert et al. 2020; Roy et al. 2020). In this study, the impact of SPL12 on alfalfa root architecture and nodulation was assessed by comparing *SPL12*-RNAi with WT plants. Since *SPL12*-RNAi plants displayed an enhancement in alfalfa root regenerative capacity during vegetative propagation, it can be concluded that SPL12 plays a role in the negative regulation of root emergence from the stem cuttings. In addition, plants with silenced *SPL12* showed an increase in nodulation and nitrogen fixation, while overexpression of *SPL12* in alfalfa resulted in reduced nodulation, indicating the negative effect of SPL12 on nitrogen fixation and nodulation. miR156-OE plants also showed similar phenotypic changes according to Aung et al. (2015), establishing that silencing of *SPL12*, either alone or in combination with other SPLs, causes phenotypic changes related to plant root architecture and nodulation in alfalfa. Furthermore, I found that SPL12 directly binds to the promoter of *AGL6*, and since it was observed that plants with silenced *AGL6* improved nodulation, it could be concluded that the miR156/SPL12 regulatory pathway is involved in regulating nodulation by directly targeting and activating the expression of *AGL6*. Additionally, my finding that *L. japonicus spl12* mutant had similar nodulation traits as those of alfalfa *SPL12*-RNAi plants indicates that SPL12 may be functionally conserved in at least some other legume plants.

My investigation of the SPL12 function also revealed that SPL12 and its direct target, AGL6, regulate nodulation under osmotic stress, as plants with reduced *SPL12* and *AGL6* showed an enhanced number of nodules under osmotic stress. This resulted in the maintenance of nodulation in *SPL12*-RNAi and *AGL6*-RNAi plants despite the adverse

stress conditions. This study, combined with the previous investigations of miR156 that showed miR156-OE plants had increased tolerance to drought (Arshad et al. 2017a; Feyissa et al. 2019), and the observation by Aung et al. (2017) that showed miR156-OE plants improved nodulation and nitrogen fixation, provided evidence that miR156-targeted *SPL12* is a regulator of nodulation under osmotic stress in alfalfa. Moreover, maintenance of nodulation by *AGL*6-RNAi as well suggests a role for AGL6 in the control of nodulation in alfalfa under osmotic stress.

To conserve energy, plants inhibit nodulation when nitrogen is available in the rhizosphere (Streeter and Wong 1988) by activating the AON signaling pathway, resulting in a decrease in nodulation and nitrogen fixation (Lin et al. 2018; Moreau et al. 2021). My results showed that the role of SPL12 in alfalfa is not restricted to regulating nodulation under normal conditions, but also controls this process under nitrate sufficient conditions. Rhizobia-inoculated alfalfa roots with reduced levels of *SPL12* were found to develop more active nodules, relative to WT under nitrate sufficient conditions, demonstrating the role of the miR156/SPL12-mediated system in controlling rhizobia-alfalfa symbiosis. SPL12 regulates nodulation under nitrate treatment in alfalfa by targeting *AGL21*. *AGL21* is an ANR1 MADS box protein-coding gene. *At*ANR1 MADS box proteins were previously shown to mediate the effect of externally applied nitrate lateral root development in Arabidopsis (Gan et al. 2012; Zhang and Forde 1998). In the current experiment, RNAseq followed by gene ontology analysis showed *AGL21* is upregulated in *SPL12*-RNAi alfalfa roots, where its transcript levels were induced by nitrate. As a negative regulator of *AGL21*, SPL12 silencing upregulates *AGL21* and enhances the production of active nodules under sufficient nitrate conditions.

Taken together, my results suggest that SPL12 along with *AGL6* and *AGL21* modulate alfalfa nodulation. Here, I report that SPL12 negatively regulates nodulation in alfalfa at least partially by targeting *AGL6* and *AGL21*. However, it is unclear how AGL6 is involved in the nodulation pathway, and further research on AGL6 target genes, and specifically AGL6-regulated genes associated with stress response would provide a better understanding of the role of the miR156/*SP*L12/AGL6 network in regulation of nodulation. Examining phenotypic traits in transgenic alfalfa with increased *AGL6* (*AGL6*-OE) could further uncover the role of SPL12/AGL6 module in alfalfa nodulation. Future research should also focus on understanding AGL21 function by comparing the molecular and morphological characters among *AGL21*-RNAi and *AGL21* overexpression alfalfa. Furthermore, the identification of the potential existence of a regulatory relationship between *SPL12* and *CLE13* was exciting because it provided the possible involvement of SPL12 in the AON signaling pathway. However, additional work is needed to directly demonstrate that this relationship indeed exists. The regulation of nodulation may not be limited to the SPL12, as SPLs are known to work in a redundant manner (Schwarz et al. 2008; Shikata et al. 2009; Yu et al. 2015b). Thus, the role of other SPLs in the miR156-mediated regulatory system in nodulation should be evaluated.

While miR156 has been found to be involved in response to a number of different abiotic stresses in alfalfa, including drought, and heat (Arshad et al. 2017a; Feyissa et al. 2019; Matthews et al. 2019), this study determined the role of SPL12/miR156 in nodulation under osmotic stress as a mimic of drought, and hence the role of SPL12 in miR156-mediated nodulation and stress tolerance should next be evaluated under actual drought and other abiotic stress conditions.

In conclusion, understanding the molecular function of miR156-targeted SPL12 and its targets, *AGL6* and *AGL21,* in alfalfa root architecture and nodulation should provide an important molecular tool that can be used in marker-assisted improvements not only for alfalfa, but also potentially for other legume crops. Results described in this thesis provide an insight into these molecular mechanisms, but further studies are still needed to understand the potential of the miR156/SPL system in legume and non-legume crop improvement.

References

Abdul-Jabbar A, Sammis T, Lugg D, Kallsen C, Smeal D (1983) Water use by alfalfa, maize, and barley as influenced by available soil water. Agricultural Water Management 6:351-363

Ahmad S, Shahzad R, Jamil S, Tabassum J, Chaudhary MAM, Atif RM, Iqbal MM, Monsur MB, Lv Y, Sheng Z (2021) Regulatory aspects, risk assessment, and toxicity associated with RNAi and CRISPR methods. In: Lim KAA-EaK-T (ed) CRISPR and RNAi Systems. Elsevier, pp 687-721

Alvarez-Buylla ER, García-Ponce B, Sánchez MdlP, Espinosa-Soto C, García-Gómez ML, Piñeyro-Nelson A, Garay-Arroyo A (2019) MADS-box genes underground becoming mainstream: plant root developmental mechanisms. New Phytologist 223:1143-1158

Anderson A, Spencer D (1950) Sulphur in nitrogen metabolism of legumes and non-legumes. Australian Journal of Biological Sciences 3:431-449

Andrews S (2010) FastQC: a quality control tool for high throughput sequence data. Babraham Bioinformatics, Babraham Institute, Cambridge, United Kingdom,

Andriankaja A, Boisson-Dernier A, Frances L, Sauviac L, Jauneau A, Barker DG, de Carvalho-Niebel FJTPC (2007) AP2-ERF transcription factors mediate Nod factor–dependent *Mt ENOD11* activation in root hairs via a novel cis-regulatory motif. The Plant Cell 19:2866-2885

Ané J-M, Kiss GB, Riely BK, Penmetsa RV, Oldroyd GE, Ayax C, Lévy J, Debellé F, Baek J-M, Kalo P (2004) *Medicago truncatula DMI1* required for bacterial and fungal symbioses in legumes. Science 303:1364-1367

Angus J, Peoples M (2012) Nitrogen from Australian dryland pastures. Crop & Pasture Science 63:746-758

Annicchiarico P, Barrett B, Brummer EC, Julier B, Marshall AH (2015) Achievements and challenges in improving temperate perennial forage legumes. Critical Reviews in Plant Sciences 34:327-380

Arrighi J-F, Barre A, Amor BB, Bersoult A, Soriano LC, Mirabella R, de Carvalho-Niebel F, Journet E-P, Ghérardi M, Huguet T (2006) The *Medicago truncatula* lysine motif-receptor-like kinase gene family includes *NFP* and new nodule-expressed genes. Plant Physiology 142:265-279

Arshad M, Feyissa BA, Amyot L, Aung B, Hannoufa A (2017a) MicroRNA156 improves drought stress tolerance in alfalfa (*Medicago sativa*) by silencing *SPL13*. Plant Sciences 258:122-136

Arshad M, Gruber MY, Hannoufa A (2018) Transcriptome analysis of microRNA156 overexpression alfalfa roots under drought stress. Scientific Reports 8:9363

Arshad M, Gruber MY, Wall K, Hannoufa A (2017b) An insight into microRNA156 role in salinity stress responses of alfalfa. Frontiers in Plant Science 8:356

Ashraf M, Iram A (2005) Drought stress induced changes in some organic substances in nodules and other plant parts of two potential legumes differing in salt tolerance. Flora-Morphology, Distribution, Functional Ecology of Plants 200:535-546

Aung B, Gao R, Gruber MY, Yuan Z-C, Sumarah M, Hannoufa A (2017) MsmiR156 affects global gene expression and promotes root regenerative capacity and nitrogen fixation activity in alfalfa. Transgenic Research 26:541-557

Aung B, Gruber MY, Amyot L, Omari K, Bertrand A, Hannoufa A (2015) MicroRNA156 as a promising tool for alfalfa improvement. Plant Biotechnology Journal 13:779-790

Badhan A, Jin L, Wang Y, Han S, Kowalczys K, Brown DC, Ayala CJ, Latoszek-Green M, Miki B, Tsang AJBfb (2014) Expression of a fungal ferulic acid esterase in alfalfa modifies cell wall digestibility. Biotechnology for Biofuels 7:39-53

Batool S, Uslu VV, Rajab H, Ahmad N, Waadt R, Geiger D, Malagoli M, Xiang C-B, Hedrich R, Rennenberg H (2018) Sulfate is incorporated into cysteine to trigger ABA production and stomatal closure. The Plant Cell 30:2973-2987

Becana M, Wienkoop S, Matamoros MA (2018) Sulfur transport and metabolism in legume root nodules. Frontiers in Plant Science 9:1434

Bélanger G, Castonguay Y, Bertrand A, Dhont C, Rochette P, Couture L, Drapeau R, Mongrain D, Chalifour F-P, Michaud R (2006) Winter damage to perennial forage crops in eastern Canada: Causes, mitigation, and prediction. Canadian Journal of Plant Science 86:33-47

Bensmihen S (2015) Hormonal control of lateral root and nodule development in legumes. Plants 4:523-547

Beringer JE (1974) R factor transfer in Rhizobium leguminosarum. Microbiology and Molecular Biology Reviews 84:188-198

Bernstein E, Caudy AA, Hammond SM, Hannon G (2001) Role for a bidentate ribonuclease in the initiation step of RNA interference. Nature communications 409:363-366

Bersoult A, Camut S, Perhald A, Kereszt A, Kiss GB, Cullimore JV (2005) Expression of the *Medicago truncatula DMI2* gene suggests roles of the symbiotic nodulation receptor kinase in nodules and during early nodule development. Molecular Plant-Microbe Interactions 18:869-876

Birkenbihl RP, Jach G, Saedler H, Huijser P (2005) Functional dissection of the plant-specific SBP-domain: overlap of the DNA-binding and nuclear localization domains. Journal of Molecular Biology 352:585-596

Blondon F, Marie D, Brown S, Kondorosi A (1994) Genome size and base composition in *Medicago sativa* and *M. truncatula* species. Genome Biology 37:264-270

Breakspear A, Liu C, Roy S, Stacey N, Rogers C, Trick M, Morieri G, Mysore KS, Wen J, Oldroyd GE (2014) The root hair "infectome" of *Medicago truncatula* uncovers changes in cell cycle genes and reveals a requirement for auxin signaling in rhizobial infection. The Plant Cell 26:4680-4701

Burgeff C, Liljegren SJ, Tapia-López R, Yanofsky MF, Alvarez-Buylla ER (2002) MADS-box gene expression in lateral primordia, meristems and differentiated tissues of *Arabidopsis thaliana* roots. Planta 214:365-372

Caetano-Anollés G, Gresshoff PM (1991) Plant genetic control of nodulation. Annual Review of Microbiology 45:345-382

Cai Y, Chen L, Sun S, Wu C, Yao W, Jiang B, Han T, Hou W (2018) CRISPR/Cas9-mediated deletion of large genomic fragments in soybean. International Journal of Molecular Sciences 19:3835

Canfield DE, Glazer AN, Falkowski PGJs (2010) The evolution and future of Earth's nitrogen cycle. Science 330:192-196

Cao MJ, Wang Z, Zhao Q, Mao JL, Speiser A, Wirtz M, Hell R, Zhu JK, Xiang CB (2014) Sulfate availability affects ABA levels and germination response to ABA and salt stress in *Arabidopsis thaliana*. The Plant Journal 77:604-615

Capoen W, Sun J, Wysham D, Otegui MS, Venkateshwaran M, Hirsch S, Miwa H, Downie JA, Morris RJ, Ané J-M (2011) Nuclear membranes control symbiotic calcium signaling of legumes. Proceedings of the National Academy of Sciences of the United States of America 108:14348-14353

Cardon G, Höhmann S, Klein J, Nettesheim K, Saedler H, Huijser P (1999) Molecular characterisation of the *Arabidopsis* SBP-box genes. Gene Expression Patterns 237:91-104

Castonguay Y, Laberge S, Brummer EC, Volenec JJ (2006) Alfalfa winter hardiness: a research retrospective and integrated perspective. Advances in Agronomy 90:203-265

Castonguay Y, Michaud J, Dubé M-P (2015) Reference genes for RT-qPCR analysis of environmentally and developmentally regulated gene expression in alfalfa. American Journal of Plant Sciences 6:132-143

Charpentier M, Sun J, Martins TV, Radhakrishnan GV, Findlay K, Soumpourou E, Thouin J, Véry A-A, Sanders D, Morris R (2016) Nuclear-localized cyclic nucleotide–gated channels mediate symbiotic calcium oscillations. Science 352:1102-1105

Chaulagain D, Frugoli J (2021) The regulation of nodule number in legumes is a balance of three signal transduction pathways. International Journal of Molecular Sciences 22:1117-1130

Chen D-S, Liu C-W, Roy S, Cousins D, Stacey N, Murray JD (2015) Identification of a core set of rhizobial infection genes using data from single cell-types. Frontiers in Plant Science 6:575-585

Chen H, Li Z, Xiong L (2012) A plant microRNA regulates the adaptation of roots to drought stress. FEBS Letters 586:1742-1747

Chen H, Zeng Y, Yang Y, Huang L, Tang B, Zhang H, Hao F, Liu W, Li Y, Liu Y (2020) Allele-aware chromosome-level genome assembly and efficient transgene-free genome editing for the autotetraploid cultivated alfalfa. Nature Communications 11:1-11

Chen WW, Jin JF, Lou HQ, Liu L, Kochian LV, Yang JL (2018) LeSPL-CNR negatively regulates Cd acquisition through repressing nitrate reductase-mediated nitric oxide production in tomato. Planta 248:893-907

Chen X-C, Feng J, Hou B-H, Li F-Q, Li Q, Hong G-F (2005) Modulating DNA bending affects NodD-mediated transcriptional control in *Rhizobium leguminosarum*. Nucleic Acids Research 33:2540-2548

Chen X (2012) Small RNAs in development–insights from plants. Current Opinion in Genetics & Development 22:361-367

Chen Z, Zhao P-X, Miao Z-Q, Qi G-F, Wang Z, Yuan Y, Ahmad N, Cao M-J, Hell R, Wirtz M (2019) SULTR3s function in chloroplast sulfate uptake and affect ABA biosynthesis and the stress response. Plant Physiology 180:593-604

Choi H-K, Kim D, Uhm T, Limpens E, Lim H, Mun J-H, Kalo P, Penmetsa RV, Seres A, Kulikova O (2004) A sequence-based genetic map of *Medicago truncatula* and comparison of marker colinearity with *M. sativa*. Genetics 166:1463-1502

Comas L, Becker S, Cruz VMV, Byrne PF, Dierig DA (2013) Root traits contributing to plant productivity under drought. Frontiers in Plant Science 4:442-457

Crespi M, Frugier F (2008) De novo organ formation from differentiated cells: root nodule organogenesis. Science Signaling 1:re11

Curtis MD, Grossniklaus U (2003) A gateway cloning vector set for high-throughput functional analysis of genes in planta. Plant Physiology 133:462-469

Dakora FD, Joseph CM, Phillips DA (1993) Alfalfa (*Medicago sativa* L.) root exudates contain isoflavonoids in the presence of *Rhizobium meliloti*. Plant Physiology 101:819-824

Davidian J-C, Kopriva S (2010) Regulation of sulfate uptake and assimilation—the same or not the same? Molecular Plant 3:314-325

De Folter S, Shchennikova AV, Franken J, Busscher M, Baskar R, Grossniklaus U, Angenent GC, Immink RG (2006) A Bsister MADS-box gene involved in ovule and seed development in petunia and Arabidopsis. The Plant Journal 47:934-946

De Zélicourt A, Diet A, Marion J, Laffont C, Ariel F, Moison M, Zahaf O, Crespi M, Gruber V, Frugier F (2012) Dual involvement of a *Medicago truncatula* NAC transcription factor in root abiotic stress response and symbiotic nodule senescence. The Plant Journal 70:220-230

Deb S, Choudhury A, Kharbyngar B, Satyawada RR (2022) Applications of CRISPR/Cas9 technology for modification of the plant genome. Genetica 150:1-12

Defez R, Esposito R, Angelini C, Bianco C (2016) Overproduction of indole-3-acetic acid in free-living rhizobia induces transcriptional changes resembling those occurring in nodule bacteroids. Molecular Plant-Microbe Interactions 29:484-495

Delaux PM, Radhakrishnan G, Oldroyd G (2015) Tracing the evolutionary path to nitrogen-fixing crops. Current Opinion in Plant Biology 26:95-99

Den Herder G, Van Isterdael G, Beeckman T, De Smet I (2010) The roots of a new green revolution. Trends in Plant Science 15:600-607

Dilworth M (1966) Acetylene reduction by nitrogen-fixing preparations from Clostridium pasteurianum. Biochimica et Biophysica Acta -General Subjects 127:285-294

Doench JG, Fusi N, Sullender M, Hegde M, Vaimberg EW, Donovan KF, Smith I, Tothova Z, Wilen C, Orchard R (2016) Optimized sgRNA design to maximize activity and minimize off-target effects of CRISPR-Cas9. Nature Biotechnology 34:184-191

Doench JG, Hartenian E, Graham DB, Tothova Z, Hegde M, Smith I, Sullender M, Ebert BL, Xavier RJ, Root DE (2014) Rational design of highly active sgRNAs for CRISPR-Cas9–mediated gene inactivation. Nature Biotechnology 32:1262-1267

Dong T, Hu Z, Deng L, Wang Y, Zhu M, Zhang J, Chen G (2013) A tomato MADS-box transcription factor, SlMADS1, acts as a negative regulator of fruit ripening. Plant Physiology 163:1026-1036

Duan K, Cheng Y, Ji J, Wang C, Wei Y, Wang Y (2021) Large chromosomal segment deletions by CRISPR/LbCpf1-mediated multiplex gene editing in soybean. Journal of Integrative Plant Biology 63:1620-1631

Ernst L, Goodger JQ, Alvarez S, Marsh EL, Berla B, Lockhart E, Jung J, Li P, Bohnert HJ, Schachtman DP (2010) Sulphate as a xylem-borne chemical signal precedes the expression of ABA biosynthetic genes in maize roots. Journal of Experimental Botany 61:3395-3405

Fan J, McConkey B, Wang H, Janzen H (2016) Root distribution by depth for temperate agricultural crops. Field Crops Research 189:68-74

Felekkis K, Touvana E, Stefanou C, Deltas C (2010) microRNAs: a newly described class of encoded molecules that play a role in health and disease. Hippokratia 14:236

Ferguson BJ, Indrasumunar A, Hayashi S, Lin MH, Lin YH, Reid DE, Gresshoff PM (2010) Molecular analysis of legume nodule development and autoregulation. Journal of Integrative Plant Biology 52:61-76

Feyissa BA, Amyot L, Nasrollahi V, Papadopoulos Y, Kohalmi SE, Hannoufa A (2021) Involvement of the miR156/SPL module in flooding response in *Medicago sativa*. Scientific Reports 11:1-16

Feyissa BA, Arshad M, Gruber MY, Kohalmi SE, Hannoufa A (2019) The interplay between *miR156/SPL13* and *DFR/WD40–1* regulate drought tolerance in alfalfa. BMC Plant Biology 19:1-19

Fischer H-M (1994) Genetic regulation of nitrogen fixation in rhizobia. Microbiology and Molecular Biology Reviews 58:352-386

Fonseca-García C, López-García CM, Pacheco R, Armada E, Nava N, Pérez-Aguilar R, Solis-Miranda J, Quinto C (2022) Metallothionein1A regulates rhizobial infection and nodulation in *Phaseolus vulgaris*. International Journal of Molecular Sciences 23:1491

Froger A, Hall JE (2007) Transformation of plasmid DNA into *E. coli* using the heat shock method. Journal of Visualized Experiments 6. doi:10.3791/253

Fukaki H, Tasaka M (2009) Hormone interactions during lateral root formation. Plant Molecular Biology 69:437-449

Gallardo K, Courty P-E, Le Signor C, Wipf D, Vernoud V (2014) Sulfate transporters in the plant's response to drought and salinity: regulation and possible functions. Frontiers in Plant Science 5:580-586

Gan Y, Bernreiter A, Filleur S, Abram B, Forde BG (2012) Overexpressing the *ANR1* MADS-box gene in transgenic plants provides new insights into its role in the nitrate regulation of root development. Plant & Cell Physiology 53:1003-1016

Gao R, Austin RS, Amyot L, Hannoufa A (2016) Comparative transcriptome investigation of global gene expression changes caused by miR156 overexpression in *Medicago sativa*. BMC Genomics 17:1-15

Gao R, Feyissa BA, Croft M, Hannoufa A (2018a) Gene editing by CRISPR/Cas9 in the obligatory outcrossing *Medicago sativa*. Planta 247:1043-1050

Gao R, Gruber MY, Amyot L, Hannoufa A (2018b) SPL13 regulates shoot branching and flowering time in *Medicago sativa*. Plant Molecular Biology 96:119-133

Gao R, Wang Y, Gruber MY, Hannoufa A (2018c) miR156/SPL10 modulates lateral root development, branching and leaf morphology in Arabidopsis by silencing *AGAMOUS-LIKE 79*. Frontiers in Plant Science 8:2226-2238

Gautrat P, Laffont C, Frugier F (2020) Compact root architecture 2 promotes root competence for nodulation through the miR2111 systemic effector. Current Biology 30:1339-1345

Gautrat P, Mortier V, Laffont C, De Keyser A, Fromentin J, Frugier F, Goormachtig S (2019) Unraveling new molecular players involved in the autoregulation of nodulation in *Medicago truncatula*. Journal of Experimental Botany 70:1407-1417

Gendrel A-V, Lippman Z, Martienssen R, Colot V (2005) Profiling histone modification patterns in plants using genomic tiling microarrays. Nature Methods 2:213-218

Gifford ML, Dean A, Gutierrez RA, Coruzzi GM, Birnbaum KD (2008) Cell-specific nitrogen responses mediate developmental plasticity. Proceedings of the National Academy of Sciences of the United States of America 105:803-808

Glass AD, Britto DT, Kaiser BN, Kinghorn JR, Kronzucker HJ, Kumar A, Okamoto M, Rawat S, Siddiqi M, Unkles SE (2002) The regulation of nitrate and ammonium transport systems in plants. Journal of Experimental Botany 53:855-864

Gommers CM (2019) Plastid Sulfate Transporters Open Doors to Abiotic Stress Resistance. Plant physiology 180:12-13

Gonzalez A, Zhao M, Leavitt JM, Lloyd AM (2008) Regulation of the anthocyanin biosynthetic pathway by the TTG1/bHLH/Myb transcriptional complex in Arabidopsis seedlings. The Plant Journal 53:814-827

Gou J, Debnath S, Sun L, Flanagan A, Tang Y, Jiang Q, Wen J, Wang ZY (2018) From model to crop: functional characterization of SPL8 in *M. truncatula* led to genetic improvement of biomass yield and abiotic stress tolerance in alfalfa. Plant Biotechnology Journal 16:951-962

Graham PH, Vance CP (2003) Legumes: importance and constraints to greater use. Plant Physiology 131:872-877

Gramzow L, Theissen G (2010) A hitchhiker's guide to the MADS world of plants. Genome Biology 11:1-11

Groth M, Takeda N, Perry J, Uchida H, Dräxl S, Brachmann A, Sato S, Tabata S, Kawaguchi M, Wang TL (2010) *NENA*, a *Lotus japonicus* homolog of *Sec13*, is required for rhizodermal infection by arbuscular mycorrhiza fungi and rhizobia but dispensable for cortical endosymbiotic development. The Plant Cell 22:2509-2526

Guerriero G, Legay S, Hausman J-F (2014) Alfalfa cellulose synthase gene expression under abiotic stress: a hitchhiker’s guide to RT-qPCR normalization. PLOS One 9. doi:10.1371/journal.pone.0103808

Handberg K, Stougaard J (1992) *Lotus japonicus*, an autogamous, diploid legume species for classical and molecular genetics. The Plant Journal 2:487-496

Hanly A, Karagiannis J, Lu QSM, Tian L, Hannoufa A (2020) Characterization of the role of SPL9 in drought stress tolerance in *Medicago sativa*. International Journal of Molecular Sciences 21:6003-6016

Heim HC, Bernhardt TM, Lang SM, Barnett RN, Landman U (2016) Interaction of iron–sulfur clusters with N2: Biomimetic systems in the gas phase. The Journal of Physical Chemistry C 120:12549-12558

Held M, Hossain MS, Yokota K, Bonfante P, Stougaard J, Szczyglowski K (2010) Common and not so common symbiotic entry. Trends in Plant Science 15:540-545

Helliwell C, Waterhouse P (2003) Constructs and methods for high-throughput gene silencing in plants. Methods 30:289-295

Herrbach V, Remblière C, Gough C, Bensmihen S (2014) Lateral root formation and patterning in *Medicago truncatula*. Journal of Plant Physiology 171:301-310

Hirsch S, Kim J, Muñoz A, Heckmann AB, Downie JA, Oldroyd GE (2009) GRAS proteins form a DNA binding complex to induce gene expression during nodulation signaling in *Medicago truncatula*. The Plant Cell 21:545-557

Höfgen R, Willmitzer L (1988) Storage of competent cells for Agrobacterium transformation. Nucleic Acids Research 16:9877

Hollmann F, Schmid A (2004) Electrochemical regeneration of oxidoreductases for cell-free biocatalytic redox reactions. Biocatalysis & Biotransformation 22:63-88

Hossain MS, Shrestha A, Zhong S, Miri M, Austin RS, Sato S, Ross L, Huebert T, Tromas A, Torres-Jerez I (2016) *Lotus japonicus* NF-YA1 plays an essential role during nodule differentiation and targets members of the *SHI/STY* gene family. Molecular Plant-Microbe Interactions 29:950-964

Huang B, Routaboul J-M, Liu M, Deng W, Maza E, Mila I, Hu G, Zouine M, Frasse P, Vrebalov JT (2017) Overexpression of the class D MADS-box gene *Sl-AGL11* impacts fleshy tissue differentiation and structure in tomato fruits. Journal of Experimental Botany 68:4869-4884

Hyung D, Lee C, Kim J-H, Yoo D, Seo Y-S, Jeong S-C, Lee J-H, Chung Y, Jung K-H, Cook DR (2014) Cross-family translational genomics of abiotic stress-responsive genes between Arabidopsis and *Medicago truncatula*. PLOS One 9:91721-91733

Íñiguez LP, Nova-Franco B, Hernández G, behavior (2015) Novel players in the AP2-miR172 regulatory network for common bean nodulation. Plant Signaling & Behavior 10:1062957

Innocenti G, Pucciariello C, Le Gleuher M, Hopkins J, de Stefano M, Delledonne M, Puppo A, Baudouin E, Frendo P (2007) Glutathione synthesis is regulated by nitric oxide in *Medicago truncatula* roots. Planta 225:1597-1602

Issah G, Schoenau JJ, Lardner HA, Knight JD (2020) Nitrogen fixation and resource partitioning in alfalfa (*Medicago sativa* L.), cicer milkvetch (*Astragalus cicer* L.) and sainfoin (*Onobrychis viciifolia* Scop.) using 15N enrichment under controlled environment conditions. Agronomy 10:1438-1451

Jeelani G, Husain A, Sato D, Ali V, Suematsu M, Soga T, Nozaki T (2010) Two atypical L-cysteine-regulated NADPH-dependent oxidoreductases involved in redox maintenance, L-cystine and iron reduction, and metronidazole activation in the enteric protozoan Entamoeba histolytica. Journal of Biological Chemistry 285:26889-26899

Jia C, Zhao F, Wang X, Han J, Zhao H, Liu G, Wang Z (2018) Genomic prediction for 25 agronomic and quality traits in alfalfa (*Medicago sativa*). Frontiers in Plant Science 9:1220-1226

Jiang S, Cheng Q, Yan J, Fu R, Wang X (2020) Genome optimization for improvement of maize breeding. Theoretical and Applied Genetics 133:1491-1502

Jiang W, Zhou H, Bi H, Fromm M, Yang B, Weeks DP (2013) Demonstration of CRISPR/Cas9/sgRNA-mediated targeted gene modification in Arabidopsis, tobacco, sorghum and rice. Nucleic Acids Research 41:188-199

Jin Y, Liu H, Luo D, Yu N, Dong W, Wang C, Zhang X, Dai H, Yang J, Wang E (2016) DELLA proteins are common components of symbiotic rhizobial and mycorrhizal signalling pathways. Nature Communications 7:1-14

Jogawat A, Yadav B, Lakra N, Singh AK, Narayan OP (2021) Crosstalk between phytohormones and secondary metabolites in the drought stress tolerance of crop plants: A review. Physiologia Plantarum 172:1106-1132

Kalloniati C, Krompas P, Karalias G, Udvardi MK, Rennenberg H, Herschbach C, Flemetakis E (2015) Nitrogen-fixing nodules are an important source of reduced sulfur, which triggers global changes in sulfur metabolism in *Lotus japonicus*. The Plant Cell 27:2384-2400

Kaló P, Gleason C, Edwards A, Marsh J, Mitra RM, Hirsch S, Jakab J, Sims S, Long SR, Rogers J (2005) Nodulation signaling in legumes requires NSP2, a member of the GRAS family of transcriptional regulators. Science 308:1786-1789

Kamboj R, Nanda V (2018) Proximate composition, nutritional profile and health benefits of legumes-A review. Legume Research-An International Journal 41:325-332

Kanamori N, Madsen LH, Radutoiu S, Frantescu M, Quistgaard EM, Miwa H, Downie JA, James EK, Felle HH, Haaning LL (2006) A nucleoporin is required for induction of Ca2+ spiking in legume nodule development and essential for rhizobial and fungal symbiosis. Proceedings of the National Academy of Sciences of the United States of America 103:359-364

Khan M, Gemenet DC, Villordon A (2016) Root system architecture and abiotic stress tolerance: current knowledge in root and tuber crops. Frontiers in Plant Science 7:1584

Khan M, Kiran U, Ali A, Abdin MZ, Zargar M, Ahmad S, Sofi PA, Gulzar S (2017) Molecular markers and marker-assisted selection in crop plants. In: Abdin ZK, UK Athar, A (ed) Plant Biotechnology: Principles and Applications. Springer, pp 295-328

Kibido T, Kunert K, Makgopa M, Greve M, Vorster J (2020) Improvement of rhizobium-soybean symbiosis and nitrogen fixation under drought. Food and Energy Security 9:e177

Kim HJ, Lee HJ, Kim H, Cho SW, Kim J-S (2009) Targeted genome editing in human cells with zinc finger nucleases constructed via modular assembly. Genome Research 19:1279-1288

Klein J, Saedler H, Huijser P (1996) A new family of DNA binding proteins includes putative transcriptional regulators of the *Antirrhinum majus* floral meristem identity gene *SQUAMOSA*. Molecular and General Genetics 250:7-16

Koevoets IT, Venema JH, Elzenga JT, Testerink C (2016) Roots withstanding their environment: exploiting root system architecture responses to abiotic stress to improve crop tolerance. Frontiers in Plant Science 7:1335

Kosslak RM, Bohlool BB (1984) Suppression of nodule development of one side of a split-root system of soybeans caused by prior inoculation of the other side. Plant Physiology 75:125-130

Krouk G, Mirowski P, LeCun Y, Shasha DE, Coruzzi GM (2010) Predictive network modeling of the high-resolution dynamic plant transcriptome in response to nitrate. Genome Biology 11:1-19

Krusell L, Krause K, Ott T, Desbrosses G, Krämer U, Sato S, Nakamura Y, Tabata S, James EK, Sandal N (2005) The sulfate transporter SST1 is crucial for symbiotic nitrogen fixation in *Lotus japonicus* root nodules. The Plant Cell 17:1625-1636

Krusell L, Madsen LH, Sato S, Aubert G, Genua A, Szczyglowski K, Duc G, Kaneko T, Tabata S, de Bruijn F (2002) Shoot control of root development and nodulation is mediated by a receptor-like kinase. Nature Communications 420:422-426

Kumar S, Stecher G, Tamura K (2016) MEGA7: molecular evolutionary genetics analysis version 7.0 for bigger datasets. Molecular Biology and Evolution 33:1870-1874

Kumar T, Bao A-K, Bao Z, Wang F, Gao L, Wang S-M (2018) The progress of genetic improvement in alfalfa (*Medicago sativa* L.). Czech Journal of Genetics and Plant Breeding 54:41-51

Lei Y, Hannoufa A, Yu P (2017) The use of gene modification and advanced molecular structure analyses towards improving alfalfa forage. International Journal of Molecular Sciences 18:298

Lerouge P, Roche P, Faucher C, Maillet F, Truchet G, Promé JC, Dénarié J (1990) Symbiotic host-specificity of *Rhizobium meliloti* is determined by a sulphated and acylated glucosamine oligosaccharide signal. Nature Communications 344:781-784

Li D, Su Z, Dong J, Wang T (2009) An expression database for roots of the model legume *Medicago truncatula* under salt stress. BMC Genomics 10:1-9

Liang G, Zhang H, Lou D, Yu D (2016) Selection of highly efficient sgRNAs for CRISPR/Cas9-based plant genome editing. Scientific Reports 6:1-8

Lim CW, Lee YW, Lee SC, Hwang CH (2014) Nitrate inhibits soybean nodulation by regulating expression of *CLE* genes. Plant Science 229:1-9

Limpens E, Franken C, Smit P, Willemse J, Bisseling T, Geurts R (2003) LysM domain receptor kinases regulating rhizobial Nod factor-induced infection. Science 302:630-633

Lin J-s, Li X, Luo Z, Mysore KS, Wen J, Xie F (2018) NIN interacts with NLPs to mediate nitrate inhibition of nodulation in *Medicago truncatula*. Nature Plants 4:942-952

Linkohr BI, Williamson LC, Fitter AH, Leyser HO (2002) Nitrate and phosphate availability and distribution have different effects on root system architecture of Arabidopsis. The Plant Journal 29:751-760

Liu C-W, Murray JD (2016) The role of flavonoids in nodulation host-range specificity: an update. Plants 5:33-45

Liu H, Ding Y, Zhou Y, Jin W, Xie K, Chen L-L (2017) CRISPR-P 2.0: an improved CRISPR-Cas9 tool for genome editing in plants. Molecular Plant 10:530-532

Liu H, Yu H, Tang G, Huang TJPcr (2018) Small but powerful: function of microRNAs in plant development. Plant Cell Reports 37:515-528

Liu W, Han X, Zhan G, Zhao Z, Feng Y, Wu C (2015) A novel sucrose-regulatory MADS-box transcription factor GmNMHC5 promotes root development and nodulation in soybean (*Glycine max* L. Merr.). International Journal of Molecular Sciences 16:20657-20673

Lynch JP (2007) Roots of the second green revolution. Australian Journal of Botany 55:493-512

Ma L, Liu X, Liu W, Wen H, Zhang Y, Pang Y, Wang X (2021) Characterization of Squamosa-Promoter Binding Protein-Box family genes reveals the critical role of *MsSPL20* in Alfalfa flowering time regulation. Frontiers in Plant Science 12. doi:https://doi.org/10.3389/fpls.2021.775690

Ma X, Zhao F, Zhou B (2022) The characters of non-coding RNAs and their biological roles in plant development and abiotic stress response. International Journal of Molecular Sciences 23:4124

Madsen LH, Fukai E, Radutoiu S, Yost CK, Sandal N, Schauser L, Stougaard J (2005) LORE1, an active low-copy-number TY3-gypsy retrotransposon family in the model legume *Lotus japonicus*. The Plant Journal 44:372-381

Madsen LH, Tirichine L, Jurkiewicz A, Sullivan JT, Heckmann AB, Bek AS, Ronson CW, James EK, Stougaard J (2010) The molecular network governing nodule organogenesis and infection in the model legume *Lotus japonicus*. Nature Communications 1:1-12

Magne K, Couzigou J-M, Schiessl K, Liu S, George J, Zhukov V, Sahl L, Boyer F, Iantcheva A, Mysore KS (2018) *MtNODULE ROOT1* and *MtNODULE ROOT2* are essential for indeterminate nodule identity. Plant Physiology 178:295-316

Magori S, Kawaguch M (2010) Analysis of two potential long-distance signaling molecules, *LjCLE-RS1/2* and jasmonic acid, in a hypernodulating mutant *too much love*. Plant Signaling & Behavior 5:403-405

Mahmood F, Shahzad T, Hussain S, Shahid M, Azeem M, Wery J (2018) Grain legumes for the sustainability of european farming systems. In: Lichtfouse E (ed) Sustainable Agriculture Reviews 32. Springer, pp 105-133

Malcheska F, Ahmad A, Batool S, Müller HM, Ludwig-Müller J, Kreuzwieser J, Randewig D, Hänsch R, Mendel RR, Hell R (2017) Drought-enhanced xylem sap sulfate closes stomata by affecting ALMT12 and guard cell ABA synthesis. Plant Physiology 174:798-814

Małolepszy A, Mun T, Sandal N, Gupta V, Dubin M, Urbański D, Shah N, Bachmann A, Fukai E, Hirakawa H (2016) The LORE 1 insertion mutant resource. The Plant Journal 88:306-317

Marsh JF, Rakocevic A, Mitra RM, Brocard L, Sun J, Eschstruth A, Long SR, Schultze M, Ratet P, Oldroyd GE (2007) *Medicago truncatula NIN* is essential for rhizobial-independent nodule organogenesis induced by autoactive calcium/calmodulin-dependent protein kinase. Plant Physiology 144:324-335

Matsunami T, Kaihatsu A, Maekawa T, Takahashi M, Kokubun M (2004) Characterization of vegetative growth of a supernodulating soybean genotype, Sakukei 4. Plant Production Science 7:165-171

Matthews C, Arshad M, Hannoufa A (2019) Alfalfa response to heat stress is modulated by microRNA156. Physiologia Plantarum 165:830-842

Maxwell CA, Edwards R, Dixon RA, biophysics (1992) Identification, purification, and characterization of S-adenosyl-L-methionine: isoliquiritigenin 2′-O-methyltransferase from alfalfa (*Medicago sativa* L.). Archives of Biochemistry and Biophysics 293:158-166

Maxwell CA, Hartwig UA, Joseph CM, Phillips DA (1989) A chalcone and two related flavonoids released from alfalfa roots induce nod genes of *Rhizobium meliloti*. Plant Physiology 91:842-847

Meng Y, Hou Y, Wang H, Ji R, Liu B, Wen J, Niu L, Lin H (2017) Targeted mutagenesis by CRISPR/Cas9 system in the model legume *Medicago truncatula*. Plant Cell Reports 36:371-374

Mergaert P, Kereszt A, Kondorosi E (2020) Gene expression in nitrogen-fixing symbiotic nodule cells in *Medicago truncatula* and other nodulating plants. The Plant Cell 32:42-68

Messinese E, Mun J-H, Yeun LH, Jayaraman D, Rougé P, Barre A, Lougnon G, Schornack S, Bono J-J, Cook DR (2007) A novel nuclear protein interacts with the symbiotic DMI3 calcium-and calmodulin-dependent protein kinase of *Medicago truncatula*. Molecular Plant-Microbe Interactions 20:912-921

Michaels SD, Ditta G, Gustafson-Brown C, Pelaz S, Yanofsky M, Amasino RM (2003) *AGL24* acts as a promoter of flowering in *Arabidopsis* and is positively regulated by vernalization. The Plant Journal 33:867-874

Middleton PH, Jakab J, Penmetsa RV, Starker CG, Doll J, Kaló P, Prabhu R, Marsh JF, Mitra RM, Kereszt A (2007) An ERF transcription factor in *Medicago truncatula* that is essential for Nod factor signal transduction. The Plant Cell 19:1221-1234

Moreau C, Gautrat P, Frugier F (2021) Nitrate-induced CLE35 signaling peptides inhibit nodulation through the SUNN receptor and miR2111 repression. Plant Physiology 185:1216-1228

Mortier V, Den Herder G, Whitford R, Van de Velde W, Rombauts S, D'haeseleer K, Holsters M, Goormachtig S (2010) CLE peptides control *Medicago truncatula* nodulation locally and systemically. Plant Physiology 153:222-237

Mortier V, Holsters M, Goormachtig S, environment (2012) Never too many? How legumes control nodule numbers. Plant, Cell & Environment 35:245-258

Mouradi M, Farissi M, Bouizgaren A, Lahrizi Y, Qaddoury A, Ghoulam C (2018) Alfalfa and its symbiosis responses to osmotic stress. New Perspectives in Forage Crops 17:149-168

Mun T, Bachmann A, Gupta V, Stougaard J, Andersen SU (2016) Lotus Base: An integrated information portal for the model legume *Lotus japonicus*. Scientific Reports 6:1-18

Muqbil I, Bao B, Badi Abou-Samra A, M Mohammad R, S Azmi A (2013) Nuclear export mediated regulation of microRNAs: potential target for drug intervention. Current Drug Targets 14:1094-1100

Murphy E, Smith S, De Smet I (2012) Small signaling peptides in *Arabidopsis* development: how cells communicate over a short distance. The Plant Cell 24:3198-3217

Murray JD, Liu C-W, Chen Y, Miller AJ (2017) Nitrogen sensing in legumes. Journal of Experimental Botany 68:1919-1926

Murray M, Thompson WF (1980) Rapid isolation of high molecular weight plant DNA. Nucleic Acids Research 8:4321-4326

Nishimura R, Hayashi M, Wu G-J, Kouchi H, Imaizumi-Anraku H, Murakami Y, Kawasaki S, Akao S, Ohmori M, Nagasawa M (2002) HAR1 mediates systemic regulation of symbiotic organ development. Nature Communications 420:426-429

Nova-Franco B, Íñiguez LP, Valdés-López O, Alvarado-Affantranger X, Leija A, Fuentes SI, Ramírez M, Paul S, Reyes JL, Girard L (2015) The micro-RNA172c-APETALA2-1 node as a key regulator of the common bean-*Rhizobium etli* nitrogen fixation symbiosis. Plant Physiology 168:273-291

Okamoto S, Shinohara H, Mori T, Matsubayashi Y, Kawaguchi M (2013) Root-derived CLE glycopeptides control nodulation by direct binding to HAR1 receptor kinase. Nature Communications 4:1-7

Oldroyd GE (2013) Speak, friend, and enter: signalling systems that promote beneficial symbiotic associations in plants. Nature Reviews Microbiology 11:252-263

Oldroyd GE, Downie JA (2004) Calcium, kinases and nodulation signalling in legumes. Nature Reviews Molecular Cell Biology 5:566-576

Oldroyd GE, Downie JA (2008) Coordinating nodule morphogenesis with rhizobial infection in legumes. Annual Review of Plant Biology 59:519-546

Oldroyd GE, Murray JD, Poole PS, Downie JA (2011) The rules of engagement in the legume-rhizobial symbiosis. Annual Review of Genetics 45:119-144

Oliveros JC (2007) VENNY. An interactive tool for comparing lists with Venn Diagrams. http://bioinfogp.cnb.csic.es/tools/venny/index.html

Osmont KS, Sibout R, Hardtke CS (2007) Hidden branches: developments in root system architecture. Annual Review of Plant Biology 58:93-113

Pacyna S, Schulz M, Scherer H (2006) Influence of sulphur supply on glucose and ATP concentrations of inoculated broad beans (*Vicia faba minor* L.). Biology and Fertility of Soils 42:324-329

Pan C, Ye L, Qin L, Liu X, He Y, Wang J, Chen L, Lu G (2016) CRISPR/Cas9-mediated efficient and heritable targeted mutagenesis in tomato plants in the first and later generations. Scientific Reports 6:1-9

Pang Y, Wenger JP, Saathoff K, Peel GJ, Wen J, Huhman D, Allen SN, Tang Y, Cheng X, Tadege M (2009) A WD40 repeat protein from *Medicago truncatula* is

necessary for tissue-specific anthocyanin and proanthocyanidin biosynthesis but not for trichome development. Plant Physiology 151:1114-1129

Park J-J, Yoo CG, Flanagan A, Pu Y, Debnath S, Ge Y, Ragauskas AJ, Wang Z-Y (2017) Defined tetra-allelic gene disruption of the 4-coumarate: coenzyme A ligase 1 (Pv4CL1) gene by CRISPR/Cas9 in switchgrass results in lignin reduction and improved sugar release. Biotechnology for Biofuels 10:1-11

Peters NK, Frost JW, Long SR (1986) A plant flavone, luteolin, induces expression of *Rhizobium meliloti* nodulation genes. Science 233:977-980

Popp C, Ott T (2011) Regulation of signal transduction and bacterial infection during root nodule symbiosis. Current Opinion in Plant Biology 14:458-467

Potel F, Valadier MH, Ferrario-Méry S, Grandjean O, Morin H, Gaufichon L, Boutet-Mercey S, Lothier J, Rothstein SJ, Hirose N (2009) Assimilation of excess ammonium into amino acids and nitrogen translocation in *Arabidopsis thaliana*– roles of glutamate synthases and carbamoylphosphate synthetase in leaves. The FEBS Journal 276:4061-4076

Prell J, Poole P (2006) Metabolic changes of rhizobia in legume nodules. Trends in Microbiology 14:161-168

Preston J, Hileman L (2013) Functional evolution in the plant *SQUAMOSA-PROMOTER BINDING PROTEIN-LIKE* (*SPL*) gene family. Frontiers in Plant Science 4:80

Provorov N, Tikhonovich I (2003) Genetic resources for improving nitrogen fixation in legume-rhizobia symbiosis. Genetic Resources and Crop Evolution 50:89-99

Puig J, Meynard D, Khong GN, Pauluzzi G, Guiderdoni E, Gantet P (2013) Analysis of the expression of the *AGL17-like* clade of MADS-box transcription factors in rice. Gene Expression Patterns 13:160-170

Reid DE, Ferguson BJ, Gresshoff PM (2011a) Inoculation-and nitrate-induced CLE peptides of soybean control NARK-dependent nodule formation. Molecular Plant-Microbe Interactions 24:606-618

Reid DE, Ferguson BJ, Hayashi S, Lin Y-H, Gresshoff PM (2011b) Molecular mechanisms controlling legume autoregulation of nodulation. Annals of Botany 108:789-795

Reubens B, Poesen J, Danjon F, Geudens G, Muys B (2007) The role of fine and coarse roots in shallow slope stability and soil erosion control with a focus on root system architecture: a review. Trees 21:385-402

Rogers K, Chen X (2013) Biogenesis, turnover, and mode of action of plant microRNAs. The Plant Cell 25:2383-2399

Roux B, Rodde N, Jardinaud MF, Timmers T, Sauviac L, Cottret L, Carrère S, Sallet E, Courcelle E, Moreau S (2014) An integrated analysis of plant and bacterial gene expression in symbiotic root nodules using laser-capture microdissection coupled to RNA sequencing. The Plant Journal 77:817-837

Roy S, Liu W, Nandety RS, Crook A, Mysore KS, Pislariu CI, Frugoli J, Dickstein R, Udvardi MK (2020) Celebrating 20 years of genetic discoveries in legume nodulation and symbiotic nitrogen fixation. The Plant Cell 32:15-41

Rozema J, Flowers T (2008) Crops for a salinized world. Science 322:1478-1480

Saito K, Yoshikawa M, Yano K, Miwa H, Uchida H, Asamizu E, Sato S, Tabata S, Imaizumi-Anraku H, Umehara Y (2007) NUCLEOPORIN85 is required for calcium spiking, fungal and bacterial symbioses, and seed production in *Lotus japonicus*. The Plant Cell 19:610-624

Sander JD, Joung JK (2014) CRISPR-Cas systems for editing, regulating and targeting genomes. Nature Biotechnology 32:347-355

Sańko-Sawczenko I, Łotocka B, Mielecki J, Rekosz-Burlaga H, Czarnocka W (2019) Transcriptomic changes in *Medicago truncatula* and *Lotus japonicus* root nodules during drought stress. International Journal of Molecular Sciences 20:1204-1223

Schauser L, Roussis A, Stiller J, Stougaard J (1999) A plant regulator controlling development of symbiotic root nodules. Nature Communications 402:191-195

Scherer HW (2008) Impact of sulfur on N 2 fixation of legumes. In: Khan NS, S Umar,S (ed) Sulfur Assimilation and Abiotic Stress in Plants. Springer, pp 43-54

Scherer HW, Lange A (1996) N2 fixation and growth of legumes as affected by sulphur fertilization. Biology Fertility of Soils 23:449-453

Schilling S, Pan S, Kennedy A, Melzer R (2018) *MADS-box* genes and crop domestication: the jack of all traits. Journal of Experimental Botany 69:1447-1469

Schnabel E, Journet E-P, de Carvalho-Niebel F, Duc G, Frugoli J (2005) The *Medicago truncatula SUNN* gene encodes a CLV1-like leucine-rich repeat receptor kinase that regulates nodule number and root length. Plant Molecular Biology 58:809-822

Schwarz S, Grande AV, Bujdoso N, Saedler H, Huijser P (2008) The microRNA regulated SBP-box genes *SPL9* and *SPL15* control shoot maturation in Arabidopsis. Plant Molecular Biology 67:183-195

Searle IR, Men AE, Laniya TS, Buzas DM, Iturbe-Ormaetxe I, Carroll BJ, Gresshoff PM (2003) Long-distance signaling in nodulation directed by a CLAVATA1-like receptor kinase. Science 299:109-112

Sentmanat MF, Peters ST, Florian CP, Connelly JP, Pruett-Miller SM (2018) A survey of validation strategies for CRISPR-Cas9 editing. Scientific Reports 8:1-8

Shan Q, Wang Y, Li J, Gao C (2014) Genome editing in rice and wheat using the CRISPR/Cas system. Nature Protocols 9:2395-2410

Shan S, Soltis PS, Soltis DE, Yang B (2020) Considerations in adapting CRISPR/Cas9 in nongenetic model plant systems. Applications in Plant Sciences 8:e11314

Sheaffer CC, Seguin P (2003) Forage legumes for sustainable cropping systems. Journal of Crop Production 8:187-216

Shi M-Z, Xie D-Y (2014) Biosynthesis and metabolic engineering of anthocyanins in *Arabidopsis thaliana*. Recent Patents on Biotechnology 8:47-60

Shikata M, Koyama T, Mitsuda N, Ohme-Takagi M (2009) Arabidopsis SBP-box genes *SPL10*, *SPL11* and *SPL2* control morphological change in association with shoot maturation in the reproductive phase. Plant & Cell Physiology 50:2133-2145

Shore P, Sharrocks AD (1995) The MADS-box family of transcription factors. European Journal of Biochemistry 229:1-13

Shuai B, Reynaga-Pena CG, Springer PS (2002) The lateral organ boundaries gene defines a novel, plant-specific gene family. Plant Physiology 129:747-761

Singer SD, Burton KH, Subedi U, Dhariwal GK, Kader K, Acharya S, Chen G, Hannoufa A (2021) The CRISPR/Cas9-mediated modulation of *SQUAMOSA PROMOTER-BINDING PROTEIN-LIKE 8* in alfalfa leads to distinct phenotypic outcomes. Frontiers in Plant Science 12:774146-774146

Singer SD, Hannoufa A, Acharya S (2018) Molecular improvement of alfalfa for enhanced productivity and adaptability in a changing environment. Plant, Cell & Environment 41:1955-1971

Smit P, Raedts J, Portyanko V, Debellé F, Gough C, Bisseling T, Geurts R (2005) NSP1 of the GRAS protein family is essential for rhizobial Nod factor-induced transcription. Science 308:1789-1791

Soltis DE, Soltis PS, Morgan DR, Swensen SM, Mullin BC, Dowd JM, Martin PG (1995) Chloroplast gene sequence data suggest a single origin of the predisposition for symbiotic nitrogen fixation in angiosperms. Proceedings of the National Academy of Sciences of the United States of America 92:2647-2651

Sprent JI (2007) Evolving ideas of legume evolution and diversity: a taxonomic perspective on the occurrence of nodulation. New Phytologist 174:11-25

Stagnari F, Maggio A, Galieni A, Pisante M (2017) Multiple benefits of legumes for agriculture sustainability: an overview. Chemical and Biological Technologies in Agriculture 4:1-13

Streeter J, Wong PP (1988) Inhibition of legume nodule formation and N2 fixation by nitrate. Critical Reviews in Plant Sciences 7:1-23

Sun C-H, Yu J-Q, Hu D-G (2017) Nitrate: a crucial signal during lateral roots development. Frontiers in Plant Science 8:485

Sun G (2012) MicroRNAs and their diverse functions in plants. Plant Molecular Biology 80:17-36

Supek F, Bošnjak M, Škunca N, Šmuc T (2011) REVIGO summarizes and visualizes long lists of gene ontology terms. PLOS One 6:e21800

Suzaki T, Yoro E, Kawaguchi M (2015) Leguminous plants: inventors of root nodules to accommodate symbiotic bacteria. International Review of Cell and Molecular Biology 316:111-158

Szczyglowski K, Shaw RS, Wopereis J, Copeland S, Hamburger D, Kasiborski B, Dazzo FB, de Bruijn FJ (1998) Nodule organogenesis and symbiotic mutants of the model legume *Lotus japonicus*. Molecular Plant-Microbe Interactions 11:684-697

Takahashi F, Shinozaki K (2019) Long-distance signaling in plant stress response. Current Opinion in Plant Biology 47:106-111

Takahashi H, Buchner P, Yoshimoto N, Hawkesford MJ, Shiu S-H (2012) Evolutionary relationships and functional diversity of plant sulfate transporters. Frontiers in Plant Science 2:119

Thapanapongworakul N, Nomura M, Shimoda Y, Sato S, Tabata S, Tajima S (2010) NAD+-malic enzyme affects nitrogenase activity of *Mesorhizobium loti* bacteroids in *Lotus japonicus* nodules. Plant Biotechnology Journal 27:311-316

Theißen G, Gramzow L (2016) Structure and evolution of plant MADS domain transcription factors. In: Gonzalez D (ed) Plant Transcription Factors. Elsevier, pp 127-138

Tian QY, Sun P, Zhang WH (2009) Ethylene is involved in nitrate-dependent root growth and branching in *Arabidopsis thaliana*. New Phytologist 184:918-931

Trapnell C, Roberts A, Loyal Go GP, Daehwan Kim, David R Kelley, Harold Pimentel, Steven L Salzberg, John L Rinn, and Lior Pachter (2012) Differential gene and

transcript expression analysis of RNA-seq experiments with TopHat and Cufflinks. Nature Protocols 7:562-578

Truchet G, Roche P, Lerouge P, Vasse J, Camut S, de Billy F, Promé J-C, Dénarié J (1991) Sulphated lipo-oligosaccharide signals of *Rhizobium meliloti* elicit root nodule organogenesis in alfalfa. Nature Communications 351:670-673

Tsay Y-F, Chiu C-C, Tsai C-B, Ho C-H, Hsu P-K (2007) Nitrate transporters and peptide transporters. FEBS Letters 581:2290-2300

Tsikou D, Yan Z, Holt DB, Abel NB, Reid DE, Madsen LH, Bhasin H, Sexauer M, Stougaard J, Markmann KJS (2018) Systemic control of legume susceptibility to rhizobial infection by a mobile microRNA. Science 362:233-236

Urbański DF, Małolepszy A, Stougaard J, Andersen SU (2012) Genome-wide LORE1 retrotransposon mutagenesis and high-throughput insertion detection in *Lotus japonicus*. The Plant Journal 69:731-741

van Velzen R, Doyle JJ, Geurts R (2019) A resurrected scenario: single gain and massive loss of nitrogen-fixing nodulation. Trends in Plant Science 24:49-57

Varin S, Cliquet J-B, Personeni E, Avice J-C, Lemauviel-Lavenant S (2010) How does sulphur availability modify N acquisition of white clover (*Trifolium repens* L.)? Journal of Experimental Botany 61:225-234

Vera-Estrella R, Barkla BJ, Bohnert HJ, Pantoja O (2004) Novel regulation of aquaporins during osmotic stress. Plant Physiology 135:2318-2329

Volenec J, Cunningham S, Haagenson D, Berg W, Joern B, Wiersma D (2002) Physiological genetics of alfalfa improvement: past failures, future prospects. Field Crops Research 75:97-110

Voytas DF, Gao C (2014) Precision genome engineering and agriculture: opportunities and regulatory challenges. PLOS Biology 12:e1001877

Wang H, Wang HJMp (2015) The miR156/SPL module, a regulatory hub and versatile toolbox, gears up crops for enhanced agronomic traits. Molecular Plant 8:677-688

Wang L, Sun Z, Su C, Wang Y, Yan Q, Chen J, Ott T, Li X (2019) A GmNINa-miR172c-NNC1 regulatory network coordinates the nodulation and autoregulation of nodulation pathways in soybean. Molecular Plant 12:1211-1226

Wang Q, Liu J, Zhu H (2018) Genetic and molecular mechanisms underlying symbiotic specificity in legume-rhizobium interactions. Frontiers in Plant Science 9:313

Wang W, Akhunova A, Chao S, Akhunov E (2016) Optimizing multiplex CRISPR/Cas9-based genome editing for wheat. BioRxiv:051342. doi:https://doi.org/10.1101/051342

Wang Y, Wang L, Zou Y, Chen L, Cai Z, Zhang S, Zhao F, Tian Y, Jiang Q, Ferguson BJ (2014) Soybean miR172c targets the repressive AP2 transcription factor NNC1 to activate *ENOD40* expression and regulate nodule initiation. The Plant Cell 26:4782-4801

Wang Y, Wang Z, Amyot L, Tian L, Xu Z, Gruber MY, Hannoufa A (2015) Ectopic expression of miR156 represses nodulation and causes morphological and developmental changes in *Lotus japonicus*. Molecular Genetics and Genomics 290:471-484

Wei L, HOU W-s, Shi S, JIANG B-j, HAN T-f, FENG Y-j, WU C-x (2019) GmNMH7, a MADS-box transcription factor, inhibits root development and nodulation of soybean (*Glycine max* L. Merr.). Journal of Integrative Agriculture 18:553-562

Wei S, Gruber MY, Yu B, Gao M-J, Khachatourians GG, Hegedus DD, Parkin IA, Hannoufa A (2012) Arabidopsis mutant *sk156* reveals complex regulation of *SPL15* in a *miR156*-controlled gene network. BMC Plant Biology 12:1-17

Wolabu TW, Cong L, Park J-J, Bao Q, Chen M, Sun J, Xu B, Ge Y, Chai M, Liu Z (2020) Development of a highly efficient multiplex genome editing system in outcrossing tetraploid alfalfa (*Medicago sativa*). Frontiers in Plant Science 11:1063

Woo JW, Kim J, Kwon SI, Corvalán C, Cho SW, Kim H, Kim S-G, Kim S-T, Choe S, Kim J-S (2015) DNA-free genome editing in plants with preassembled CRISPR-Cas9 ribonucleoproteins. Nature Biotechnology 33:1162-1164

Wu M-F, Tian Q, Reed JW (2006) Arabidopsis microRNA167 controls patterns of *ARF6* and *ARF8* expression, and regulates both female and male reproduction. Development 133:4211-4218

Xiong L, Wang R-G, Mao G, Koczan JM (2006) Identification of drought tolerance determinants by genetic analysis of root response to drought stress and abscisic acid. Plant Physiology 142:1065-1074

Xu M, Hu T, Zhao J, Park M-Y, Earley KW, Wu G, Yang L, Poethig RS (2016) Developmental functions of miR156-regulated *SQUAMOSA PROMOTER BINDING PROTEIN-LIKE* (*SPL*) genes in *Arabidopsis thaliana*. PLOS Genetics 12:e1006263

Xu W, Dubos C, Lepiniec L (2015) Transcriptional control of flavonoid biosynthesis by MYB–bHLH–WDR complexes. Trends in Plant Science 20:176-185

Yamasaki K, Kigawa T, Inoue M, Tateno M, Yamasaki T, Yabuki T, Aoki M, Seki E, Matsuda T, Nunokawa E, Ishizuka Y, Terada T, Shirouzu M, Osanai T, Tanaka A, Seki M, Shinozaki K, Yokoyama S (2004) A novel zinc-binding motif revealed by solution structures of DNA-binding domains of Arabidopsis SBP-family transcription factors. Journal of Molecular Biology 337:49-63

Yamasaki K, Kigawa T, Inoue M, Yamasaki T, Yabuki T, Aoki M, Seki E, Matsuda T, Tomo Y, Terada T (2006) An Arabidopsis SBP-domain fragment with a disrupted C-terminal zinc-binding site retains its tertiary structure. FEBS Letters 580:2109-2116

Yan Z, Hossain MS, Wang J, Valdés-López O, Liang Y, Libault M, Qiu L, Stacey G (2013) miR172 regulates soybean nodulation. Molecular Plant-Microbe Interactions 26:1371-1377

Yano K, Yoshida S, Müller J, Singh S, Banba M, Vickers K, Markmann K, White C, Schuller B, Sato S (2008) CYCLOPS, a mediator of symbiotic intracellular accommodation. Proceedings of the National Academy of Sciences of the United States of America 105:20540-20545

Yu B, Yang Z, Li J, Minakhina S, Yang M, Padgett RW, Steward R, Chen X (2005) Methylation as a crucial step in plant microRNA biogenesis. Science 307:932-935

Yu C, Liu Y, Zhang A, Su S, Yan A, Huang L, Ali I, Liu Y, Forde BG, Gan Y (2015a) MADS-box transcription factor *OsMADS25* regulates root development through affection of nitrate accumulation in rice. PLoS One 10:e0135196

Yu H, Ito T, Wellmer F, Meyerowitz EM (2004) Repression of AGAMOUS-LIKE 24 is a crucial step in promoting flower development. Nature Genetics 36:157-161

Yu L-H, Miao Z-Q, Qi G-F, Wu J, Cai X-T, Mao J-L, Xiang C-B (2014) MADS-box transcription factor AGL21 regulates lateral root development and responds to multiple external and physiological signals. Molecular Plant 7:1653-1669

Yu N, Niu QW, Ng KH, Chua NH (2015b) The role of miR156/SPLs modules in Arabidopsis lateral root development. The Plant Journal 83:673-685

Yu Y, Jia T, Chen X (2017) The ‘how’and ‘where’of plant microRNAs. New Phytologist 216:1002-1017

Yun J, Sun Z, Jiang Q, Wang Y, Wang C, Luo Y, Zhang F, Li X (2022) The miR156b-GmSPL9d module modulates nodulation by targeting multiple core nodulation genes in soybean. New Phytologist 233:1881-1899

Zhang H, Forde BG (1998) An *Arabidopsis* MADS box gene that controls nutrient-induced changes in root architecture. Science 279:407-409

Zhang J, Wang Y, Naeem M, Zhu M, Li J, Yu X, Hu Z, Chen G (2019) An AGAMOUS MADS-box protein, SlMBP3, regulates the speed of placenta liquefaction and controls seed formation in tomato. Journal of Experimental Botany 70:909-924

Zhao L, Liu F, Crawford NM, Wang Y (2018) Molecular regulation of nitrate responses in plants. International Journal of Molecular Sciences 19:2039

Zia R, Nawaz MS, Siddique MJ, Hakim S, Imran A (2021) Plant survival under drought stress: Implications, adaptive responses, and integrated rhizosphere management strategy for stress mitigation. Microbiological Research 242:126626

Zimny T, Sowa S, Tyczewska A, Twardowski T (2019) Certain new plant breeding techniques and their marketability in the context of EU GMO legislation–recent developments. New Biotechnology 51:49-56

Zong Y, Wang Y, Li C, Zhang R, Chen K, Ran Y, Qiu J-L, Wang D, Gao C (2017) Precise base editing in rice, wheat and maize with a Cas9-cytidine deaminase fusion. Nature Biotechnology 35:438-440

Zou Q, Luo S, Wu H, He D, Li X, Cheng G (2020) A GMC Oxidoreductase GmcA is required for symbiotic nitrogen fixation in *Rhizobium leguminosarum* bv. viciae. Frontiers in Microbiology 11:394

Appendices

ATGGAGTGGAATTTGAAAGCACCTTCTTGGGATTTGGGGGGTATAGAAGAGGCAACATTACCCAACATAGAAACAATGGAAGAAT
CAAACAGATTTGGAGTTTATAAAATGAAAGGGGAGTTTTCTGTTGATTTGAAGCTTGGTCAGGTTGGGAACTCTGCCACTGATCA
ATCACCACTTCCTTTGTCTAATGATGCTGTTGTTGTCTCCAAAATTGCAACACCTACTTCTTCTTCAGGATCTTCTAAGAGAGCT
AGAGCTATGAATAATGCAACATTG**ACAGTGTCTTGTCTTGTGGATGGGTGCAATTCTGATCTTAGTAATTGTAGAGATTATCATA**
GGCGTCATAAGGTTTGTGAACTTCATTCTAAGACTCCAGAGGTTACAATTTGTGGCCTTAAACAAAGGTTCTGCCAACAGTGTAG
CAGGTTTCATTCGCTGGAGCAATTTGATGAAAGAAAAAGAAGCTGTAGGAAACGTTTAGATGGACACAACCGAAGAAGAAGAAAA
CCACAGCCTGAACCTATCACGCGACCTGCTGGTAGTTTTTTGTCCAATTACCAAGGCACCCAGGTGCTACCCTTTTCAAGTTCTA
CTGCCATGGTGAATTCAGCTTGGAGTAGCGGACTCATTACTTCCTGTGAAAGTGGTAGACTTCACATCCACAACCAACACCAGCA
AGTTCATGTGGTTGATAAACAAGATCATTTTCTTGGTTCTACTGCAACCACCTACGAAGAAGGGAAACAACTTCAATTCTTACAC
AATGACAACAACAATCCCTCACTTCATAGCCAAACCACACCTCTTCTTAGGACAAGTAGCAAAATGTTCTGTGATAGTTTAGCAA
CTTCAGTACACGAGTCACCTTGTGCTCTCTCTCTTCTGTCATCATCACAGACGCACACACCTGATAATGGTTTGAATCAAATGGT
GCAGCAGCCTCATTCAATGTCTCTTATGCAGCCCTTGGGACTGAGTCTGCATGGTAACAATAGCTTTGAGTCCATG**GAAGGAGTG**
TTGGTCCCAAATGGGAGTGAGAGTGATCATTGTTCCTCGTTGTATAACATGGGTTCTGATGGATCACAAGGCAATGATGCACCTC
AACTATTTCCCTATCAATGGGAATAG

Figure S1 The original coding sequence of *SPL13* in alfalfa and positions of different gRNAs selected for CRISPR experiments

Different exons are indicated with bold and normal sequences. Sequences in green (gRNA1): GCATCATTAGACAAAGGAAG, sequences in red (gRNA2): GAACCTATCACGCGACCTGC and sequences in purple (gRNA3): GAAGGAGTGTTGGTCCCAAA.

CTTTCTGTGTTATGTGATGCTGAGGTTGCTCTTATCATTTTCTCCGGTCTTGGCAAGCTTTTTCAATACAGTACCACAGAGTGAGCAATTCATTTTCTTT
TAATATATATATCTTTAAGCAATTTTTTATCTCTTCGTTAGTTTTTTAAATACAAGCTTGGTCATAATTAAAAATATTCTAGGGGTTGTAAAATTATCTGTT
TAGCGCATTTTTGTTTGCCAAGAGAAATATCATAAGGTAAAAGCTACCGGCCGGTGGATTGGTCATTCATGAAGACAACTTGTTTGGCAAAGCACAA
CCACTTGATAGTTCTAGCAACATTCACTCATCATTTGACTAAGTTATTCCTTCTTGTCTTGGTTATAAGTAAACTAATTTCACACATTAAGAAATTCAGTA
AATATAATTAATCTTCTTGCAACAAAAAAAATGGTACCCATCATAAAAATTTGTTTCATAAGAATGAAATGTCACTAAAAAAATAAAATATATATAAATTA
AAGAGTATTTTAGGATATGAGTCTTTATATCAAAAGTAGTCATATTAGCTTAATTATATTTTAAAAAAGTATGCACTTTTTTTTTTTTTTATCTTTATTTGA
GATTGGAATTAGGGGTGTCAATTTCATCTCTGAATGGGGATCTAAGCGGGTACCATCAAATTTGAAGTTACGTAGACGGAGAATTTTTTTCTATTGG
GGATGGGGGAGAAAGTATTCTCTGATAATAGTGCAGGGACACGATCATACCCCCCGATACATGGAGACTCGTCCCCGAGCAATTCAGTATAATATATT
TTATATTGGTATATACAAATATTTCCTATGTTATATTTATTTATCATTTTACGCAATTTTTTTATATGTAATGTTTACTGTAATGCCTTAATTATATTATATTTGT
TTTAATGTTAAATTTTAATTTTTTTAAAATAATATAAATTTAGTTATTTTTACATGCCGATGGATCTCTGTGGGACCGTGGTGATGTGCGGGGGTGAGG
ACAGGGAGGAAAAACTCTCCAAGACGGGGAATGGGGATGAGGGACAATTTAAGTGGCGGGAGAGGAAACATAGATGTACTCCTTGTCTCCTCCC
CACCCCATCCATTGACATCCCTGACTAGAATAGCTAGTAGAGTATTTTTTTTTTTTTTGACAAAAAACAAGTAGAGTACGATAAAAAGGATTATTTTA
GTCATGGATTGAACTATAATATTCCAAGATAATTTGACCTTAATGAAGTTTTACTAACTACTTAAACTCAACCATTTAGTTAGACTTTAACATCAAAATG
TGTTTGAGTTGTGTAAGTTTGAGGTGGATTTGTGGGAGTAACTTGATAGCGGTTATAAAATTAAATTTGAGTTTCTTACAAATTTGTCATTGGAGATG
TTCTAAGGATCATACTAGCTTATATTCTAAGAGCACATGTTAAAGATTTTTACCAATAGTAATTATAATTGAAAAAAGTAATTTTCAACTTTTTGAAGAA
TGTACAAAGTTTTCAATAAGAAATTTCTATATTTAATGCACTAACAAGTGCCTTAACTATAAGGGTGCATTTTAACATTCCTCTTGTTGTAATACAAACA
ATGATGTTAGTTTTATTCAACGGGAGAGAATGTAGTTGTTAGTCCCTATATTTTTATAACGTATTATCTTTTTTTTTTTGTTTCACGGTTTATTTCAATAAT
TTAACTCAAGTCAAAATTATATGGTACTAACCAATATAATTGATATACCTTGTTCATTCTGATCAGCTTGAACAAAATCATTGAGAAGTATCGTCAATGTT
GCTTCAACAATATGTCTGAGAATGGTGACTTAGGAGAACATGAGTCACAGG

Figure S2 Promoter sequence of the alfalfa *AGL6* gene with putative SBD binding elements

Nucleotides that are highlighted in yellow represent putative SPL binding elements with ‘GTAC’ core sequences, and those in blue represent forward and reverse primer sequences used for ChIP-qPCR . The red text shows coding sequences of *AGL6*.

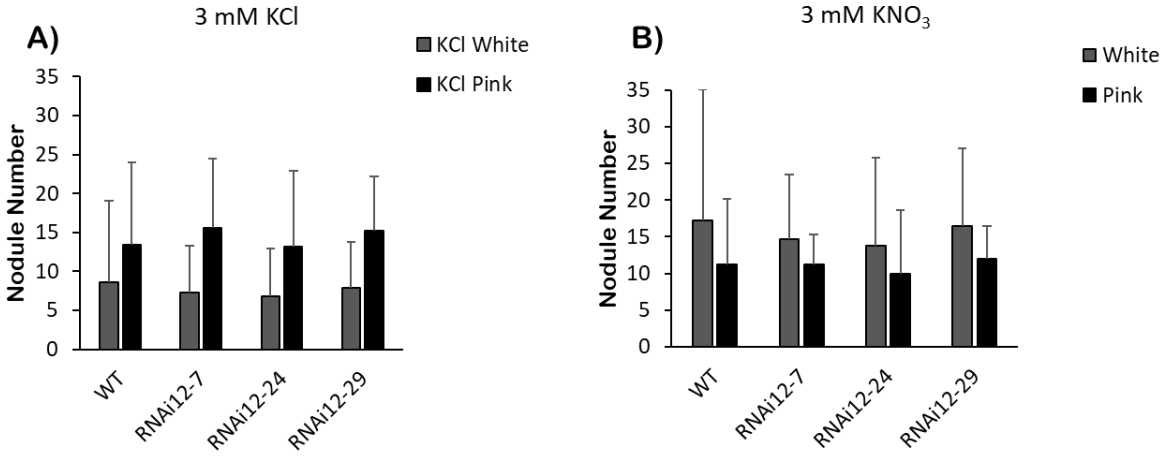

Figure S3 Effect of nitrate on nodulation in *SPL12*-RNAi plants

The average numbers of pink and white nodules in WT and *SPL12*-RNAi at 21 dai (n = 15-22) under 3 Mm **A)** KCl and **B)** KNO_3. Error bars indicate standard deviation.

GGAGGTTACAACTATATATACTAATAGGACTAATACTACTTGTAACTAAACTATGTATCTCTAATAGGTGTTTTGATGTGCGAGGTGTAAGGTT
TTCTTTTGGTGTTCCGCATATATACGACGTCTTTTGTTATGTTGTTTATTCTTACCGGTCTCTAAAACATTACTCTTTAAAAAAATATGAAAGAT
TTTTCAATTTCTCCTATATTTCTCACCCCTAATGTGTTCACCTAAACCTCTAAGATTCTAAAACATGAACTTTTTCTTTTTGGAGATACCCTTTT
TAGAACGGGTGATTATGCCTCCTGAATTTGTATCAGCAGGAGTGACAACATCACTTTGCTTCTTTTTTTTTCTGCAGTTCCATGTTAACCTTT
GTTAGAGTTTCCACATGTTTGTTGGGATTGTATTCCTGCACAATTAAAGTGTTTGCGTCAGGATCATCCTCTGCTAAGTCACCCCAATGTTCC
TTAAGGATTTGTACACTCCTCTTACTAGCCTCTGTGGGTACACTCCTCTTACAAGCCTCATCAAATTTAACAAAGTTTTTTCTTCTCAAACAA
AAAAACTCTTATCCCTTTAAGCTTCTAGCTCCACTCACCCATTTTTCGAATGTAGATCTCTTCCTACTCGGATATTGCCAACAACCTAAGGAA
AACTTGCTTAAGAGAGTAGACATCAATACATCTATCATGTCAAAATTGAATTCTCCCTTCATCTTCCATTTTTTCACACGCTAAGCTCGTAAAT
TGATCCCCTTTAACCCTTCACATACGGTCTAAACAACACAAATTGTTCCATCACAAAGGAAGTTGATGACTCTGGAGAAGCCAAAGTGCTA
ACACCATACTTGGTTGACAAGACGTTTATCCATTGAGACTACCTTTATTAATAACTGCCACCTCCATTTGGTTGAAATATATTGTCTACACATG
TCCCCTAATGAATAAAGTATCAGTACGCACGCTCCCAGAAAGCGTGCGAGTGAGGACAAAACACGCTGAAAAGATTTGCGTTGATTTGTG
GGGTCAGTCGGCAATCCTAAAAGCAGTCTGAGATGTTACATTGGGAGCCCTTCTGGAGGGCACCTAAGCCTCTCTAGAAGGCATTTGTTC
CCTTAGGAATAGATTGACGATTCAATTATATTATTAAGTTTGTGTAAAATGACCAAAATGGTTTATGAGAAAGTACGTCTTGTGCAAAAATAC
TTTTTTTAAGAGGCTAGACGTGTTATCGTCATGCCTTATATTGATAAGGCTTTTAATTTTTATATTCTTTTAGAATGGCAAATGTTATTAATGAA
TTGTTAGAATAATTTCTCTCCTTTATCCGAGTTTAAACTCAGGAACTTCAACTCCTTTATCTCTTGGCTCAAACCAGTTGAGTCATCCAACCTC
CATAGATTAAGCATTTCATGATCAATGATATTGATAATTTTGGGAACAAATTAAAAATATGATTATTCTTTCTTGTGGTCAGCATGAAATCAGT
GATTGAGAGATATAACATTTGCAAGGAAGACCAACAAGGGACAAATCCAGAATCTGAAGTCAAG

Figure S4 Promoter sequence of the alfalfa *AGL21* gene with putative SBD binding elements

Nucleotides highlighted with green/yellow represent putative SPL binding elements with 'GTAC' core sequences, those highlighted in blue represent forward and reverse primer sequences used for ChIP-qPCR. The red text shows coding sequences of *AGL21*.

Table S1 Primers utilized and their nucleotide sequences

Primer Name	Primer Sequence	Primer Use	Origin
RNAiMsSPL12-F2	CACCACAGGTCTAGAAGATCCAA	*SPL12*-RNAi construct cloning	*M. sativa*
RNAiMsSPL12-R2	CGAGAACGAGATACAGGCACT	*SPL12*-RNAi construct cloning	*M. sativa*
pHELLGATE12intro	TGATTACTTTATTTCGTGTGTCTA	RNAi construct cloning	*M. sativa*
MsAGL6-RNAi-F2	CACCTACAAGATGCTTCAAAAAGAC	*AGL6*-RNAi construct cloning	*M. sativa*
MsAGL6-RNAi-R2	CAATTCTGGCATTGGGTTGGCT	*AGL6*-RNAi construct cloning	*M. sativa*
35S-F	CAATCCCACTATCCTTCGCAAGACCC	RNAi construct cloning	*M. sativa*
OEMsSPL12 F	CACCATGGAGTGGAACGTGAAATC	*SPL12*-OE construct cloning	*M. sativa*
OEMsSPL12 R	ATCCAGCTGGTTGCAAGGGAA	*SPL12*-OE construct cloning	*M. sativa*
LA-MsSPL12-F1	CCCCCAAACCAAAGATTTTA	RT-qPCR	*M. sativa*
LA-MsSPL12-R1	TCTTGGTTCCTTTGCCTTTG	RT-qPCR	*M. sativa*
qMsAGL6-1F	TGTTATGTGATGCTGAGGTTGC	RT-qPCR	*M. sativa*
qMsAGL6-1R	GTTCTCCTAAGTCACCATTCTCAG	RT-qPCR	*M. sativa*
LH_Cas9_F1	CCAGAGAAAATCAGACCACA	RT-qPCR	*M. sativa*
LH_Cas9_R1	CTTGAGGCATAGAGAGAACC	RT-qPCR	*M. sativa*
β-actin-F	CAAAAGATGGCAGATGCTGAGGAT	RT-qPCR (reference gene) – *β-actin*	*M. sativa*
β-actin-R	CATGACACCAGTATGACGAGGTCG	RT-qPCR (reference gene) – *β-actin*	*M. sativa*
ADFqF	TCAAGGCGAAAAGGACACAC	RT-qPCR (reference gene) – *ADF*	*M. sativa*
ADFqR	AAAACAGCATAGCGGCACTC	RT-qPCR (reference gene) – *ADF*	*M. sativa*
CycloqF	CAAACTTTCCTGACGAGTCACC	RT-qPCR (reference gene) – *Cyclo*	*M. sativa*
CycloqR	ACGGTCAGCAATTGCCATTG	RT-qPCR (reference gene) – *Cyclo*	*M. sativa*
q1MsAGL6-F	AATTAATCTTCTTGCAACAAA	ChIP-qPCR	*M. sativa*
q1MsAGL6-R	CCGTCTACGTAACTTCAAATT	ChIP-qPCR	*M. sativa*
q2MsAGL6-F	AAGTGGCGGGAGAGGAAACA	ChIP-qPCR	*M. sativa*
q2MsAGL6-R	TATTATAGTTCAATCCATGA	ChIP-qPCR	*M. sativa*
q3MsAGL6-F	GTAATTTTCAACTTTTTGAAG	ChIP-qPCR	*M. sativa*

Primer Name	Primer Sequence	Primer Use	Origin
q3MsAGL6-R	AAGGTATATCAATTATATTGG	ChIP-qPCR	*M. sativa*
qMsLOBF	AGATGGTGATTCGTGACCCG	ChIP-qPCR	*M. sativa*
qMsLOBR	CTGTTGCTGCTGTTGTTGATTC	ChIP-qPCR	*M. sativa*
LysM-F	TTGGAGTCGTGCTGTTGGAA	RT-qPCR	*M. sativa*
LysM-R	AGCTTTCGATGAGGCAAGGA	RT-qPCR	*M. sativa*
CLE13-F	TCCTCACACCAAGAGTTTATGCT	RT-qPCR	*M. sativa*
CLE13-R	TCCTGTAGGCACTTTGCGTT	RT-qPCR	*M. sativa*
NIN-F	TGGATCTGCTGCTGATTTTG	RT-qPCR	*M. sativa*
NIN-R	TGTTGTTGTTGGGAAGGTGA	RT-qPCR	*M. sativa*
NSP2-F	CGGTTATCCGAAGATGAGGA	RT-qPCR	*M. sativa*
NSP2-R	AGAATCACCTCACCGGATTG	RT-qPCR	*M. sativa*
DMI1-F	GCACTTTGGCATTCTTGGAC	RT-qPCR	*M. sativa*
DMI1-R	ATTTGTCACTCCAGCCAAGG	RT-qPCR	*M. sativa*
DMI2-F	TGCAGACCAATACCCGAAAT	RT-qPCR	*M. sativa*
DMI2-R	CTCCCTCGATTTCCAAGTCC	RT-qPCR	*M. sativa*
DMI3F	GAAGCTGCAACTGTGGTTCA	RT-qPCR	*M. sativa*
DMI3R	CAGAACTCAACCCAAAATCCA	RT-qPCR	*M. sativa*
DELLA-F	TAACGGACCGGTTTTCGTAG	RT-qPCR	*M. sativa*
DELLA-R	CCTTCATAAGCCACCACGTT	RT-qPCR	*M. sativa*
miR172-F	TTGTTCCTTGTGGCCTCATT	RT-qPCR	*M. sativa*
miR172-R	CATTGAGTTTTGCACCTCCA	RT-qPCR	*M. sativa*
NOOT1-F1	ACCCAATAGGAGGAGGAGGA	RT-qPCR	*M. sativa*
NOOT1-R1	GCACCCTCTCTCACCACAAT	RT-qPCR	*M. sativa*
NOOT2-F1	TTCAGCGACGTTGTTTTCAG	RT-qPCR	*M. sativa*
NOOT2-R1	AGACCTAGCTGAACCGGATG	RT-qPCR	*M. sativa*
ChOMT-F1	CTTTCATTTGAGCCATTGGT	RT-qPCR	*M. sativa*
ChOMT-R1	TTCGAGGCAATTGAGGATGT	RT-qPCR	*M. sativa*
IPD3-F	ATCCCGGAGTCATGCAAACC	RT-qPCR	*M. sativa*

Primer Name	Primer Sequence	Primer Use	Origin
IPD3-R	GGAAGCTGTTCCGCCTTGTA	RT-qPCR	*M. sativa*
nifA-F	CCTCTGGAAAGGCGTTCACT	RT-qPCR	*M. sativa*
nifA-R	CTTTCGGCGGAACGTCATTG	RT-qPCR	*M. sativa*
fixK-F	TCGGTCGTCAAAGTGCGATT	RT-qPCR	*M. sativa*
fixK-R	TCGAACCTGCGTGAATAGCC	RT-qPCR	*M. sativa*
RpoH1-F	CCAAGCGGTATCAGGAGCAT	RT-qPCR	*M. sativa*
RpoH1-R	GCCTTCGGAAATGACTTCGC	RT-qPCR	*M. sativa*
AGL21-F	GGGAGGCAGAAATTTTAAGG	RT-qPCR	*M. sativa*
AGL21-R	TGGAGGCTAAGTTCCAGTTGA	RT-qPCR	*M. sativa*
WRKY41-F	ACCAAACATCCAAGGTGAGG	RT-qPCR	*M. sativa*
WRKY41-R	TGATCTCTGCACTTGCTTCG	RT-qPCR	*M. sativa*
ABA-F	AGAAGCATGAGGCCAAGAAA	RT-qPCR	*M. sativa*
ABA-R	GGTGGTGCTTCTTTCCATGT	RT-qPCR	*M. sativa*
LOB39-F	AAGCGATCAGGTGCTGAAGT	RT-qPCR	*M. sativa*
LOB39-R	ATCTCCTCCGATCCCACTTT	RT-qPCR	*M. sativa*
GRASS-F	CATGCCACTCAGATCACCAC	RT-qPCR	*M. sativa*
GRASS-R	GCTGCCGTAACTGTCAACAA	RT-qPCR	*M. sativa*
Nod26-F	CCGGTAACAGGAGCATCAAT	RT-qPCR	*M. sativa*
Nod26-R	ACGTCCAGCTTCTTTGAGGA	RT-qPCR	*M. sativa*
NAR2-F	CAACAAAACGGTCCAAACCT	RT-qPCR	*M. sativa*
NAR2-R	AACACGCCTAGGGACACAAC	RT-qPCR	*M. sativa*
NR1-F	CAACAAGCAGTGTAGATGA	RT-qPCR	*M. sativa*
NR1-R	GAGACATTAGGCCACCATTAG	RT-qPCR	*M. sativa*
NR2-F	TCCACTACCCCCAAAAAGTG	RT-qPCR	*M. sativa*
NR2-R	GTTGCTGGGATTGAAGGTGT	RT-qPCR	*M. sativa*
NPF4.4-F	ATATCCCAGGAGGGTGAGGT	RT-qPCR	*M. sativa*
NPF4.4-R	GTCTGCCCACAAAAGAGACC	RT-qPCR	*M. sativa*
SULTR1.3-F	CAAGGGCCATGGAAGAAATA	RT-qPCR	*M. sativa*

Primer Name	Primer Sequence	Primer Use	Origin
SULTR1.3-R	CTTGGCAAAAGGGTCATCAG	RT-qPCR	*M. sativa*
SULTR3.4-F	TGGAAATTCACAGGGTTCGT	RT-qPCR	*M. sativa*
SULTR3.4-R	CTCAGGACCCCATTGAAAAA	RT-qPCR	*M. sativa*
SULTR3.5-F	GCACTTTTCCCTGATGATCC	RT-qPCR	*M. sativa*
SULTR3.5-R	TGGCAAGACTAGCAATGGTG	RT-qPCR	*M. sativa*
RR19-F	TTGTACCAACGTGGTGGAGA	RT-qPCR	*M. sativa*
RR19-R	GTGGGAAAAGAGAGGTGGAA	RT-qPCR	*M. sativa*
q1MsAGL21-F	AAGTGTTTGCGTCAGGATCA	ChIP-qPCR	*M. sativa*
q1MsAGL21-R	CGAAAAATGGGTGAGTGGAG	ChIP-qPCR	*M. sativa*
q2MsAGL21-F	CCACCTCCATTTGGTTGAAA	ChIP-qPCR	*M. sativa*
q2MsAGL21-R	TCAGCGTGTTTTGTCCTCAC	ChIP-qPCR	*M. sativa*
q3MsAGL21-F	CCTCTCTAGAAGGCATTTGTTC	ChIP-qPCR	*M. sativa*
q3MsAGL621-R	AAGGCATGACGATAACACGTC	ChIP-qPCR	*M. sativa*
SPL12i-35S-F	AACCTCCTCGGATTCCATT	Southern blot-Probe	*M. sativa*
SPL12i-35S-R	GGGTCTTGCGAAGGATAGTG	Southern blot-Probe	*M. sativa*
WD40-1-F	GGATGAATCTGTGAACGCCG	RT-qPCR	*M. sativa*
WD40-1-R	CTTTGTCCACGGCTCAAACA	RT-qPCR	*M. sativa*
CRISPR-SPL13g1-F	AAGCACCTTCTTGGGATTTG	PCR-SPL13-gRNA1	*M. sativa*
CRISPR-SPL13g1-R	CACTGTTGGCAGAACCTTTG	PCR-SPL13-gRNA1	*M. sativa*
CRISPR-SPL13g2-F	GATCCTTGCGTTTGTGTTCA	PCR-SPL13-gRNA2	*M. sativa*
CRISPR-SPL13g2-R	TGTGGGGATCTTTAGGCAAC	PCR-SPL13-gRNA2	*M. sativa*
CRISPR-SPL13g3-F	CCAGGTGCTACCCTTTTCAA	PCR-SPL13-gRNA3	*M. sativa*
CRISPR-SPL13g3-R	CACATTTGCCAAAGGAATTG	PCR-SPL13-gRNA3	*M. sativa*
GSH-F	ACGCTTCCCAGCTTTAATGA	RT-qPCR	*M. sativa*
GSH-R	CCCCAACAAGAAGACCATTG	RT-qPCR	*M. sativa*
Spl12-1-LORE1-F	TTGGCCTGGTAATACAGCCAGCCT	PCR-genotyping LORE1 insertion *spl12* alleles	*L. japonicus*

Primer Name	Primer Sequence	Primer Use	Origin
Spl12-1-LORE1-R	TGAACTCCTTGAGGAAGTAGCGGCA	PCR-genotyping LORE1 insertion *spl12* alleles	*L. japonicus*
Spl12-2-LORE1-F	GCGTGTTCGGATCAGTGCTTGTCA	PCR-genotyping LORE1 insertion *spl12* alleles	*L. japonicus*
Spl12-2-LORE1-R	TGACTCAAAGGGCGCGCTCAACAG	PCR-genotyping LORE1 insertion *spl12* alleles	*L. japonicus*
P2 (LORE1 reverse)	CCATGGCGGTTCCGTGAATCTTAGG	PCR-genotyping LORE1 insertion *spl12* alleles	*L. japonicus*

Table S2 Composition of alfalfa transformation media

Basal SH2K Medium		
Component	Amount/Litre	Final concentration
10x Schenk and Hildebrandt salt	3.2 g	
Nicotinic acid	5 mg	
Pyridoxine HCL	0.5 mg	
Thiamine HCL	5 mg	
Myo-inositol	200 mg	
Potassium sulfate	4.35 g	50 mM
Proline	0.288 g	25 mM
Kinentin (10 mg/mL)	40 μL	2.14 μM
2,4-D (100 mg/mL)	40 μL	18.12 μM
Sucrose,	30 g	3% (w/v)
Adjust pH to 5.8 Plant tissue culture agar,	8 g	
Thioproline (100 mg/L)	530 μL	53 mg/L

Co-cultivation medium		
Component	Amount/Litre	Final concentration
Basal SH2K medium plus: Acetosyringone (10 mM)	2 mL	20 Mm

Callus Induction medium		
Component	Amount/Litre	Final concentration
Basal SH2K medium plus: Timentin (300 mg/mL)	1 mlL	300 mg/L

Callus Induction with antibiotics (RNAi constructs)

Component	Amount/Litre	Final concentration
Basal SH2K medium plus:		
Timentin (300 mg/mL)	1 mL	300 mg/L
Kanamycin (100 mg/ml) (first 10 days)	500 µL	50 mg/L
(after 10 days)	750 µL	75 mg/L

Callus Induction with antibiotics (Overexpression constructs)

Component	Amount/Litre	Final concentration
Basal SH2K medium plus:		
Timentin (300 mg/mL)	1 mL	300 mg/L
Hygromycin (50 mg/mL) (first 10 days)	1 mL	50 mg/L
(after 10 days)	1.5 mL	75 mg/L

Callus Induction with antibiotics (sgRNA-Cas9 constructs)

Component	Amount/Litre	Final concentration
Basal SH2K medium plus:		
Timentin (300 mg/mL)	1 mL	300 mg/L
Glufosinate ammonium (10 mg/mL) (first 10 days)	1 mL	10 mg/L
(after 10 days)	1.5 mL	15 mg/L

Embryo Development medium (BOi2Y)

Component	Amount/Litre	Final concentration
10x Blade's Stock with myo-inositol	100 ml	
Yeast extract	2 g	
Sucrose	30 g	3% (w/v)
pH to 5.8 with HCl		
Plant TC agar (Sigma A7921)	8 g	
Timentin (300 mg/mL)	1 ml	300 mg/L
Appropriate antibiotics		75 mg/L

Embryo Germination medium (½ MSO)

Component	Amount/Litre	Final concentration
MS Basal Salts	2.165 g	
10X MS-modified vitamins	100 mL	
Sucrose	30 g	3% (w/v)
pH to 5.8 with KOH		
Plant TC agar (Sigma A7921)	8 g	
Timentin (300 mg/mL)	1 mL	300 mg/L
Appropriate antibiotics		75 mg/L

Plant development medium (MSO)

Component	Amount/Litre	Final concentration
MS Basal Salts	4.33 g	
10X MS-modified vitamins	100 mL	
Glycine (10 mg/mL)	100 μL	
Sucrose	30 g	3% (w/v)
Plant TC agar (Sigma A7921)	8 g	
Timentin (300 mg/mL)	1 mL	300 mg/L
Appropriate antibiotics		75 mg/L

10x SH modified vitamins with myo-inositol

Component	Amount/Litre	Final concentration
Nicotinic acid	100 mg	5 mg/L
(B6) pyridoxine HCl (10 mg/mL)	1 mL	0.5 mg/L
(B1) thiamine HCl	100 mg	5 mg/L
Myo-inositol	4g	200 mg/L

10x SH modified vitamins with myo-inositol

Component	Amount/2Litre	Final concentration
$MgSO_4$-$7H_2O$	700 mg	35 mg/L
$MnSO_4$-H_2O	88 mg	4.4 mg/L
$Ca(NO_3)_2$-$4H_2O$	6.94 g	347 mg/L
NH_4NO_3	20 g	1000 mg/L
KNO_3	20 g	1000 mg/L
KH_2PO_4	6 g	300 mg/L
KCl	1.3 g	65 mg/L
H_3BO_3	32 mg	1.6 mg/L
$ZnSO_4$-$7H_20$	30 mg	1.5 mg/L
KI	16 mg	0.8 mg/L
Fe(III)EDTA	720 mg	3.6 mg/L
VITAMINS:		
Nicotinic acid	10 mg	0.5 mg/L
(B_6) pyridoxine HCl (10 mg/mL)	200 µL	0.1 mg/L
(B_1) thiamine HCl (10 mg/mL)	200 µL	0.1 mg/L
Glycine (10 mg/mL)	4 mL	2 mg/L

10X MS-modified vitamins

Component	Amount/2Litre	Final concentration
Nicotinic acid	10 mg	0.5 mg/L
(B_6) pyridoxine HCl (10 mg/mL)	1 mL	0.5 mg/L
(B_1) thiamine HCl (10 mg/mL)	2 mL	1 mg/L
myo-inositol	4 g	200 mg/L

Table S3 Buffers and extraction reagent used in Southern blot analysis and their components

Buffers	Chemicals	Concentration
hybridization buffer	Na_2HPO_4 (pH 7.2)	0.25M
	EDTA (pH 8.0)	1 mM
	BSA	1%
	SDS	20%
Post hybridization wash buffer	Na_2HPO_4 (pH 7.2)	20 mM
	EDTA (pH 8.0)	1 mM
	SDS	1%
Blocking buffer	Tris-HCl (pH 7.6)	100 mM
	NaCl	150 mM
	BSA	0.1%-0.5%
	Skim Milk	2-5%
Antibody wash buffer	Tris-HCl (pH 7.6)	100 mM
	NaCl	150 mM
Activation buffer	Tris-HCl (pH 9.5)	100 mM
	NaCl	100 mM

Table S4 Buffers used in ChIP assay and their components

Buffers	Chemicals	Concentration
Extraction buffer 1	Sucrose	0.4 M
	Tris-HCl (pH=8)	10 mM
	$MgCl_2$	10 mM
	β-ME	5 mM
	PMSF	0.1 mM
	Protease inhibitor1	2 tablets/ 100 mL
Extraction buffer 2	Sucrose	0.25 M
	Tris-HCl (pH=8)	10 mM
	$MgCl_2$	10 mM
	Triton X-100	1%
	β-ME	5 mM
	PMSF	0.1 mM
	Protease inhibitor1	1 tablet/10 mL
Extraction buffer 3	Sucrose	1.7 M
	Tris-HCl (pH=8)	10 mM
	$MgCl_2$	2 mM
	Triton X-100	0.15%
	β-ME	5 mM
	PMSF	0.1 mM
	Protease inhibitor1	1 tablet/10 mL
	Sucrose	1.7 M
Nuclei lysis buffer	Tris-HCl (pH=8)	50 mM
	EDTA	10 mM
	SDS	1%
	Protease inhibitor1	1 tablet/10 mL

Buffers	Chemicals	Concentration
ChIP dilution buffer	Triton X-100	1.10%
	EDTA	1.2 mM
	Tris-HCl (pH=8)	16.7 mM
	NaCl	167 mM
Elution buffer	SDS	1%
	NaHCO3	0.1M
High salt wash buffer	SDS	0.10%
	Triton X-100	1%
	EDTA	2 mM
	Tris-HCl pH=8)	20 mM
	NaCl	500 mM
Low salt wash buffer	SDS	0.10%
	Triton X-100	1%
	EDTA	2 mM
	Tris-HCl (pH=8)	20 mM
	NaCl	150 mM
LiCl wash buffer	LiCl	0.25 M
	IGEPAL-CA630	1%
	Deoxycholic acid	1%
	EDTA	1 mM
	Tris-HCl (pH=8)	10 mM
TE buffer	EDTA	1 mM
	Tris-HCl (pH=8)	10 mM

[1]Obtained from Sigma-Aldrich, Canada

Table S5 Top 50 out of 1710 differentially expressed genes and their functions in RNAi12-29

No.	Gene	Function	No.	Gene	Function
1	Medtr1g008740	NAC transcription factor-like protein	18	Medtr1g018750	carbohydrate esterase plant-like protein
2	Medtr1g009200	peptide/nitrate transporter plant	19	Medtr1g019130	wuschel-related homeobox protein
3	Medtr1g009613	shikimate kinase-like protein, putative	20	Medtr1g019410	cytochrome P450 family ABA 8'-hydroxylase
4	Medtr1g009720	plasma membrane H+-ATPase	21	Medtr1g019670	EF hand protein
5	Medtr1g010120	glucan endo-1,3-beta-glucosidase-like protein	22	Medtr1g021642	cysteine-rich receptor-kinase-like protein
6	Medtr1g011580	gibberellin 2-beta-dioxygenase	23	Medtr1g023120	beta-like galactosidase
7	Medtr1g011800	plant/F18G18-200 protein	24	Medtr1g024095	filament-plant-like protein
8	Medtr1g013150	glycoside hydrolase family 18 protein	25	Medtr1g025950	cinnamyl alcohol dehydrogenase-like protein
9	Medtr1g014320	hypothetical protein	26	Medtr1g026110	syringolide-induced protein 14-1-1
10	Medtr1g015890	glutaredoxin-like protein, putative	27	Medtr1g027290	flavonol synthase/flavanone 3-hydroxylase
11	Medtr1g016780	vacuolar processing enzyme	28	Medtr1g027490	wall-associated receptor kinase-like protein
12	Medtr1g017500	hypothetical protein	29	Medtr1g028290	receptor-like kinase
13	Medtr1g017700	phytosulfokine precursor protein	30	Medtr1g028970	glycolipid transfer protein (GLTP) family protein
14	Medtr1g018200	TPR 7B-like protein	31	Medtr1g029600	receptor-like kinase plant, putative
15	Medtr1g018420	C2H2-type zinc finger protein	32	Medtr1g029610	receptor-like kinase plant-like protein, putative
16	Medtr1g018510	calcium-binding EF hand-like protein	33	Medtr1g030810	pathogenesis-related protein bet V I family protein
17	Medtr1g018640	gibberellin-regulated family protein	34	Medtr1g032290	nudix hydrolase-like protein

No.	Gene	Function	No.	Gene	Function
35	Medtr1g038680	cationic peroxidase	47	Medtr1g060490	GDSL-like lipase/acylhydrolase
36	Medtr1g043320	hypothetical protein	48	Medtr1g061590	LRR receptor-like kinase
37	Medtr1g046490	disease resistance-responsive, dirigent domain protein	49	Medtr1g066530	pentameric polyubiquitin
38	Medtr1g040430	hypothetical protein	50	Medtr1g066380	cationic peroxidase
39	Medtr1g051810	IQ calmodulin-binding motif protein, putative			
40	Medtr1g052640	hypothetical protein			
41	Medtr1g052885	hypothetical protein			
42	Medtr1g053130	hypothetical protein			
43	Medtr1g054035	hypothetical protein			
44	Medtr1g054205	peroxidase family protein			
45	Medtr1g054935	white-brown-complex ABC transporter family protein			
46	Medtr1g057790	BEL1-related homeotic protein			

Table S6 Top 50 out of 840 differentially expressed genes and their functions in RNAi12-24

No.	Gene	Function	No.	Gene	Function
1	Medtr5g081030	leghemoglobin Lb120-1	18	Medtr7g103390	Myb/SANT-like DNA-binding domain protein
2	Medtr4g085800	PLC-like phosphodiesterase superfamily protein	19	Medtr4g068000	lipid-binding protein
3	Medtr3g087730	linoleate 13S-lipoxygenase 2-1, related protein	20	Medtr5g084040	Nodule-specific Glycine Rich Peptide
4	Medtr1g069825	G1-like protein	21	Medtr2g087830	hypothetical protein
5	Medtr1g054635	fatty acyl-CoA reductase-like protein	22	Medtr2g076010	pathogenesis-like protein
6	Medtr5g099060	nodule inception protein	23	Medtr3g069420	peptide/nitrate transporter
7	Medtr4g094812	caffeoyl-CoA 3-O-methyltransferase	24	Medtr8g059150	MADS-box transcription factor family protein
8	Medtr7g114870	IQ calmodulin-binding motif protein	25	Medtr1g051120	hypothetical protein
9	Medtr1g049330	leghemoglobin Lb120-1	26	Medtr2g438260	adenine nucleotide alpha hydrolase-like domain kinase
10	Medtr4g094338	hypothetical protein	27	Medtr8g006790	plasma membrane H+-ATPase
11	Medtr6g038390	oxidoreductase family, NAD-binding rossmann fold protein	28	Medtr1g101500	carbohydrate-binding X8 domain protein
12	Medtr1g052840	hypothetical protein	29	Medtr3g073150	nitrate reductase NADH-like protein
13	Medtr4g081190	ABC transporter B family protein	30	Medtr7g089640	F-box plant-like protein
14	Medtr3g415610	histone deacetylase family protein	31	Medtr7g099870	ion channel regulatory protein UNC-93
15	Medtr5g018480	cytochrome P450 family protein	32	Medtr2g064310	ZIP zinc/iron transport family protein
16	Medtr3g078623	formin-like 2 domain protein	33	Medtr2g031750	transmembrane amino acid transporter family protein
17	Medtr6g093180	beta-amyrin synthase	34	Medtr1g067150	RabGAP/TBC domain protein

No.	Gene	Function	No.	Gene	Function
35	Medtr3g021430	caffeic acid O-methyltransferase	48	Medtr8g445170	PPR containing plant-like protein
36	Medtr5g095400	hypothetical protein	49	Medtr8g103233	PPR containing plant-like protein
37	Medtr1g097220	carbohydrate-binding X8 domain protein	50	Medtr8g036075	EF hand calcium-binding family protein
38	Medtr5g059820	Serine/Threonine kinase family protein			
39	Medtr4g059730	glutathione S-transferase, amino-terminal domain protein			
40	Medtr7g011090	casparian strip membrane protein			
41	Medtr4g045990	wound-responsive family protein			
42	Medtr8g087710	hypothetical protein			
43	Medtr7g011790	DUF1336 family protein			
44	Medtr2g006870	hypothetical protein			
45	Medtr7g092230	oligopeptide transporter OPT family protein			
46	Medtr8g014930	LRR receptor-like kinase			
47	Medtr8g083280	magnesium transporter NIPA2-like protein			

Table S7 Differentially increased genes and their functions common in both *SPL12*-RNAi plants

No.	Gene	Function	No.	Gene	Function
1	Medtr6g038390	oxidoreductase family, NAD-binding rossmann fold protein	13	Medtr1g075180	sieve element occlusion protein
2	Medtr1g101500	MATE efflux family protein	14	Medtr1g092690	GDSL-like lipase/acylhydrolase
3	Medtr7g089640	F-box plant-like protein	15	Medtr6g086170	sulfate/bicarbonate/oxalate exchanger and transporter sat-1
4	Medtr3g021430	caffeic acid O-methyltransferase	16	Medtr4g011970	sulfate/bicarbonate/oxalate exchanger and transporter sat-1
5	Medtr5g059820	nitrate reductase NADH-like protein	17	Medtr7g027960	cytochrome P450 family flavone synthase
6	Medtr3g073180	nitrate reductase NADH-like protein	18	Medtr1g036460	caffeic acid O-methyltransferase
7	Medtr4g059730	glutathione S-transferase, amino-terminal domain protein	19	Medtr4g094772	cytochrome P450 family 81 protein
8	Medtr8g087710	major intrinsic protein (MIP) family transporter	20	Medtr7g079010	WRKY family transcription factor
9	Medtr0056s0160	flavonol synthase/flavanone 3-hydroxylase	21	Medtr3g099020	palmitoyl-acyl carrier thioesterase
10	Medtr8g445170	embryonic abundant-like protein	22	Medtr2g009450	leguminosin group485 secreted peptide
11	Medtr8g103233	peptide/nitrate transporter plant	23	Medtr3g465470	tyrosine kinase family protein
12	Medtr2g092930	phosphoenolpyruvate carboxylase	24	Medtr8g089300	CASP POPTRDRAFT-like protein

No.	Gene	Function	No.	Gene	Function
25	Medtr8g089300	CASP POPTRDRAFT-like protein	41	Medtr5g016320	indole-3-acetic acid-amido synthetase
26	Medtr4g063090	tonoplast intrinsic protein	42	Medtr3g088630	two-component response regulator ARR3-like protein
27	Medtr4g063090	tonoplast intrinsic protein	43	Medtr5g070010	cytochrome P450 family-dependent fatty acid hydroxylase
28	Medtr4g108690	GDSL-like lipase/acylhydrolase	44	Medtr8g030620	glycerol-3-phosphate acyltransferase
29	Medtr4g108690	GDSL-like lipase/acylhydrolase	45	Medtr1g076930	isoflavone-7-O-methyltransferase
30	Medtr5g014100	anionic peroxidase swpb3 protein	46	Medtr5g031210	cinnamyl alcohol dehydrogenase-like protein
31	Medtr5g014100	anionic peroxidase swpb3 protein	47	Medtr4g091150	FAD-binding berberine family protein
32	Medtr8g079050	GDSL-like lipase/acylhydrolase	48	Medtr3g463060	cytochrome P450 family-dependent fatty acid hydroxylase
33	Medtr3g102450	receptor-like kinase			
34	Medtr7g009780	polyvinylalcohol dehydrogenase-like protein	49	Medtr7g090970	glycerol-3-phosphate dehydrogenase
35	Medtr8g031390	GDSL-like lipase/acylhydrolase	50	Medtr8g078480	BEL1-related homeotic protein
36	Medtr7g065080	peptide/nitrate transporter plant	51	Medtr8g030590	cytochrome P450 family 94 protein
37	Medtr4g077930	ABC transporter B family protein	52	Medtr3g435540	GDSL-like lipase/acylhydrolase
38	Medtr7g009960	O-acyltransferase WSD1-like protein	53	Medtr4g415290	glycerol-3-phosphate acyltransferase
39	Medtr3g075390	KDEL-tailed cysteine endopeptidase CEP1	54	Medtr1g034360	long-chain fatty acyl CoA ligase
40	Medtr8g028780	oxidoreductase/ferric-chelate reductase	55	Medtr3g104920	mechanosensitive ion channel family protein

No.	Gene	Function	No.	Gene	Function
56	Medtr1g085680	cytochrome P450 family 709 protein	71	Medtr7g118170	3-ketoacyl-CoA synthase-like protein
57	Medtr0097s0070	CASP POPTRDRAFT-like protein	72	Medtr4g104700	component of high affinity nitrate transporter
58	Medtr5g006940	Lipid transfer protein	73	Medtr4g099430	inhibitor of apoptosis-promoting Bax1 protein
59	Medtr6g084430	NAC transcription factor-like protein	74	Medtr7g013660	copper chaperone
60	Medtr6g017205	FAD-binding berberine family protein	75	Medtr1g052640	stress up-regulated Nod 19 protein
61	Medtr8g031070	oxidoreductase/ferric-chelate reductase	76	Medtr1g011640	drug resistance transporter-like ABC domain protein
62	Medtr7g112360	chaperone DnaJ domain protein	77	Medtr2g008470	high affinity sulfate transporter type 1
63	Medtr5g049280	peroxidase family protein	78	Medtr2g046150	DUF538 family protein
64	Medtr2g005130	peptide/nitrate transporter	79	Medtr8g107250	tubulin
65	Medtr4g117390	endo-1,3-1,4-beta-D-glucanase-like protein	80	Medtr3g437870	ABC transporter A family protein
66	Medtr5g018990	cytochrome P450 family 71 protein	81	Medtr2g062220	oxidoreductase/transition metal ion-binding protein
67	Medtr3g074070	transducin/WD40 repeat protein	82	Medtr8g045490	pathogenesis-related protein bet V I family protein
68	Medtr8g045300	polyketide cyclase/dehydrase and lipid transporter	83	Medtr5g007450	cytochrome P450 family 71 protein
69	Medtr4g065113	extensin-like region protein	84	Medtr2g055250	F-box protein
70	Medtr5g031000	MADS-box transcription factor			

Table S8 Differentially decreased genes and their functions common in both *SPL12*-RNAi plants

No.	Gene	Function	No.	Gene	Function
1	Medtr2g098890	EF hand calcium-binding family protein	13	Medtr5g430440	hypothetical protein
2	Medtr4g129820	UDP-D-glucuronate 4-epimerase	14	Medtr7g082570	class I glutamine amidotransferase
3	Medtr5g081710	triose-phosphate transporter family protein	15	Medtr5g025690	EF hand calcium-binding family protein
4	Medtr5g015590	calcium-transporting ATPase 2, plasma membrane-type protein	16	Medtr7g116850	glycoside hydrolase family 18 protein
5	Medtr7g071120	WRKY transcription factor	17	Medtr8g061360	tyrosine/nicotianamine family aminotransferase
6	Medtr7g090630	dehydration-induced protein ERD15	18	Medtr4g090970	calmodulin-binding protein
7	Medtr5g015880	lateral organ boundaries (LOB) domain protein	19	Medtr4g091100	F-box SKIP27-like protein
8	Medtr6g027540	calcium-dependent lipid-binding (CaLB domain) family protein	20	Medtr3g114750	syringolide-induced protein 14-1-1
9	Medtr4g081440	dihydroflavonol 4-reductase-like protein	21	Medtr8g090205	calmodulin-binding transcription activator
10	Medtr1g052885	calcium-binding EF-hand protein	22	Medtr1g076800	DUF1442 family protein
11	Medtr3g074230	TPR repeat thioredoxin TTL1-like protein	23	Medtr7g105870	harpin-induced-like protein
12	Medtr2g020710	sugar porter (SP) family MFS transporter	24	Medtr3g093830	WRKY family transcription factor

No.	Gene	Function	No.	Gene	Function
25	Medtr1g048610	ethylene response factor	41	Medtr5g006450	acetyltransferase (GNAT) domain protein
26	Medtr1g018420	C2H2-type zinc finger protein	42	Medtr8g033220	MADS-box transcription factor
27	Medtr7g085850	hypothetical protein	43	Medtr4g133660	GRAS family transcription factor
28	Medtr2g039910	calmodulin-binding family protein	44	Medtr2g086920	F-box plant-like protein
29	Medtr2g084875	arogenate/prephenate dehydratase	45	Medtr3g092640	membrane-related protein CP5, putative
30	Medtr3g095040	WRKY family transcription factor	46	Medtr1g026110	syringolide-induced protein 14-1-1
31	Medtr4g064570	zinc finger (C3HC4-type RING finger) family protein	47	Medtr2g039620	basic helix loop helix (BHLH) DNA-binding family protein
32	Medtr3g070230	nematode resistance HSPRO2-like protein	48	Medtr8g100065	GRAM domain protein/ABA-responsive-like protein
33	Medtr3g085180	squamosa promoter-binding-like protein	49	Medtr3g088845	2-oxoisovalerate dehydrogenase subunit alpha
34	Medtr2g097620	zinc finger, C3HC4 type (RING finger) protein, putative	50	Medtr4g129650	nodulin MtN21/EamA-like transporter family protein
35	Medtr5g071560	MAP kinase kinase kinase	51	Medtr4g035180	Serine/Threonine-kinase CCR3-like protein
36	Medtr1g029610	receptor-like kinase plant-like protein, putative	52	Medtr8g107110	EF hand calcium-binding family protein
37	Medtr2g081580	calcium-binding EF-hand protein	53	Medtr7g010820	peptide/nitrate transporter
38	Medtr8g104510	calmodulin-binding-like protein	54	Medtr7g010820	peptide/nitrate transporter
39	Medtr1g034300	extra-large GTP-binding protein	55	Medtr3g102980	C2H2-type zinc finger protein
40	Medtr1g034300	extra-large GTP-binding protein	56	Medtr3g102980	C2H2-type zinc finger protein

No.	Gene	Function	No.	Gene	Function
57	Medtr3g078800	late embryogenesis abundant hydroxyproline-rich glycoprotein, putative	72	Medtr6g086365	arabinogalactan protein
58	Medtr3g078800	late embryogenesis abundant hydroxyproline-rich glycoprotein, putative	73	Medtr3g065080	Avr9/Cf-9 rapidly elicited protein
59	Medtr1g106915	gibberellin-regulated family protein	74	Medtr3g065080	Avr9/Cf-9 rapidly elicited protein
60	Medtr3g086830	hypothetical protein	75	Medtr3g070880	ARM repeat CCCH-type zinc finger protein
61	Medtr5g077510	Avr9/Cf-9 rapidly elicited protein	76	Medtr2g436100	RING-H2 zinc finger protein
62	Medtr5g011980	Lipid transfer protein	77	Medtr8g099350	WRKY family transcription factor
63	Medtr4g007060	WRKY transcription factor	78	Medtr4g116530	stress induced protein
64	Medtr4g126020	calmodulin-binding family protein	79	Medtr6g049280	heavy metal-associated domain protein
65	Medtr4g066240	cyanogenic beta-glucosidase, putative	80	Medtr0008s0390	myb-related transcription factor
66	Medtr5g017980	myb-like DNA-binding domain, shaqkyf class protein	81	Medtr8g432390	BON1-associated-like protein
67	Medtr4g106500	UVI1, putative	82	Medtr5g084570	leguminosin group485 secreted peptide
68	Medtr5g023980	Serine/Threonine-kinase Cx32, related protein	83	Medtr3g092890	2OG-Fe(II) oxygenase family oxidoreductase
69	Medtr1g032290	nudix hydrolase-like protein	84	Medtr7g100100	Cys2-His2 zinc finger transcription factor
70	Medtr8g086820	DUF1685 family protein	85	Medtr5g067370	serine-glyoxylate aminotransferase-like protein
71	Medtr1g087710	DUF761 domain protein			

Table S9 GO-term analysis represented molecular function, biological process and cellular components in leaf tissues

Biological process (top 45)	Molecular function	Cellular component
"catalytic activity"	"metabolic process"	"membrane"
"binding"	"primary metabolic process"	"integral component of membrane"
"hydrolase activity"	"cellular biosynthetic process"	"intracellular anatomical structure"
"nucleotide binding"	"cellular aromatic compound metabolic process"	"cytoplasm"
"nucleic acid binding"	"transport"	"nucleus"
"metal ion binding"	"regulation of transcription DNA-templated"	"extracellular region"
"oxidoreductase activity"	"proteolysis"	"endoplasmic reticulum"
"DNA binding"	"cellular amino acid metabolic process"	"integral component of plasma membrane"
"transporter activity"	"lipid metabolic process"	"chloroplast"
"transferase activity transferring phosphorus-containing groups"	"intracellular signal transduction"	"ubiquitin ligase complex"
"RNA binding"	"sulfur compound metabolic process"	"microtubule associated complex"
"hydrolase activity acting on ester bonds"	"transcription DNA-templated"	"nucleosome"
"phosphotransferase activity alcohol group as acceptor"	"fatty acid metabolic process"	"protein phosphatase type 2A complex"
"protein binding"	"proton transmembrane transport"	"photosystem I"
"DNA-binding transcription factor activity"	"defense response"	"TIM23 mitochondrial import inner membrane translocase complex"
"ligase activity"	"protein folding"	"transcription factor TFIIE complex"

Biological process (top 45)	Molecular function	Cellular component
"structural molecule activity"	"ubiquitin-dependent protein catabolic process"	"cytochrome b6f complex"
"methyltransferase activity"	"protein dephosphorylation"	
"structural constituent of ribosome"	"protein targeting"	
"endopeptidase activity"	"isoprenoid biosynthetic process"	
"magnesium ion binding"	"porphyrin-containing compound biosynthetic process"	
"sequence-specific DNA binding"	"'de novo' IMP biosynthetic process"	
"hydrolase activity hydrolyzing O-glycosyl compounds"	"lipid transport"	
"iron ion binding"	"amino acid transmembrane transport"	
"heme binding"	"pseudouridine synthesis"	
"GTPase activity"	"embryo development"	
"monooxygenase activity"	"regulation of translational fidelity"	
"electron transfer activity"	"thiamine biosynthetic process"	
"protein dimerization activity"	"ubiquinone biosynthetic process"	
"calcium ion binding"	"defense response to bacterium"	
"N-acetyltransferase activity"	"glycerol ether metabolic process"	
"transferase activity transferring alkyl or aryl (other than methyl) groups"	"sulfate assimilation"	
"carbohydrate binding"	"regulation of cyclin-dependent protein serine/threonine kinase activity"	
"intramolecular transferase activity"	"sucrose metabolic process"	
"ubiquitin-protein transferase activity"	"allantoin catabolic process"	
"FMN binding"	"protein retention in ER lumen"	
"actin binding"	"lignin catabolic process"	

Biological process (top 45)	Molecular function	Cellular component
"aminopeptidase activity"	"photosynthetic electron transport in photosystem II"	
"translation initiation factor activity"	"flavonoid biosynthetic process"	
"carbon-nitrogen ligase activity with glutamine as amido-N-donor"	"xenobiotic transmembrane transport"	
"transcription cis-regulatory region binding"	"division septum site selection"	
"peptidyl-prolyl cis-trans isomerase activity"		
"cytoskeletal motor activity"		
"potassium ion transmembrane transporter activity"		
"transcription coregulator activity"		

Curriculum Vitae

Name:	Vida Nasrollahi
Post-secondary Education and Degrees:	**The University of Western Ontario** London, Ontario, Canada (PhD) **Bu-Ali Sina University** Hamedan, Iran (MSc) **Shiraz University** Shiraz, Iran (BSc)
Honors and Awards:	Western Graduate Research Scholarship (WGRS) 2017-2021
Related Work Experience:	**Teaching Assistant** Western University 2017-2022 **Research Assistant** Agriculture and Agri-Food Canada, London, Ontario, Canada 2017-2022

Articles in refereed journals:

Nasrollahi, V, Yuan Z-C, Kohalmi SE and Hannoufa A. SPL12 directly regulates *AGL6* and *AGL21* in modulating nodulation and root regeneration under osmotic stress and nitrate sufficient conditions in *Medicago sativa*. Plants (submitted)

Nasrollahi, V., Z.-C. Yuan, Q. Lu, T. McDowell, S. Kohalmi and A. Hannoufa, 2022. Deciphering the role of SPL12 and AGL6 from a genetic module that functions in nodulation and root regeneration in *Medicago sativa*. Accepted for publication in Plant Molecular Biology (https://doi.org/10.1007/s11103-022-01303-7).

Feyissa, B.A., L. Amyot, V. **Nasrollahi**, Y. Papadopoulos, S.E. Kohalmi and A. Hannoufa, 2021. Involvement of the mir156/SPL module in flooding response in *Medicago sativa*. Scientific Reports, 11: 1-16.

Feyissa BA, Renaud J, **Nasrollahi V**, Kohalmi SE, Hannoufa A, 2020 Transcriptome-IPMS analysis reveals a tissue-dependent miR156/SPL13 regulatory mechanism in alfalfa drought tolerance, BMC Genomics 21:721.

Selected scientific presentation:

Nasrollahi V, Kohalmi SE, Hannoufa A,. (2021) miR156/SPL12 regulates nodulation and root regeneration in *Medicago sativa*. Plant Science and Genomics (Online). [Presentation].

Nasrollahi V, Kohalmi SE, Hannoufa A,. (2021) Characterization of SPL12 role in regulating root architecture, nodulation and nitrogen fixation in *Medicago sativa* . CSPB/SCBV Annual Business Meeting (Online). [Presentation].

Nasrollahi V, Kohalmi SE, Hannoufa A,. (2021) miR156/SPL12 modulates nodulation, nitrogen fixation and root regeneration in *Medicago sativa* by Silencing *AGAMOUS-LIKE 6*. European Nitrogen Fixation Conference, Aarhus University, Denmark (Online). [Poster].